ผลของการเติมนิกเกิล โคบอลต์ และอินเดียมต่อโครงสร้างจุลภาค สมบัติทางไฟฟ้า และสมบัติเชิงกลของโลหะบัดกรีผสมดีบุก-ทองแดง

นายปิตินันท์ ปิยะวาทิน

วิทยานิพนธ์นี้เป็นส่วนหนึ่งของการศึกษาตามหลักสูตรปริญญาวิศวกรรมศาสตรมหาบัณฑิต
สาขาวิชาวิศวกรรมโลหการ ภาควิชาวิศวกรรมโลหการ
คณะวิศวกรรมศาสตร์ จุฬาลงกรณ์มหาวิทยาลัย
ปีการศึกษา 2554
ลิขสิทธิ์ของจุฬาลงกรณ์มหาวิทยาลัย

บทคัดย่อและแฟ้มข้อมูลฉบับเต็มของวิทยานิพนธ์ตั้งแต่ปีการศึกษา 2554 ที่ให้บริการในคลังปัญญาจุฬาฯ (CUIR)
เป็นแฟ้มข้อมูลของนิสิตเจ้าของวิทยานิพนธ์ที่ส่งผ่านทางบัณฑิตวิทยาลัย
The abstract and full text of theses from the academic year 2011 in Chulalongkorn University Intellectual Repository(CUIR)
are the thesis authors' files submitted through the Graduate School.

EFFECTS OF Ni, Co AND In ON MICROSTRUCTURES, ELECTRICAL PROPERTIES AND MECHANICAL PROPERTIES OF Sn-Cu SOLDER ALLOY

Mr. Pitinan Piyavatin

A Thesis Submitted in Partial Fulfillment of the Requirements
for the Degree of Master of Engineering Program in Metallurgical Engineering
Department of Metallurgical Engineering
Faculty of Engineering
Chulalongkorn University
Academic Year 2011
Copyright of Chulalongkorn University

Thesis Title	EFFECTS OF Ni, Co AND In ON MICROSTRUCTURES, ELECTRICAL PROPERTIES AND MECHANICAL PROPERTIES OF Sn-Cu SOLDER ALLOY
By	Mr. Pitinan Piyavatin
Field of Study	Metallurgical Engineering
Thesis Advisor	Boonrat Lohwongwatana, Ph.D.
Thesis Co-advisor	Associate Professor Gobboon Lothongkum, Dr.Ing.

Accepted by the Faculty of Engineering, Chulalongkorn University in Partial Fulfillment of the Requirements for the Master's Degree

………………………………………….. Dean of the Faculty of Engineering

(Associate Professor Boonsom Lerdhirunwong, Dr.Ing.)

THESIS COMMITTEE

………………………………………….. Chairman

(Associate Professor Prasonk Sricharoenchai, D.Eng.)

………………………………………….. Thesis Advisor

(Boonrat Lohwongwatana, Ph.D.)

………………………………………….. Thesis Co-Advisor

(Associate Professor Gobboon Lothongkum, Dr.Ing.)

………………………………………….. Examiner

(Associate Professor Charkorn Jarupisitthorn)

………………………………………….. External Examiner

(Ekkarut Viyanit, Dr.Ing.)

ปิตินันท์ ปิยะวาทิน: ผลของการเติมนิกเกิล โคบอลต์ และอินเดียมต่อโครงสร้างจุลภาค สมบัติทางไฟฟ้า และสมบัติเชิงกลของโลหะบัดกรีผสมดีบุก-ทองแดง. (EFFECTS OF Ni, Co AND In ON MICROSTRUCTURES, ELECTRICAL PROPERTIES AND MECHANICAL PROPERTIES OF Sn-Cu SOLDER ALLOY) อ. ที่ปรึกษาวิทยานิพนธ์หลัก: อ.ดร.บุญรัตน์ โล่ห์วงศ์วัฒน, อ.ที่ปรึกษาวิทยานิพนธ์ร่วม : รศ.ดร.กอบบุญ หล่อทองคำ, 81 หน้า.

โลหะตะกั่วบัดกรีถูกใช้อย่างแพร่หลายในอุตสาหกรรมอิเล็กทรอนิกส์มาหลายทศวรรษ แต่เนื่องจากความเป็นพิษของตะกั่วเป็นผลให้มีการออกระเบียบห้ามการใช้งานในชิ้นส่วนอิเล็กทรอนิกส์ทุกประเภท โลหะบัดกรีไร้ตะกั่วจึงถูกพัฒนาขึ้น โดยโลหะผสมระบบ Sn-Ag-Cu เป็นที่ได้รับความนิยมมากที่สุด แต่เนื่องจากราคาที่ผันผวนของโลหะเงิน โลหะผสม Sn-Cu จึงได้รับความสนใจมากขึ้นจากผู้ผลิต โลหะผสม Sn-Cu แม้ต้นทุนจะถูกกว่ามาก แต่ยังมีสมบัติด้อยกว่า Sn-Ag-Cu งานวิจัยนี้จึงได้ทำการศึกษาผลของการเติมนิกเกิล โคบอลต์ และอินเดียม ต่อสมบัติของโลหะบัดกรีระบบ Sn-Cu เพื่อปรับปรุงสมบัติสำคัญในการนำไปใช้งานทางอิเล็กทรอนิกส์

ผลการทดลองพบว่าการเติมอินเดียมทำให้จุดหลอมเหลวของโลหะบัดกรี Sn-Cu ลดลงใกล้เคียงกับ Sn-3.0Ag-0.5Cu การเติมนิกเกิล โคบอลต์ และอินเดียมในปริมาณที่เหมาะสมยังส่งผลดีต่อค่าความแข็งและความเค้นแรงเฉือนโดยการสร้างสารประกอบเชิงโลหะซึ่งส่งผลให้รอยประสานบัดกรีแข็งแรงขึ้น แต่ส่งผลให้สัมประสิทธ์ความต้านทานไฟฟ้าเพิ่มขึ้น นอกจากนี้โลหะบัดกรี Sn-Cu-Ni-Co-In ยังสามารถรักษาความแข็งแรงได้หลังผ่านการอบที่อุณหภูมิ 150 องศาเซลเซียส เป็นเวลา 1,000 ชั่วโมง ในขณะที่ค่าความเค้นแรงเฉือนของ Sn-3.0Ag-0.5Cu ลดลง 25.33% โลหะบัดกรี Sn-Cu-Ni-Co-In มีค่าความเค้นแรงเฉือนลดลงเพียง 3.82% เนื่องมาจากผลของสารประกอบเชิงโลหะที่กระจายตัวอย่างสม่ำเสมอซึ่งขัดขวางการเคลื่อนที่ของดิสโลเคชันและเป็นตำแหน่งจำนวนมากที่เกิดความเค้นรวมศูนย์

ภาควิชา..วิศวกรรมโลหการ..... ลายมือชื่อนิสิต...
สาขาวิชา..วิศวกรรมโลหการ.... ลายมือชื่อ อ.ที่ปรึกษาวิทยานิพนธ์หลัก...............................
ปีการศึกษา....2554................. ลายมือชื่อ อ.ที่ปรึกษาวิทยานิพนธ์ร่วม...............................

5170381021 : MAJOR METALLURGICAL ENGINEERING

KEYWORDS : LEAD-FREE SOLDER / INTERMETALLIC COMPOUND / SOLDERING / MOLYBDENUM EFFECT / SHEAR STRENGTH / Sn-Cu-Ni-Co-In

PITINAN PIYAVATIN : EFFECTS OF Ni, Co AND In ON MICROSTRUCTURES, ELECTRICAL PROPERTIES AND MECHANICAL PROPERTIES OF Sn-Cu SOLDER ALLOY. ADVISOR : BOONRAT LOHWONGWATANA, Ph.D., CO-ADVISOR : ASSOC.PROF. GOBBOON LOTHONGKUM, DR.-ING., 81 pp.

Pb-containing solder alloys were widely used in electronic industries for decades but due to toxicity of Pb, worldwide restrictions were emerged to ban Pb usage in all electronic parts. Subsequently, several lead-free solder alloy compositions were developed. Sn-Ag-Cu alloy systems have been proposed to be amongst the first candidates. However, due to price fluctuation of Ag, many manufacturers are moving toward Sn-Cu solder alloys. Despite of lower cost, Sn-Cu solder alloys have inferior properties. In this research, we study the effects of Ni, Co and In additions to Sn-Cu solder alloy in order to improve its key properties for electronic applications.

The result shows that addition of In lowers the melting point of Sn-Cu alloys to comparable value of that of Sn-3.0Ag-0.5Cu. The optimal amounts of Ni, Co and In additions result in improved hardness and shear strength by formation of intermetallic compounds that strengthen the soldered interface. The additions result in increased electrical resistivity. The Sn-Cu-Ni-Co-In solder alloys can maintain their shear strength after aging at 150°C for 1,000 hours. Sn-3.0Ag-0.5Cu shows 25.33% drop in its shear strength while Sn-Cu-Ni-Co-In alloys show only 3.82% drop. This is due to the uniformly distributed intermetallic compound which serves as dislocation obstacles and multiple sites for local stress concentration.

Department : Metallurgical Engineering	Student's Signature ....
Field of Study : Metallurgical Engineering	Advisor's Signature ....
Academic Year : 2011	Co-advisor's Signature ....

ACKNOWLEDGEMENTS

First of all, it is with immense gratitude that I acknowledge the support and help of my thesis advisor, Boonrat Lohwongwattana, whose encouragement and guidance from the initial to the final level enabled me to develop an understanding of this thesis. I could not have imagined having a better advisor and philosopher for my master's study.

This thesis would not have been possible without the support and help from a lot of people. I would like to thank my thesis co-advisor, Associate Professor Gobboon Lothongkum, for his valuable continuous support in number of ways. I would also like to thank Assistant Professor Arporn Teeramongkonrasmee for his guidance and support during my experiments at Department of Electrical Engineering.

This thesis was supported by the Thailand Research Fund (TRF) Master Research Grants (MAG) under Contract No. MRG-WI525E019 and The 90th Anniversary of Chulalongkorn University Fund (Ratchadaphiseksomphot Endowment Fund). The partial materials and fund were also supported by the Ultracore Corporation, Ltd.. I would like to express my thanks. Thanks also go to Chaiyaporn Tongyam and the Mektec Manufacturing Corporation (Thailand) Ltd. for equipment used.

I consider it an honor to work with my labmates at Department of Metallurgical Engineering, Anan Lawan, Chedtha Puncreobutr, Chaiyapat Tangpatjaroen and Nutnicha Teng-amnuay. I would also like to thank for their help, friendships and stimulating discussions.

Lastly, I cannot find words to express my gratitude to my parents who have given me the opportunity of an education from the best institutions and support throughout my life.

CONTENTS

Page

ABSTRACT (Thai) iv

ABSTRACT (English) v

ACKNOWLEDGEMENT........ vi

CONTENTS vii

LIST OF TABLES ix

LIST OF FIGURES x

CHAPTER I INTRODUCTION........ 1

1.1 Background 1

1.2 Objective of Research 2

1.3 Scopes of Research........ 2

1.4 Advantages of Research 2

CHAPTER II LITERATURE SURVEY........ 3

2.1 Development of Lead-Free Solder Alloys 6

2.2 Reflow Soldering Process 5

2.3 Effects of Ni and Co Additions on Sn-based Solder Alloys........ 7

2.4 Effects of In Addition on Properties of Sn-based Solder Alloys 10

CHAPTER III EXPERIMENTAL PROCEDURES 17

3.1 Sample Preparation 17

3.2 Observations of Melting and Solidification Behavior........ 17

3.3 Measurement of Wetting Characteristics........ 17

3.4 Measurement of Electrical Resistivity........ 20

3.5 Solder Joint Production........ 22

3.6 Metallographic Examination........ 24

3.7 Mechanical Testing........ 24

3.8 Isothermal Aging.. 25

CHAPTER IV EXPERIMENTAL RESULTS AND DISCUSSION 26

4.1 Wettability 26

4.2 Melting and Solidification Behavior... 30

4.3 Electrical Resistivity 32

4.4 Effects of Soldering Condition on Microstructure and Shear Strength............. 33

4.5 As-soldered Microstructures and Shear Strength.. 38

4.6 Microstructure Evolution After Isothermal Aging.. 42

4.7 Phase Identification.. 42

4.8 Elemental Distribution 49

4.9 Growth Behavior of Interfacial Intermetallic Compounds................................. 52

4.10 Shear Strength After Isothermal Aging 55

CHAPTER VI CONCLUSIONS 60

REFERENCES 63

APPENDIX... 67

BIOGRAPHY... 81

LIST OF TABLES

Table Page

2.1 Pass-Fail Criteria used by the NCMS Pb-Free Solder Project................ 4

3.1 Compositions of solder alloys used in this study (Conventional alloys, SAC305 and SC, were tested for result comparison) 19

3.2 Soldering conditions 23

4.1 Melting point and solidification behavior of the selected solder alloys .. 31

4.2 Summary of shear failure mode of solder joints..................................... 59

LIST OF FIGURES

Figure		Page
2.1	Typical reflow soldering temperature profile of 63Sn-37Pb solder	5
2.2	Backscattering electron image shows Kirkendall voids found in Cu_3Sn layer after aging at 140°C for 40 days	7
2.3	Backscattering electron image showing the interface of Sn-3.5Ag/Cu (a) and Sn-3.5Ag-0.1Ni/Cu (b) subjected to thermal aging at 150°C for 1,000 hours	8
2.4	Thickness of intermetallic compound layer after thermal aging at 160°C a) Cu_6Sn_5 (b) Cu_3Sn	8
2.5	Impact strength of Sn-Ag-Cu+X solder alloys	9
2.6	Impact strength of Sn-Ag-Cu+X solder alloys where lighter bars are values of as-soldered joint and darker bars are values of joint subjected to thermal aging for 1,000 hours	9
2.7	Effects of In addition on solidus and liquidus temperature of Sn-3.0Ag-0.7Cu solder alloy	10
2.8	Schematic of wetting curve obtained from wetting balance test	10
2.9	Wetting time and wetting force of Sn-0.3Ag-0.7Cu+XIn solder alloys....	11
2.10	Tensile strength and microhardness of Sn-0.3Ag-0.7Cu-XIn solder alloys..	12
2.11	Microstructure of Sn-0.3Ag-0.7Cu	13
2.12	SEM image of Sn-0.3Ag-0.7Cu	13
2.13	Sn distribution in Sn-0.3Ag-0.7Cu..	13
2.14	Ag distribution in Sn-0.3Ag-0.7Cu	13
2.15	Cu distribution in Sn-0.3Ag-0.7Cu	13
2.16	Microstructure of Sn-0.3Ag-0.7Cu-1.5In	14
2.17	Sn distribution in Sn-0.3Ag-0.7Cu-1.5In	14
2.18	Ag distribution in Sn-0.3Ag-0.7Cu-1.5In	14

Figure Page

2.19 Cu distribution in Sn-0.3Ag-0.7Cu-1.5In 14
2.20 In distribution in Sn-0.3Ag-0.7Cu-1.5In 14
2.21 Microstructure of Sn-0.3Ag-0.7Cu-3In 15
2.22 Sn distribution in Sn-0.3Ag-0.7Cu-3In 15
2.23 Ag distribution in Sn-0.3Ag-0.7Cu-3In 15
2.24 Cu distribution in Sn-0.3Ag-0.7Cu-3In 15
2.25 In distribution in Sn-0.3Ag-0.7Cu-3In 16
3.1 Assembly used for spread test 18
3.2 Schematic showing solder-alloy ingot spread on copper sheet in spread test 18
3.3 Measurement of spread area 20
3.4 Measurement of contact angle 20
3.5 Wired sample and contact probes used for electrical resistivity measurement 21
3.6 An example of V_s-I_0 plot used for resistance calculation 22
3.7 The assembly used for production of solder joint 23
3.8 Example of recorded temperature profile of 245°C/60s for SAC305 alloy 23
3.9 The asymmetrical four point bending shear test fixture 25
4.1 Spread-area 3-D surface of SC-Ni-Co-In solder alloys varying amounts of Ni and Co where In is fixed at 3% 27
4.2 Spread-area 3-D surface of SC-Ni-Co-In solder alloys varying amounts of Ni and In where Co is fixed at 0.5% 28
4.3 Spread-area 3-D surface of SC-Ni-Co-In solder alloys varying amounts of Co and In where Ni is fixed at 0.1% 28
4.4 Contact-angle 3-D surface of SC-Ni-Co-In solder alloys varying amounts of Ni and Co where In is fixed at 3% 29
4.5 Contact-angle 3-D surface of SC-Ni-Co-In solder alloys varying amounts of Ni and In where Co is fixed at 0.5% 29

Figure | Page

4.6 Contact-angle 3-D surface of SC-Ni-Co-In solder alloys varying amounts of In and Co where Ni is fixed at 0.1% 30
4.7 DSC curve of the selected solder alloys.. 31
4.8 Electrical resistivity of wire-drawn solder alloys and Sn......................... 33
4.9 BEI micrographs of SC-0.01Ni-0.1Co-1In with various soldering time and temperature at solder matrix and solder/Cu interface 35
4.10 BEI micrographs of SC-0.01Ni-0.1Co-3In with various soldering time and temperature at solder matrix and solder/Cu interface 36
4.11 IMC layer thickness at solder/Cu interface for various soldering time and temperature 37
4.13 BEI micrographs of solder joints for as-soldered condition.................... 39
4.14 BEI micrographs of solder joints for as-soldered condition (2).............. 40
4.15 BEI micrographs of solder joints for as-soldered condition (3) 41
4.16 AFPB shear strength of as-soldered solder joints.................................. 41
4.17 BEI micrographs showing microstructure evolution of SAC305 aged at 150°C 43
4.18 BEI micrographs showing microstructure evolution of SC-0.01Ni-0.1Co-1In aged at 150°C.. 44
4.19 BEI micrographs showing microstructure evolution of SC-0.01Ni-0.1Co-3In aged at 150°C.. 45
4.20 BEI micrographs showing microstructure evolution of SC-0.01Ni-0.5Co-3In aged at 150°C.. 46
4.21 BEI micrographs showing microstructure evolution of SC-0.1Ni-0.5Co-3In aged at 150°C.. 47
4.22 Summary of EDS analysis of as-soldered SC-0.1Ni-0.5Co-3In solder joint 48
4.23 Summary of EDS analysis of SC-0.1Ni-0.5Co-3In solder subjected to isothermal aging at 150°C for 1,000 hours 48

Figure Page

4.24 EPMA elemental mapping of SC-0.1Ni-0.5Co-3In solder joint before isothermal aging 50
4.25 EPMA elemental mapping of SC-0.1Ni-0.5Co-3In solder joint after subjected to isothermal aging at 150˚C for 250 hours........ 50
4.26 EPMA elemental mapping of SC-0.1Ni-0.5Co-3In solder joint after subjected to isothermal aging at 150˚C for 1,000 hours........ 51
4.27 Schematic of IMC-layer structure at the interface of a) SAC and b) SC-Ni-Co-In solder joint 51
4.28 Cu_3Sn Thickness as a function of time of solder joints aged at 150°C.... 53
4.29 Cu_6Sn_5 Thickness as a function of time of solder joints aged at 150°C .. 54
4.30 Total intermetallic compound thickness as a function of time of solder joints aged at 150°C 54
4.31 Cu_3Sn thickness as a function of square root time of the solder joints aged at 150°C........ 55
4.32 AFPB shear test results of SC-Ni-Co-In solder joints showing maximum shear strength as a function of aging time, SAC305 also shown as baseline 56
4.33 AFPB shear test results of SAC solder joints showing maximum shear strength as a function of aging time 57
4.34 Load-displacement curves of solder joints aged at 150°C for 1,000 hours........ 57
4.35 Illustrations of shear failure mode observed in AFPB shear test............ 58

CHAPTER I
INTRODUCTION

1.1 Background

Solder alloys for electronic applications have major effects on reliability of packaged devices. Pb-containing solder alloys have been widely used in electronic industries for decades. However, due to the toxicity of lead, worldwide restrictions were posted on electronics manufacturers to completely eliminate lead-containing solder alloys from the electronic assembly. As a consequent, advance in lead-free technology has been brought forward. Several lead-free solder alloy compositions have been proposed but still no solder alloys were considered a drop-in substitute for the conventional Pb-containing alloys. Alternative Sn-Ag-Cu (SAC) solder alloys have been widely accepted to be the first candidate. However, due to price fluctuation of Ag, most manufacturers are moving toward Sn-Cu solder alloys. Despite of lower cost, Sn-Cu solder alloys have inferior mechanical properties and higher melting point than those of Ag-containing alloys.

The focus of this research project is to improve the microstructural and mechanical properties of the eutectic Sn-Cu solder alloys by additions of nickel, cobalt and indium. Cobalt and nickel have been reported to cause microstructural changes in tin solder such as the formation of various intermetallic compounds (IMCs), enhanced heterogeneous nucleation which could result in grain refinement effect, and the change in thermal properties such as the suppression of undercooling [1-3]. For indium addition, it is known that the melting behavior of the tin-based alloys can be altered to favor the lowering of liquidus and solidus temperatures. Moreover, the addition of indium refines the tin-rich phase and unifies the distribution of IMCs [4-7]. However, further investigation is necessary to examine the effects of these alloy additions.

Key properties for soldering of new solder alloys need to be characterize. In this study melting behavior, solidification behavior, wettability, electrical

resistivity, microstructures and mechanical properties were characterized. The temperature profile of reflow soldering in surface-mount assembly was simulated to produce realistic joint microstructures. Four temperature profiles were used to produce solder joints to find proper soldering time and temperature for these new solder alloys.

1.2 Objective of Research

To study microstructures, mechanical properties and electrical properties of Sn-Cu-Ni-Co-In solder alloys and to find the appropriate amount of alloying elements and reflow soldering condition for the solder alloys

1.3 Scopes of Research

In this study, the effects of Ni, Co and In additions where the amounts of Ni, Co and In are not more than 0.1, 0.5 and 3 wt.%, respectively. The amount of Cu is fixed at 0.7wt.%. The pure elements are weighted and melted to produce solder alloys by electric arc melter machine under argon atmosphere. The solder alloys are made into solder joints by joining two copper blocks under soldering temperature/time of 230°C/30s, 240°C/45s, 245°C/60s and 260°C/120s. The solder joints are subjected to thermal aging at 150°C for 1,000 hours. Microstructures are studied by scanning electron microscope, x-ray diffractometer and electron probe micro-analyzer. Mechanical properties are measured by asymmetrical four-point bending method and micro-Vickers hardness measurement. The electrical properties are studied by electrical resistivity measurement of solder alloys using four-point probe method.

1.4 Advantages of Research

1.4.1 This research provides better understanding of effects of Ni, Co and In on Sn-0.7Cu solder alloys.

1.4.2 This research clarifies the appropriate amount of Ni, Co and In additions to Sn-0.7Cu solder alloys.

1.4.3 This research clarifies the appropriate reflow soldering profile for Sn-Cu-Ni-Co-In solder alloys.

CHAPTER II
LITERATURE SURVEY

2.1 Development of lead-free solder alloys

The traditional Sn-Pb solder alloys have been used in electronic applications for decades because of its good properties for soldering such as low melting point, low melting range, good solderability, good mechanical properties and low cost. The compositions of these alloys are varied e.g. near-eutectic 60Sn-40Pb (melting point 190ºC), eutectic 63Sn-37Pb (melting point 183ºC) and 62Sn-36Pb-2Ag (melting point 179ºC)

Advance in lead-free technology started in 1994 after emerging of global restrictions posted on electronic manufacturers to completely eliminate the use of Pb in electronic assembly production lines. Various lead-free alloy systems were developed including binary alloys i.e. Sn-Ag, Sn-Bi, Sn-Cu, and Sn-Zn and ternary alloys i.e. Sn-Ag-Cu, Sn-Ag-Bi and Sn-Bi-Zn. Although several new solder alloy compositions were proposed, no one has been considered a “drop-in” substitute for the conventional lead-containing alloys due to many inferior properties for soldering such as high melting point, solderability and microstructural stability.

The project of National Center for Manufacturing Science (NCMS) for development of candidate Pb-free alloys has created the pass-fail criteria for the alloys shown in Table 2.1 [8]. The criteria intended to illustrate limitation on soldering profiles and peak soldering temperature, acceptable level on thermomechanical fatigue life and creep strength, wettability and oxidation resistance of the alloys

Table 2.1 Pass-Fail Criteria used by the NCMS Pb-Free Solder Project [8]

Solder Property	Definition	Acceptable Levels
Liquidus Temperature	Temperature at which solder alloy is completely molten.	< 225°C
Pasty Range	Temperature difference between solidus and liquidus temperatures; temperature range where the alloy is part solid and part liquid.	< 30°C
Wettability	A wetting balance test assesses the force resulting when a copper wire is immersed in and wetted by a molten solder bath. A large force indicates good wetting, as does a short time to attain a wetting force of zero and a short time to attain a value of two-thirds of the maximum wetting force.	$F_{max} > 300\ \mu N$ $t_0 < 0.6$ s $t_{2/3} < 1$ s
Area of Coverage	Assesses the coverage of the solder on Cu after a typical dip test.	>85% coverage
Drossing	Assesses the amount of oxide formed in air on the surface of molten solder after a fixed time at the soldering temperature.	Qualitative scale
Thermo-mechanical Fatigue	Cycles-to-failure for a given percent failed of a test population based on a specific solder-joint and board configuration, compared to eutectic Sn-Pb.	Some percentage, usually > 50%
Coefficient of Thermal Expansion (CTE)	Thermal expansion coefficient of the solder alloy is the fraction change of length per °C temperature change. Value used for comparison was CTE of solder alloy at room temperature.	$< 2.9 \times 10^{-5}$/°C
Creep	Stress required at room temperature to cause failure in 10,000 minutes.	> 3.4 MPa
Elongation	Total percent elongation of material under uniaxial tension at room temperature.	>> 10%

2.2 Reflow soldering process [9]

Reflow soldering is one of the soldering methods commonly used in electronic assemblies to join surface mount components to a printed circuit board. In the process, mixture of solder ball and flux or solder paste is used to hold electrical components on the circuit board usually by stencil printing. The assembly is then conducted into reflow oven given a temperature profile which starts flux activation and melts the solder to create solder joints under a nitrogen atmosphere. A typical example of reflow temperature profile for eutectic Sn-Pb solder alloy is shown in Fig.2.1. There are four sections of their own proposes in the reflow temperature profile i.e. preheat, dryout, reflow, and cooling.

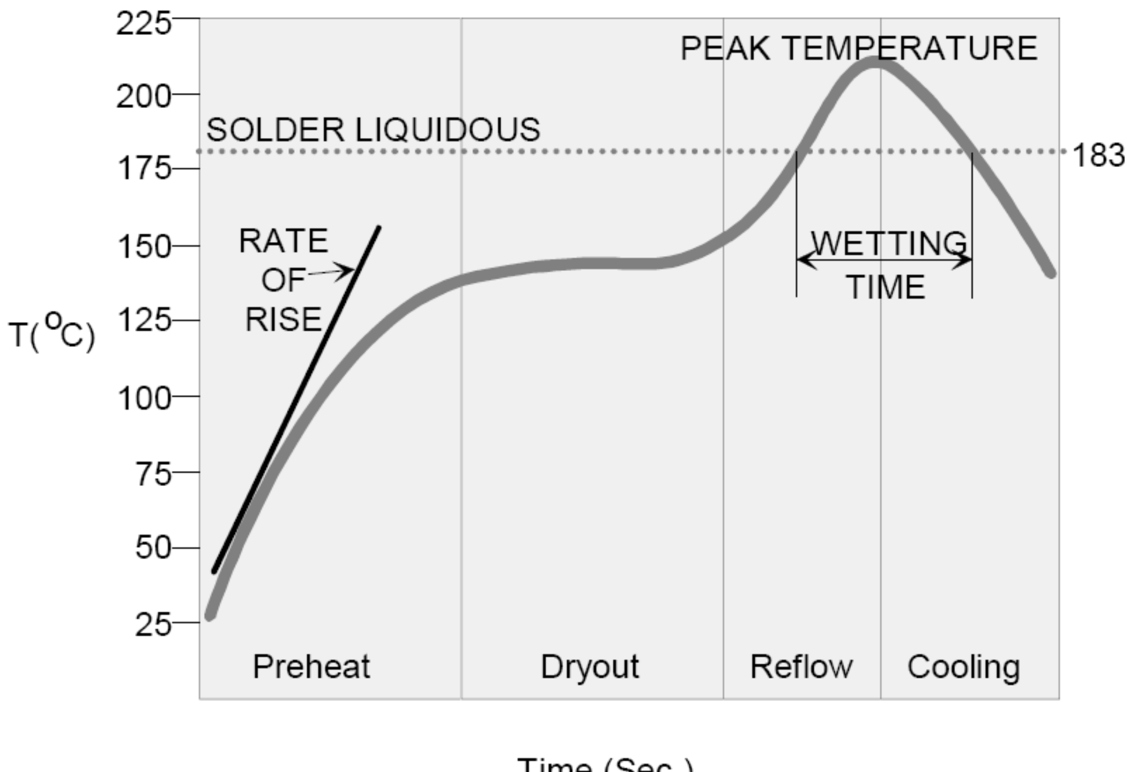

Fig 2.1 Typical reflow soldering temperature profile of 63Sn-37Pb solder [9]

Preheat

In this stage, the assembly is given a controlled heating rate usually between 1-4ºC/second. The temperature is raised up to 100-150ºC just below the flux activation temperature. The control of heating rate is the major concern because excessively fast heating rate produces thermal shock to some electronic components which susceptible to thermal cracking such as multilayer ceramic chip capacitors. Moreover, too fast heating rate may cause paste spatter.

Dryout

In this dryout stage, also known as soak or preflow stage, the temperature is hold consistently between 150-170ºC for a period of 60-120 second. The primary aims of the dryout stage is 1) to fully dry the solder paste before heating up to reflow, 2) to stabilize the temperature throughout the entire assembly, and 3) to serve as flux activation stage where flux reacts to clean the oxide surface.

Reflow

The reflow temperature stage provides a rapid rise in temperature to higher than the melting point of the solder paste where the solder paste reflows and wets to form solder joint between components and printed circuit board. The given peak temperature is generally 20ºC above the melting point. The wetting time refers to the length of time that the temperature is above the melting point which, for most solder paste, is between 30-60 second. Excessive wetting time or temperature may produce intermetallic growth which embrittles the solder joint.

Cooling

The final stage gives the assembly a cooling rate between 4-8ºC/second. The cooling rate is critical to the quality of the solder joint. Excessively slow cooling rate produces large Sn grains in the microstructure which weaken to solder joint. Rapid cooling rate may cause thermal crack to some electronic components

2.3 Effects of Ni and Co additions on Sn-based solder alloys

At temperature above 50ºC, reaction between Sn and Cu can form two intermetallic compounds including Cu_6Sn_5 and Cu_3Sn. Kirkendall void forms along with formation of Cu_3Sn at the interface between Cu_3Sn and Cu as shown in Fig.2.2. This Kirkendall void formation is resulted from faster diffusion coefficient of Cu than Sn in the Cu_3Sn layer. This void can cause brittle fracture in solder joint [10]. Luhua Xu and John H.L. Pang [11] found that growth of Kirkendall void weaken the solder joint and the fracture surface of impact test changes its position from intermetallic compound to solder interface.

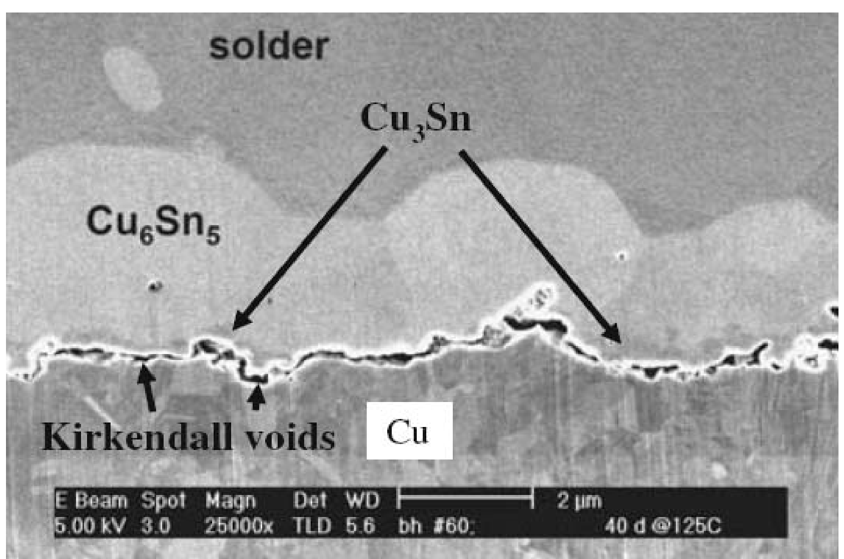

Fig.2.2 Backscattering electron image shows Kirkendall voids found in Cu_3Sn layer after aging at 140ºC for 40 days [12]

In order to suppress Kirkendall void formation, Hume-Rothery criteria is used to select alloying elements that can substitute Cu atoms in Cu_6Sn_5 and Cu_3Sn intermetallic compounds to produce lattice strain result in reduced vacancy diffusion which is the main diffusion mechanism of Cu-Sn interdiffusion. The element that could substitute Cu atom are Si, Ti, Cr, Mn, Ni, Ge, Cu, Fe and Zn. A study revealed that addition of 0.1wt.% Ni in Sn-3.5Ag can effectively suppress the growth of Cu_3Sn layer in as-soldered condition and after thermal aging as shown in Fig. 2.3 [13].

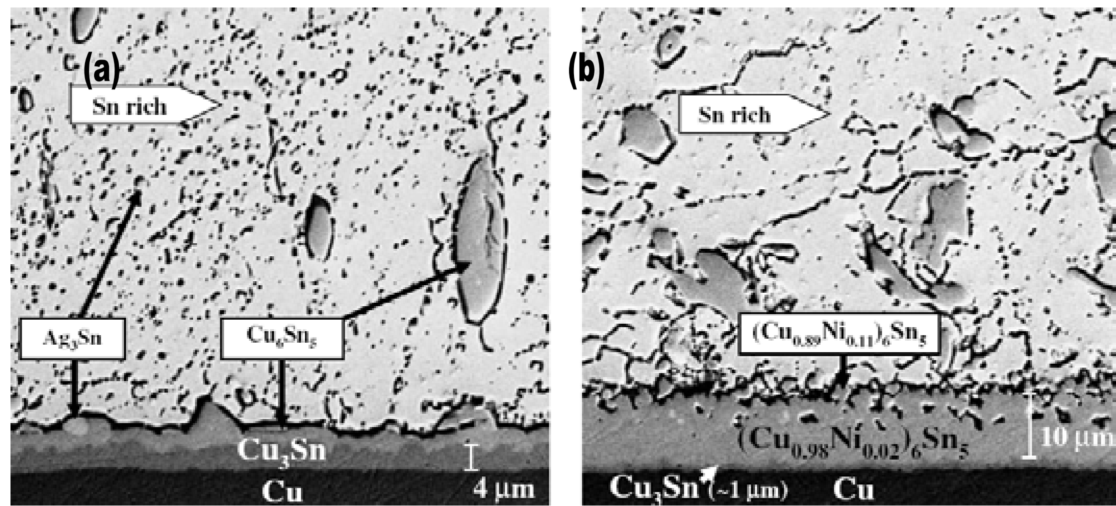

Fig.2.3 Backscattering electron image showing the interface of Sn-3.5Ag/Cu (a) and Sn-3.5Ag-0.1Ni/Cu (b) subjected to thermal aging at 150ºC for 1,000 hours [13]

Shear strength test of Sn-Ag-Cu + Co/Cu solder joint after thermal aging at 150ºC for 1,000 hours exhibit ductile fracture surface [14]. Wavelength dispersive x-ray spectroscopy found segregation of Co in Cu_6Sn_5 and Cu_3Sn [15].

Microstructure after thermal aging of Sn-based solder alloys showed that additions of Ni and/or Co could reduce Cu_3Sn growth as shown in Fig.2.4. However Ni and Co increase the thickness of Cu_6Sn_5 layer [14,16].

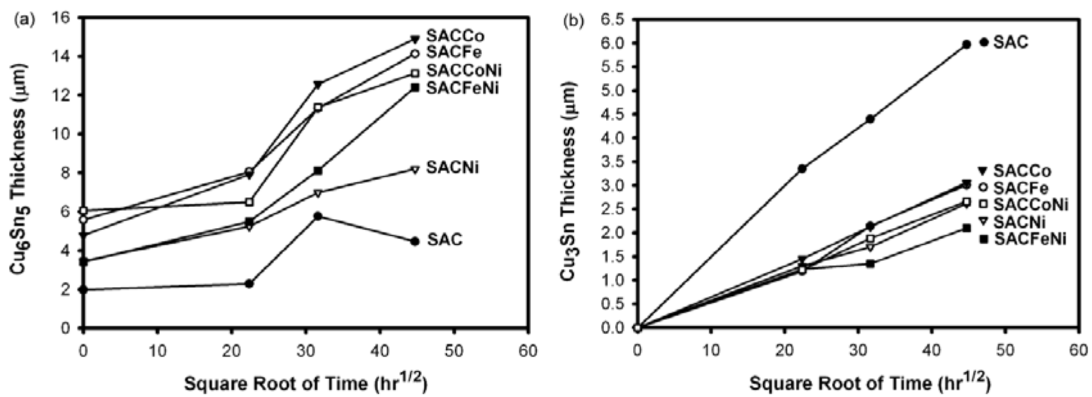

Fig.2.4 Thickness of intermetallic compound layer after thermal aging at 160ºC a) Cu_6Sn_5 (b) Cu_3Sn [16]

Although Ni and/or Co additions can suppress Cu_3Sn growth which is the cause of Kirkendall void formation, both elements effect in increase of Cu_6Sn_5 growth which can produce brittle solder joint. For this reason, effects of these elements on impact resistance of solder joint were tested.

Impact strength test results of Sn-Ag-Cu+X solder alloys where X= Si, Co, Ti, Cr, Mn, Ni, Zn and Ge are shown in Fig.2.5 [17]. Sn-Ag-Cu+Ni and Sn-Ag-Cu+Co exhibit the best impact strength among others in as-soldered condition and after-aging condition as shown in Fig.2.6.

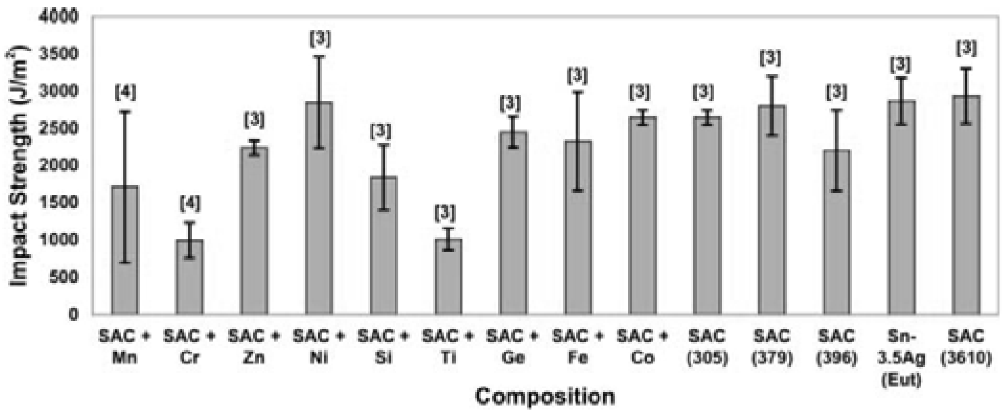

Fig. 2.5 Impact strength of Sn-Ag-Cu+X solder alloys [17]

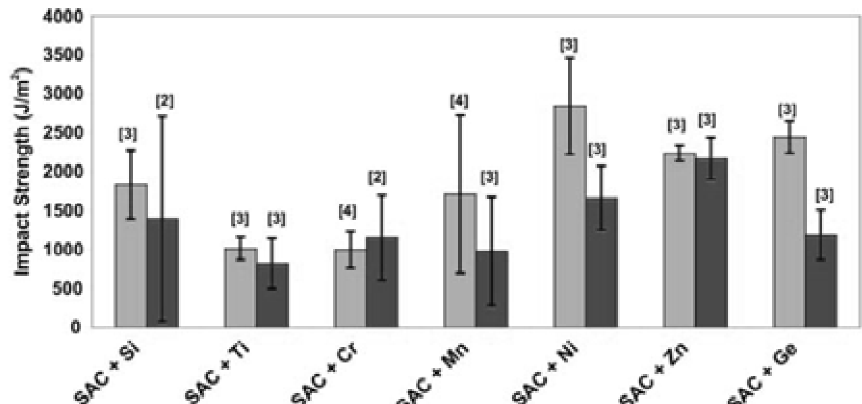

Fig. 2.6 Impact strength of Sn-Ag-Cu+X solder alloys where lighter bars are values of as-soldered joint and darker bars are values of joint subjected to thermal aging for 1,000 hours [17]

2.4 Effects of In addition on properties of Sn-based solder alloys

Solidus and liquidus temperatures of Sn-Ag-Cu+In solder alloys were measured using differential scanning calorimeter (DSC) [4]. The result in Fig.2.7 shows that addition of In in Sn-0.3Ag-0.7Cu could effectively lower the solidus and liquidus temperatures. For the alloy with 3wt.% In, the solidus and liquidus are lower than those of Sn-0.3Ag-0.7Cu for 21.7°C and 11.5°C, respectively. However, the melting range increases with the amount of In.

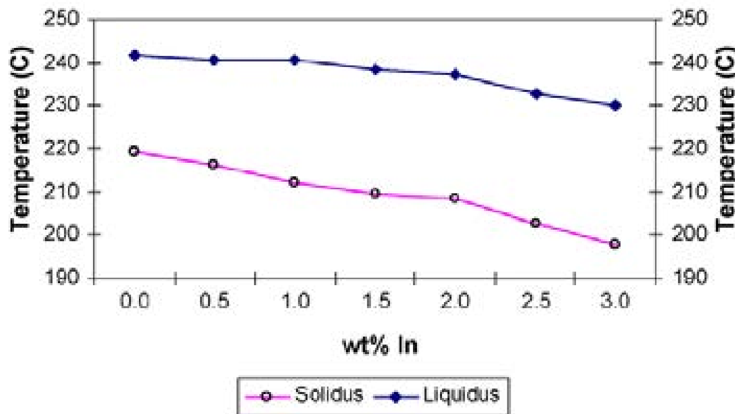

Fig.2.7 Effects of In addition on solidus and liquidus temperature of Sn-3.0Ag-0.7Cu solder alloy [4].

Wetting time and wetting force of Sn-3.0Ag-0.7Cu+XIn were measured using wetting balance tester where copper sheets were immerged in solder bath at 250°C. Schematic of wetting balance test is shown in Fig.2.8.

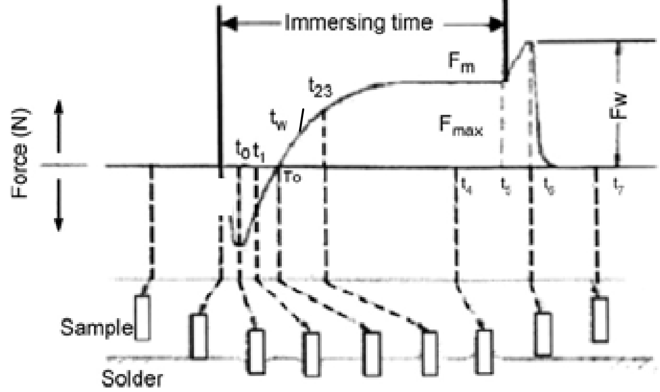

Fig.2.8 Schematic of wetting curve obtained from wetting balance test [4]

The wetting time and wetting force of solder alloys are shown in Fig. 2.9. The experimental results indicate that addition of In results in reduced wetting time and increased wetting force of the solder alloys with Cu sheet. The wetting time and wetting force are 2.1 s and 5.2 mN, respectively, for Sn-0.3Ag-0.7Cu with no In addition. When 3 wt.% In was added, wetting time was reduced to 1.1 s and wetting force increased to 7mN.

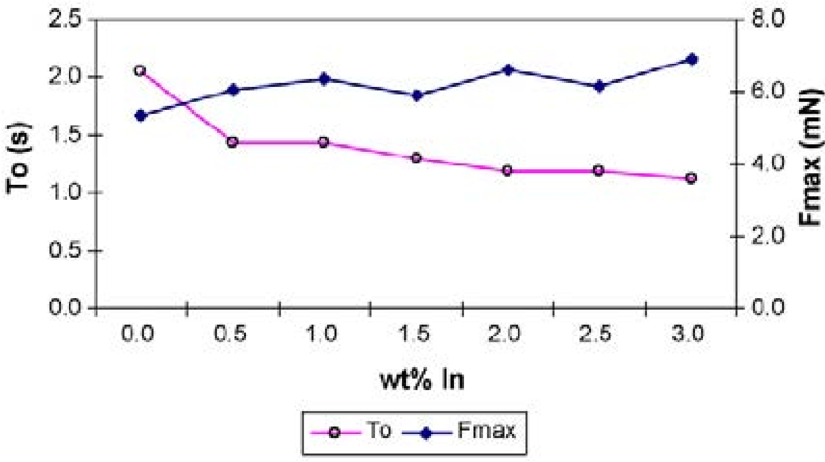

Fig. 2.9 Wetting time and wetting force of Sn-0.3Ag-0.7Cu+XIn solder alloys [4]

Fig. 2.10 shows tensile strength and micro-Vickers hardness of Sn-0.3Ag-0.7Cu+XIn solder alloys [4]. The tensile strength and hardness increase with amount of In. Sn-0.3Ag-0.7Cu with no In addition show tensile strength of 31.86 MPa. When 3wt.% In was added, the tensile strength of Sn-0.3Ag-0.7Cu-3In increased to 56.89 MPa.

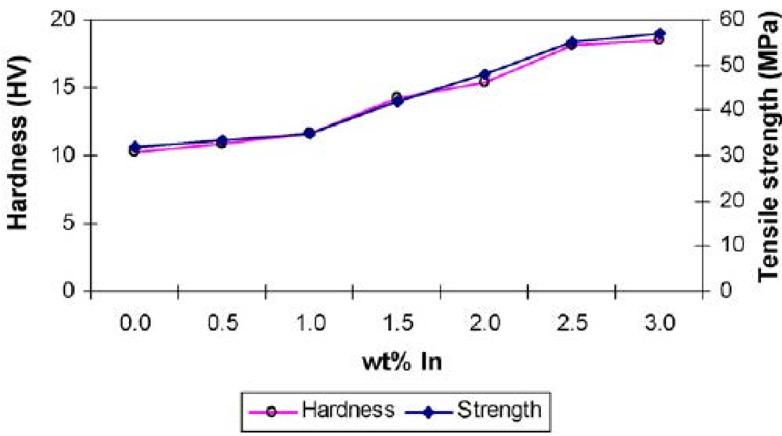

Fig. 2.10 Tensile strength and microhardness of Sn-0.3Ag-0.7Cu-XIn solder alloys [4]

The increase in tensile strength and microhardness of the Sn-0.3Ag-0.7Cu+XIn solder alloys can be described by their microstructures. It can be seen in Fig. 2.11 that Sn-rich phase is the base microstructure of Sn-0.3-Ag-0.7Cu surrounded by intermetallic compounds of Sn, Ag and Cu such as Cu_6Sn_5, Cu_3Sn and Ag_3Sn. Fig. 2.12 shows image captured by scanning electron microscope of the alloy. Fig. 2.13-2.15 show distribution of Sn, Ag and Cu, respectively.

The solder alloys with addition of In show smaller Sn-rich phase and more uniformly distribution of intermetallic compounds. Microstructure of Sn-0.3Ag-0.7Cu-1.5In is shown in Fig. 2.16. Sn, Ag, Cu and In elemental distribution of this solder alloy is shown in Fig. 2.17-2.20, respectively. Microstructure of Sn-0.3Ag-0.7Cu-3In is shown in Fig. 2.21. Sn, Ag, Cu and In elemental distribution of this solder alloy is shown in Fig. 2.22-2.25, respectively. It can be seen that more In addition leads to smaller Sn-rich phase and more uniformly distribution of intermetallic compounds. The refined and uniform microstructures of these Sn-0.3Ag-0.7Cu-XIn solder alloys are caused by adsorption phenomenon of In [4].

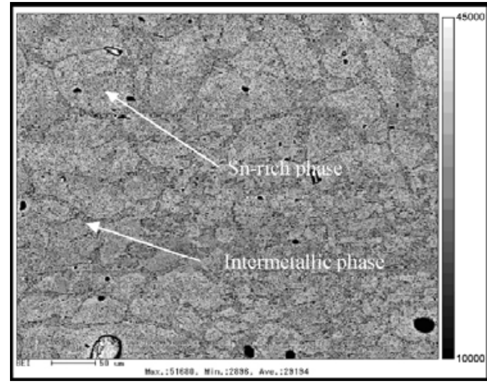

Fig.2.11 Microstructure of Sn-0.3Ag-0.7Cu [4]

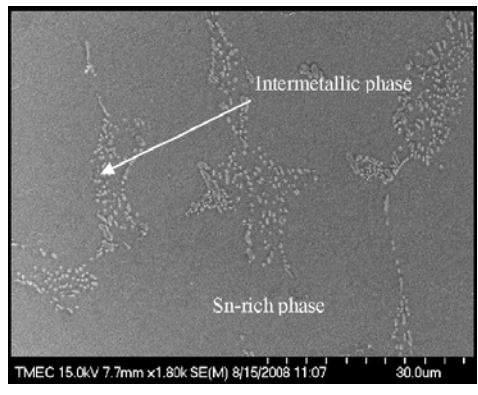

Fig.2.12 SEM image of Sn-0.3Ag-0.7Cu [4]

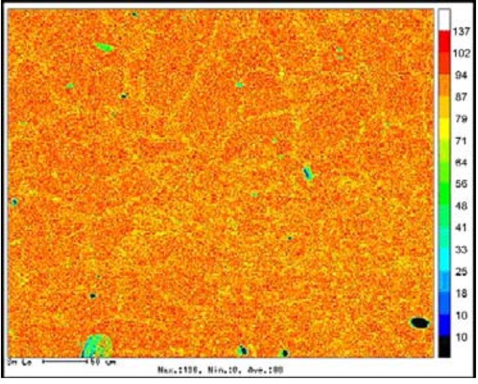

Fig.2.13 Sn distribution in Sn-0.3Ag-0.7Cu [4]

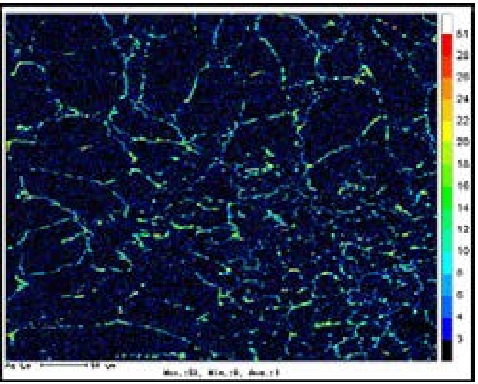

Fig.2.14 Ag distribution in Sn-0.3Ag-0.7Cu [4]

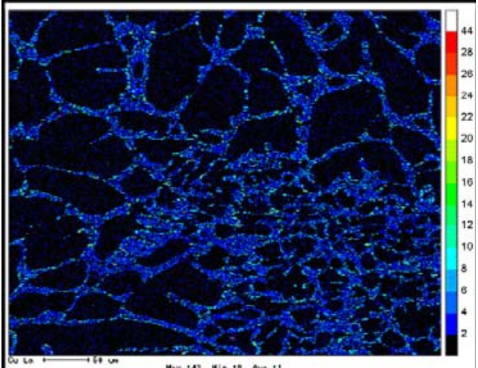

Fig.2.15 Cu distribution in Sn-0.3Ag-0.7Cu [4]

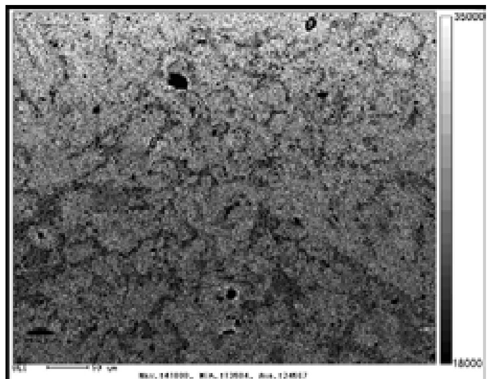

Fig.2.16 Microstructure of Sn-0.3Ag-0.7Cu-1.5In [4]

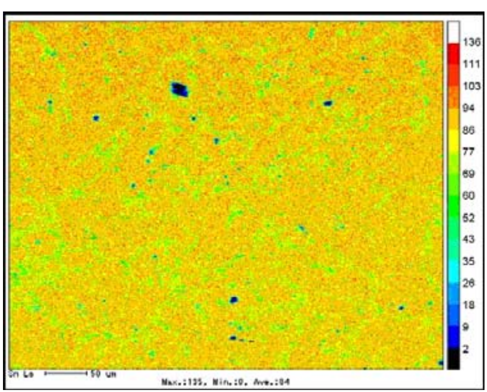

Fig.2.17 Sn distribution in Sn-0.3Ag-0.7Cu-1.5In [4]

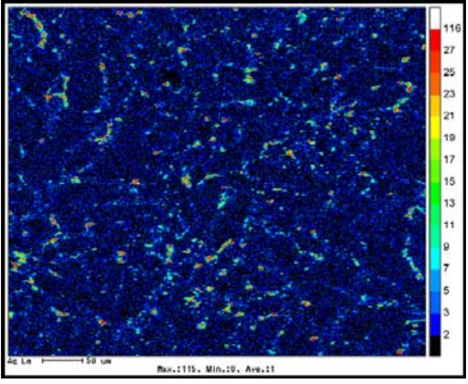

Fig.2.18 Ag distribution in Sn-0.3Ag-0.7Cu-1.5In [4]

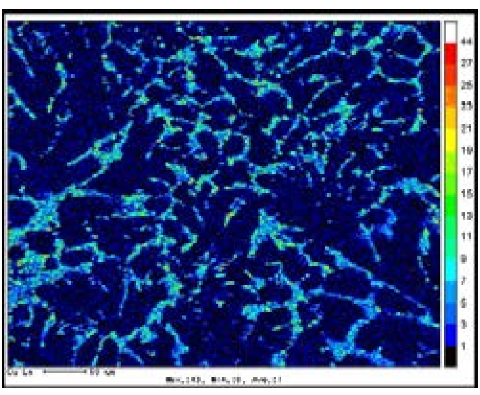

Fig.2.19 Cu distribution in Sn-0.3Ag-0.7Cu-1.5In [4]

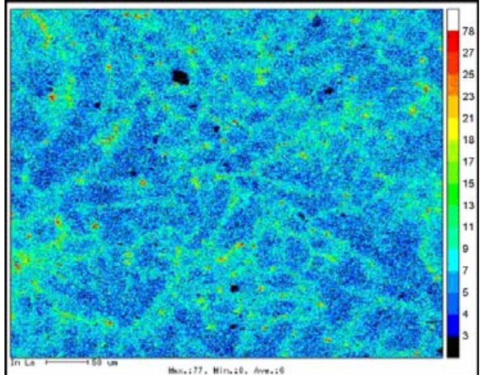

Fig.2.20 In distribution in Sn-0.3Ag-0.7Cu-1.5In [4]

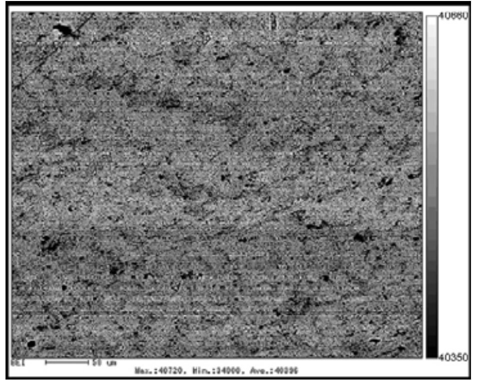

Fig.2.21 Microstructure of Sn-0.3Ag-0.7Cu-3In [4]

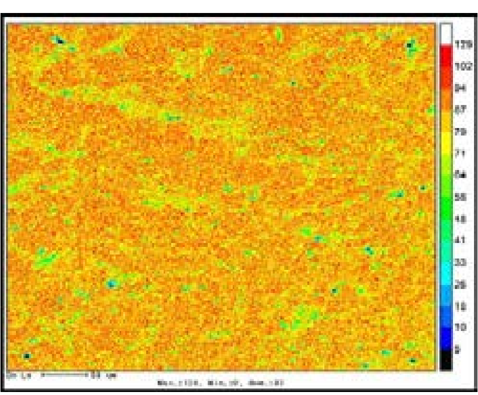

Fig.2.22 Sn distribution in Sn-0.3Ag-0.7Cu-3In [4]

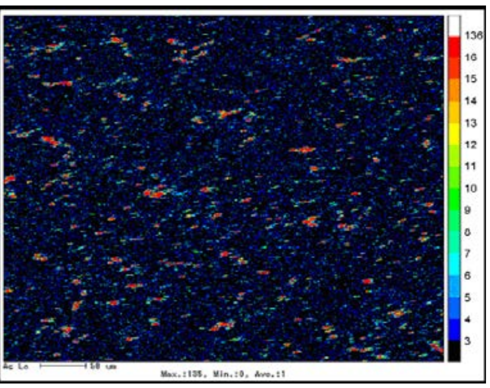

Fig.2.23 Ag distribution in Sn-0.3Ag-0.7Cu-3In [4]

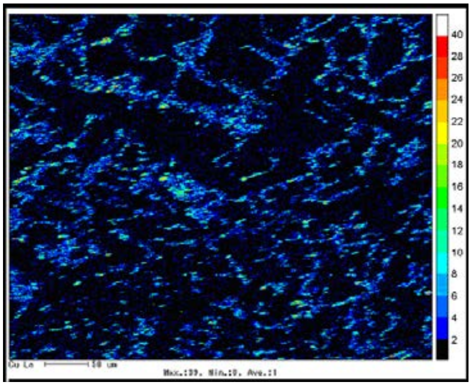

Fig.2.24 Cu distribution in Sn-0.3Ag-0.7Cu-3In [4]

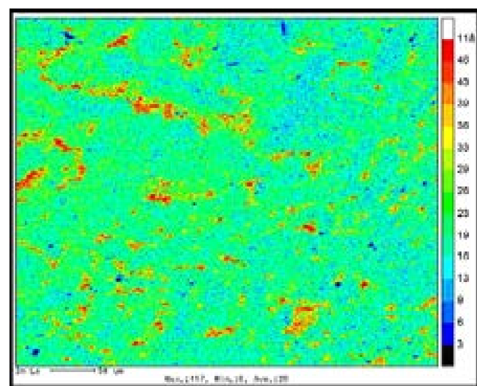

Fig.2.25 In distribution in Sn-0.3Ag-0.7Cu-3In [4]

CHAPTER III
EXPERIMENTAL PROCEDURES

3.1 Sample preparation

Solder alloys were prepared with pure metals and master alloys i.e. Sn (99.9 wt.% purity), Cu (99.99 wt.% purity), Sn-Ni master alloy (1 wt.% Ni, 99.95 wt.% purity), Sn-Co master alloy (1 wt.% Co, 99.95 wt.% purity) and In (99.99 wt.% purity). Pure metals and master alloys were weighted and melted together into ingots in an argon atmosphere by electric arc melter machine. The designed compositions and conventional alloys examined in this study are listed in Table 3.1. The solder alloy compositions were verified using inductively coupled plasma atomic emission spectroscopy (ICP-AES) (see Appendix A).

3.2 Observation of melting and solidification behavior

Before production of solder joints, differential scanning calorimeter (DSC) was performed to observe melting range, melting and solidification behavior of the solder alloys. The solder alloys were heated from 25ºC to 240ºC, hold for 10 minutes and cooled down to 25ºC with a heating rate and cooling rate of 10ºC/min. Each solder alloy was subjected to the heat cycle twice. The melting and solidification behavior results were taken form second heat cycle so that microstructural effects were eliminated.

3.3 Measurement of wetting characteristics

Wetting characteristics of the alloys was measured by spread test in which the solder alloys were cut into 1-gram pieces and then placed on copper sheet covered with flux. The copper sheet was attached with thermocouple to measure the actual temperature. The assembly used for spread area test is shown in Fig.3.1. The assembly was then placed in a furnace given a maximum temperature of 250ºC. After isothermal holding at 250ºC for two minutes, the solder alloys melted and spread out on the copper sheet as shown schematically in Fig.3.2. The flux used in this experiment

was Amtech NC-559-AS no-clean flux. The copper sheet used in this experiment was prepared using 1%Nital etched and subsequent cleansed with ethanol. The spread areas were observed from top view optical images as shown in Fig.3.3. Wetting angle was measured on cross-sectioned images as shown in Fig.3.4. The images were captured by a digital microscope at various magnifications. Area of spread and wetting angle measurement was carried out by SemAfore software. The experiment was performed twice to confirm the results. The results are shown as an average of two values.

Fig.3.1 Assembly used for spread test

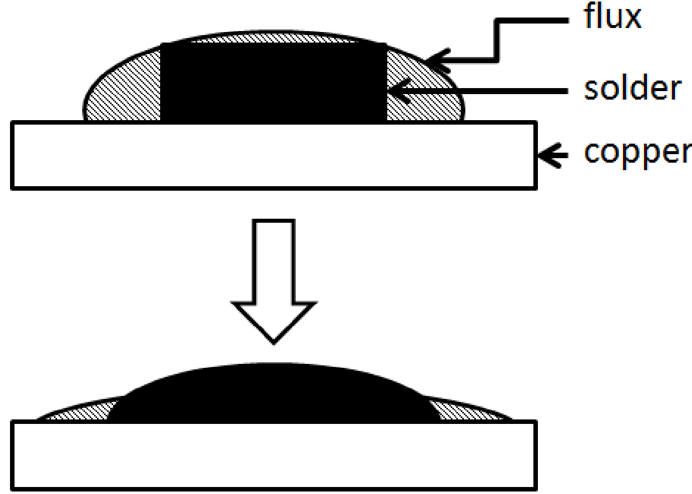

Fig.3.2 Schematic showing solder-alloy ingot spread on copper sheet in spread test

Table 3.1 Compositions of solder alloys used in this study (Conventional alloys, SAC305 and SC, were tested for result comparison)

Sample	Compositions (%)					
	Sn	Ag	Cu	Ni	Co	In
SAC305	Bal.	3	0.5	-	-	-
SC	Bal.	-	0.7	-	-	-
SC-0.01Ni	Bal.	-	0.7	0.01	-	-
SC-0.1Ni	Bal.	-	0.7	0.1	-	-
SC-0.1Co	Bal.	-	0.7	-	0.1	-
SC-0.5Co	Bal.	-	0.7	-	0.5	-
SC-1In	Bal.	-	0.7	-	-	1
SC-In	Bal.	-	0.7	-	-	3
SC-0.01Ni-0.1Co	Bal.	-	0.7	0.01	0.1	-
SC-0.01Ni-0.5Co	Bal.	-	0.7	0.01	0.5	-
SC-0.1Ni-0.1Co	Bal.	-	0.7	0.1	0.1	-
SC-0.1Ni-0.5Co	Bal.	-	0.7	0.1	0.5	-
SC-0.01Ni-1In	Bal.	-	0.7	0.01	-	1
SC-0.01Ni-1In	Bal.	-	0.7	0.01	-	3
SC-0.1Ni-3In	Bal.	-	0.7	0.1	-	1
SC-0.1Ni-3In	Bal.	-	0.7	0.1	-	3
SC-0.1Co-1In	Bal.	-	0.7	-	0.1	1
SC-0.1Co-3In	Bal.	-	0.7	-	0.1	3
SC-0.5Co-1In	Bal.	-	0.7	-	0.5	1
SC-0.5Co-3In	Bal.	-	0.7	-	0.5	3
SC-0.01Ni-0.1Co-1In	Bal.	-	0.7	0.01	0.1	1
SC-0.01Ni-0.5Co-1In	Bal.	-	0.7	0.01	0.5	1
SC-0.1Ni-0.1Co-1In	Bal.	-	0.7	0.1	0.1	1
SC-0.1Ni-0.5Co-1In	Bal.	-	0.7	0.1	0.5	1
SC-0.01Ni-0.1Co-3In	Bal.	-	0.7	0.01	0.1	3
SC-0.01Ni-0.5Co-3In	Bal.	-	0.7	0.01	0.5	3
SC-0.1Ni-0.1Co-3In	Bal.	-	0.7	0.1	0.1	3
SC-0.1Ni-0.5Co-3In	Bal.	-	0.7	0.1	0.5	3

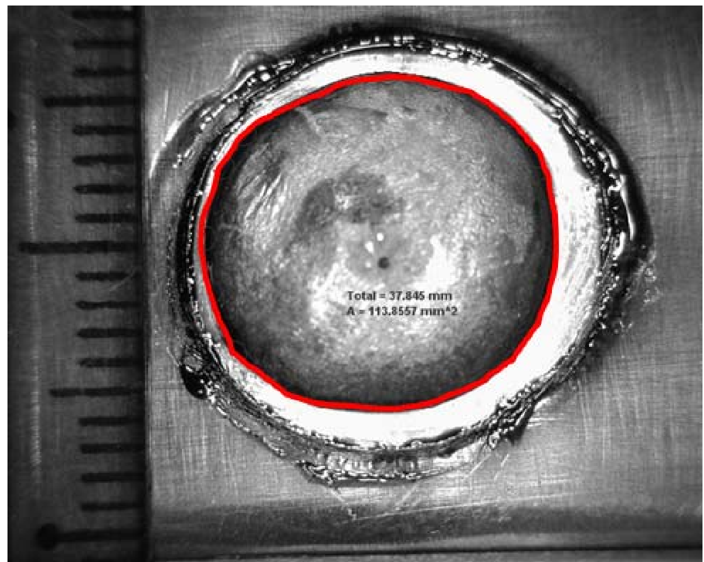

Fig.3.3 Measurement of spread area

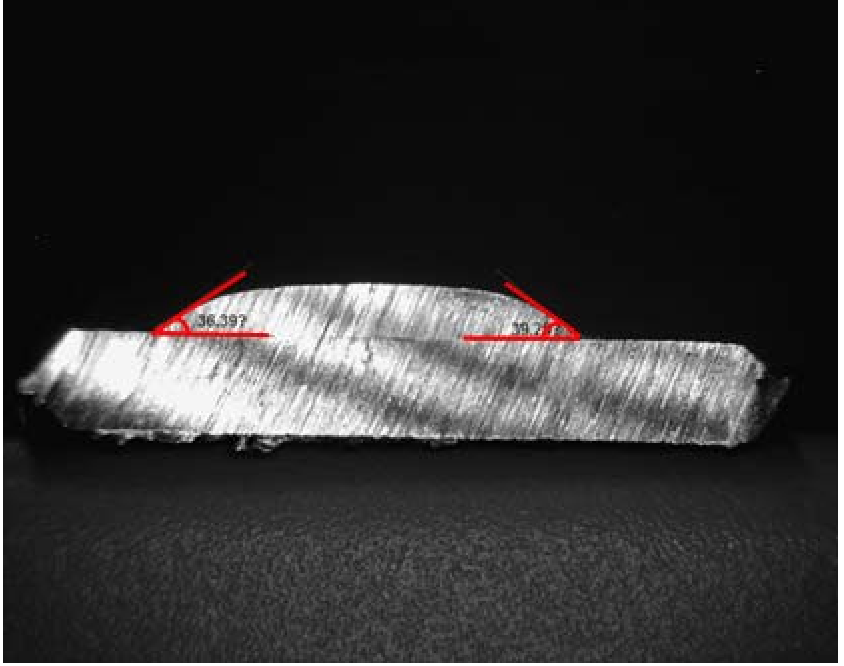

Fig.3.4 Measurement of contact angle

3.4 Measurement of electrical resistivity

The electrical resistivity (ρ) of the solder alloys was measured by DC four-point probe method at ambient temperature. The solder-alloy ingots were drawn into 1.5-mm-diameter wired samples. MCP M10-TP3005H voltage source was use to

supply DC current through iron clips located at each end of the samples. Voltage probes were made by heating 0.5-mm-diameter copper wires and put into contact with the solder wires to locally melt and embedded into them to minimize contact resistance. Agilent 34401A digital multimeter was used to measure voltage drop between each probe. The resistivity of the samples can be expressed as:

$$\rho = \frac{0.5625\pi R}{L} \qquad [3.1]$$

where L is the distance between voltage probes which was at least 30 mm in this experiment. R is the electrical resistance of the samples obtained from the slope of the V_s-I_0 plot. Where V_s is the voltage drop between voltage probes and I_0 is the DC current in the circuit. By varying I_0, each V_s-I_0 plot contains minimum of 20 data points. The wired sample and contact probes are shown in Fig.3.5. An example of V_s-I_0 plot used for sample-resistance calculation is shown in Fig.3.6.

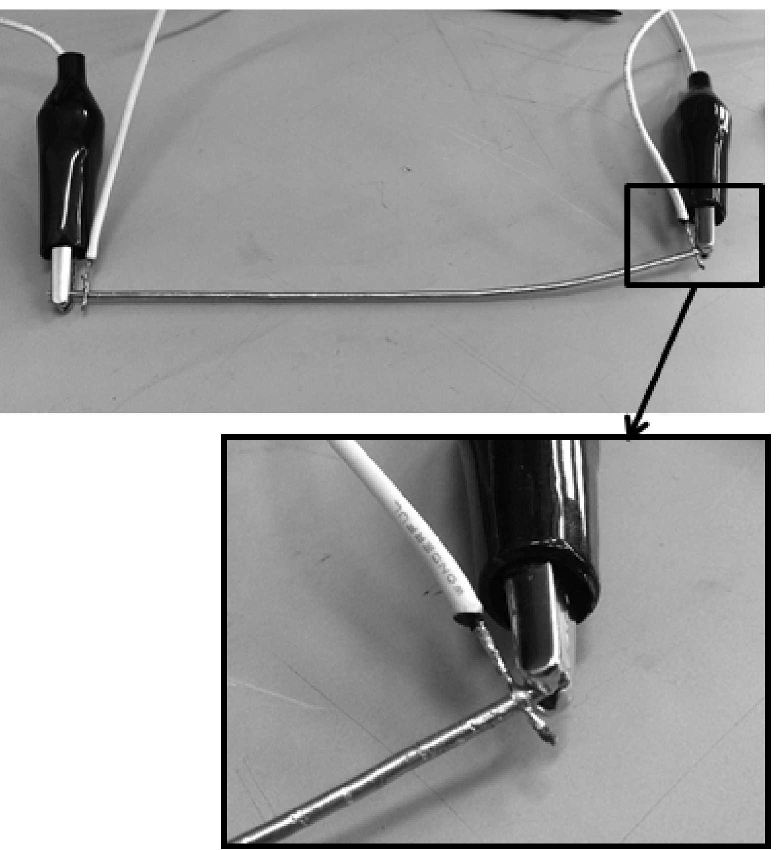

Fig.3.5 Wired sample and contact probes used for electrical resistivity measurement

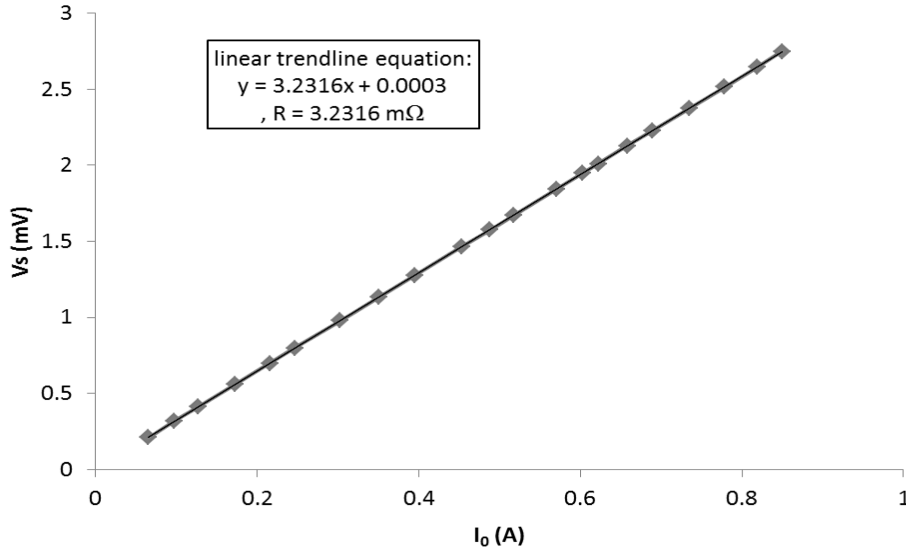

Fig.3.6 Example of V_s-I_0 plot used for resistance calculation

3.5 Solder joint production

The alloys obtained from arc melter were wire-drawn to produce 1.5 mm diameter solder wire. The temperature profile of reflow soldering in surface-mount assembly was simulated to produce joint microstructures similar to those obtained from commercial processes. Solder joints were produced by placing the solder wires between two copper blocks [18]. A stainless steel holder was used to control joint gap at as shown in Fig.3.7. Solder joint gap was controlled by inserting 200 μm between the copper blocks before screw locking. A thermocouple was attached at one end of a copper block to measure the soldering temperature. Graphite bars were used to prevent molten solder from overrunning to the steel frame. The assembly was placed on a hot plate given soldering temperature and time shown in Table 3.2. The temperature profile is recorded by computer software connected to the thermocouple by RS-485 communication cable with acquisition rate of 1 point/second. The soldering temperature is defined as peak temperature at which the assembly is hold. The soldering time is from the solder alloy start melting until it solidifies. The example of recorded temperature profile given temperature/time of 245ºC/60s is shown in Fig.3.8. After the required

soldering time was reach, the assembly was placed on huge aluminum heat sink and blew by dryer to give a typical industrial cooling rate of approximately 4-8ºC/s.

Table 3.2 Soldering conditions

Condition No.	Temperature (ºC)	Soldering Time (s)
1	235	30
2	240	45
3	245	60
4	260	120

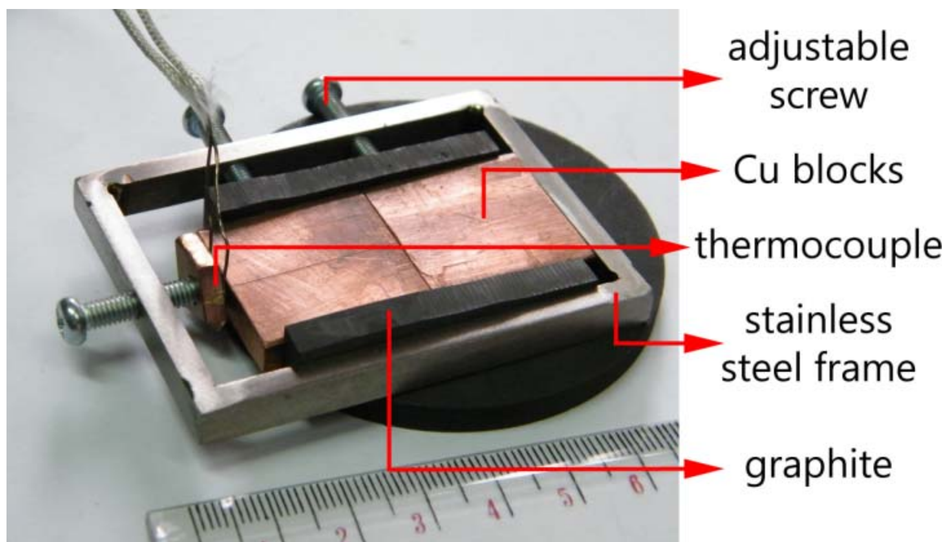

Fig.3.7 The assembly used for production of solder joint

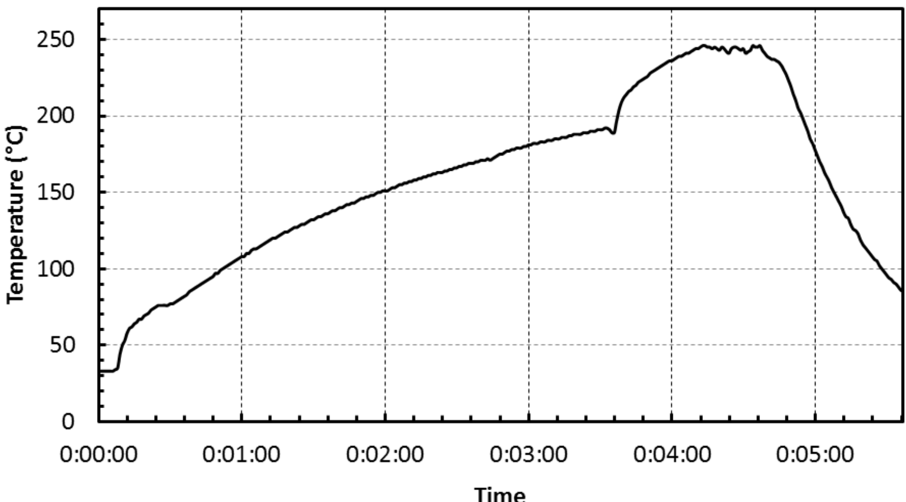

Fig.3.8 Example of recorded temperature profile of 245ºC/60s for SAC305 alloy

3.6 Metallographic examination

Solder-joint specimens were grinded with #400, #800, #1,200 and #2,000 grit sand papers followed by fine polishing with 1-μm Al_2O_3 powder. The specimens were lightly etched with 0.5%HCl in methanol for 10 sec. Microstructural observation was performed using optical microscope (OM) and scanning electron microscope (SEM) in backscattered electron mode equipped with energy dispersive x-ray spectroscopy (EDS). Electron probe micro-analysis (EPMA) was also performed to confirm the types of IMC. Thickness of IMC layers was measured using SemAfore image-digitalizer software on SEM images.

3.7 Mechanical testing

Micro-vicker hardness tests were carried out using 25-g force on the cross sections of solidified solder in the spread area test. The Vickers hardness number (VHN) was reported as an average value of at least 10 indentations.

The shear strength test was carried out by asymmetrical four point bend (AFPB) shear test method [19]. The specimens were prepared by sectioning and milling the solder blocks down to 3.2 x 4 x 40 mm bars. Bar specimens were notched along top and bottom of solder joint into 1 mm depth. The H13 carbon steel AFPB shear fixture

was shown in Fig.3.9. The loading pins were made from stainless steel and have 3 mm diameter. The fixture dimensions used is X = 4 mm and Y = 30 mm which shown satisfying result for metallic specimens. Finite element method (FEM) calculated within the linear-elastic regime shown that the shear strength was approximated by [19]:

$$\tau = \frac{F_{max}}{WH}\left[\frac{(Y-X)}{(Y+X)}\right] \qquad [3.2]$$

where, F_{max} is the maximum shear force, and W and H are the width and height of the specimen, respectively. The tests were performed at room temperature using Shimadzu EZ-S universal testing machine with a cross-head speed of 10 μm/s. The shear strength values were reported as an average value of at least 4 specimens tested. After shear test, fracture location was observed by specimen's cross-section image captured by OM.

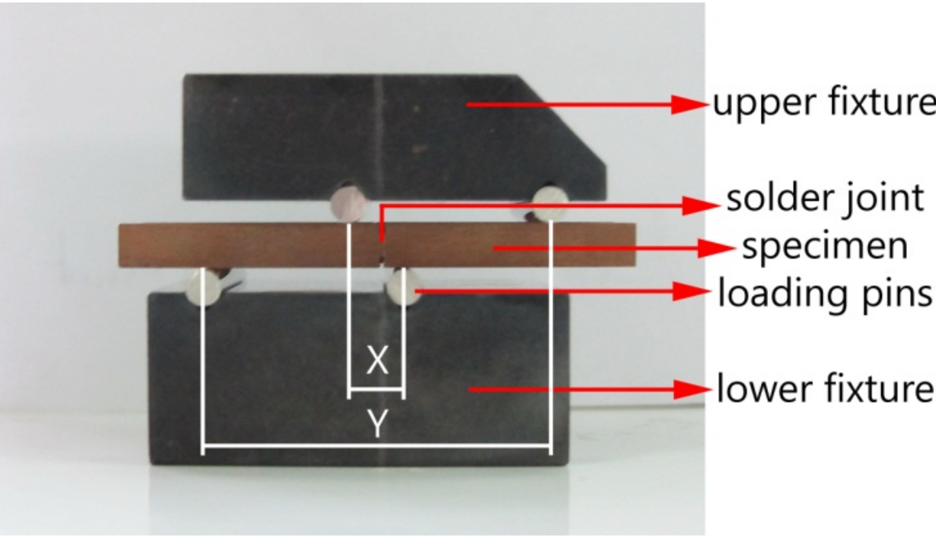

Fig.3.9 The asymmetrical four point bending shear test fixture

3.8 Isothermal aging

Bar specimens were subjected to isothermal aging at 150°C for 1,000 hours in a conventional furnace with temperature accuracy of ±5°C. Microstructures of the specimens were observed by SEM for as-soldered condition and after 250, 500, 750 and 1,000 hours aging. AFPB shear test were performed before isothermal aging and after 250 and 1000 hours.

CHAPTER IV
EXPERIMENTAL RESULTS AND DISCUSSIONS

4.1 Wettability

Wetting is very important for solder alloys because a reliable solder interconnection requires a good wetting property. There are various test methods measuring different wetting parameters in order to characterize the wettability of solder alloys. In this study, spread test was chosen because it provides fast characterization so that 28 alloy compositions can be characterized in a single experimental run. The wettability of the solder alloys was measured by spread area and wetting angle. The spread area and the wetting angle of the solder alloys are shown in Fig.4.1-4.3 and Fig.4.4-4.6, respectively. The data shows inverted relationship between spread area and wetting angel i.e. the sample with high spread area tends to have low wetting angle. It can be seen that all alloying elements affect the overall wettability by decreasing spread area and increasing wetting angle. These trends can be clearly seen in 3-D surface plot of spread area as we can see the surface slope down toward high-alloyed samples. However, the sample with 0.1wt.%Ni tends to have better wettability than those with 0.01wt.%Ni as shown in Fig.4.1 and 4.2 when 0.5wt.%Co and 3wt.%In were added, respectively. The wettability of SAC305 was the best among all solder alloys in this experiment. This indicated a positive effect of Ag addition on wettability of Sn-based solder alloys. This could be attributed the effect of Ag that improves wettability by providing better oxidation resistance [20]. For SAC305 and Sn-Cu, both alloys have more spread areas than those of Sn-Cu-Ni-Co-In alloys at 120 and 138 mm^2, respectively. Although the additions of Ni, Co and In may post a negative effect on wettability of SC solder alloys, the SC-Ni-Co-In solder alloys were ‘solderable’ by soldering method used in this research.

The influence of In addition on wettability obtained from this study exhibit opposite effect from previous study [4]. This may be due to difference in atmosphere control. Indium addition has been reported to lower oxidation resistance of solder alloys

as can be observed in severe dross formation in wave-soldering process. In this study, spread test was conducted in an ambient atmosphere. This could promotes oxide layer in molten In-containing solder alloy which worsen wettability.

In addition, the spread area is also influenced by surface tension of liquid solders which can be calculated by means of various models. One model widely approved is the Butler's method which predicts surface tension of alloys by using thermodynamic data, in particular, partial excess Gibbs energies of the components in the alloys [21].

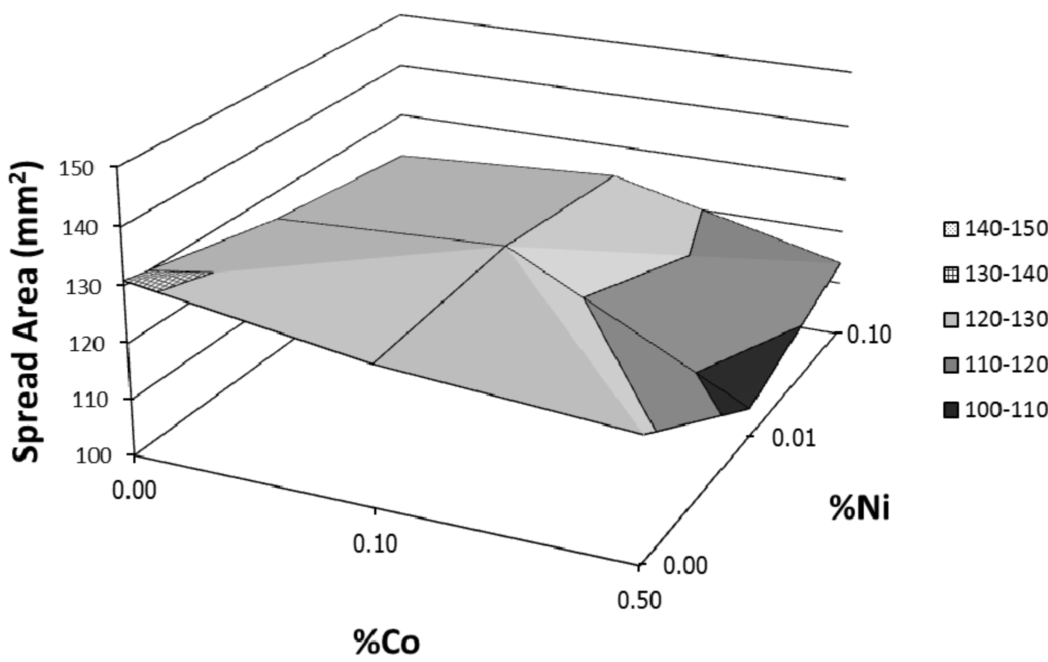

Fig 4.1 Spread-area 3-D surface of SC-Ni-Co-In solder alloys varying amounts of Ni and Co where In is fixed at 3%

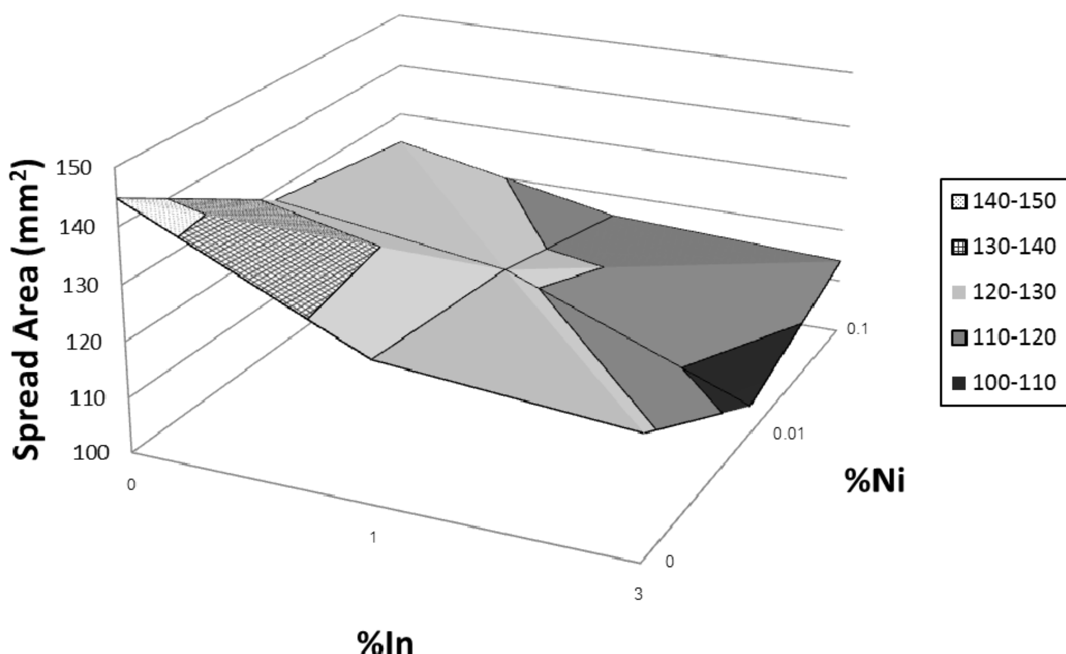

Fig 4.2 Spread-area 3-D surface of SC-Ni-Co-In solder alloys varying amounts of Ni and In where Co is fixed at 0.5%

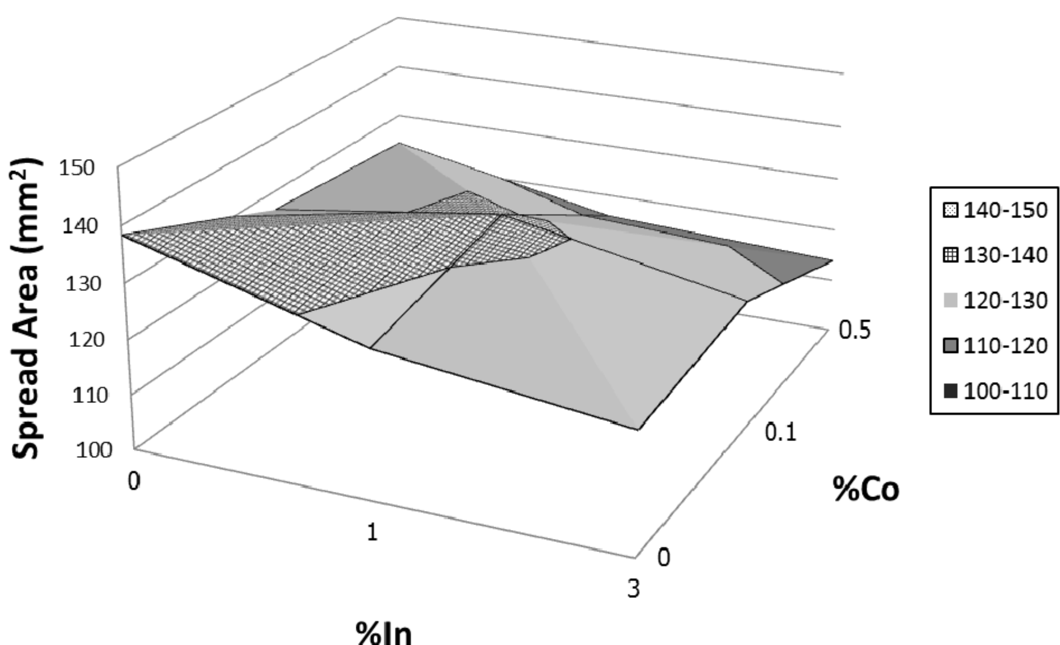

Fig 4.3 Spread-area 3-D surface of SC-Ni-Co-In solder alloys varying amounts of Co and In where Ni is fixed at 0.1%

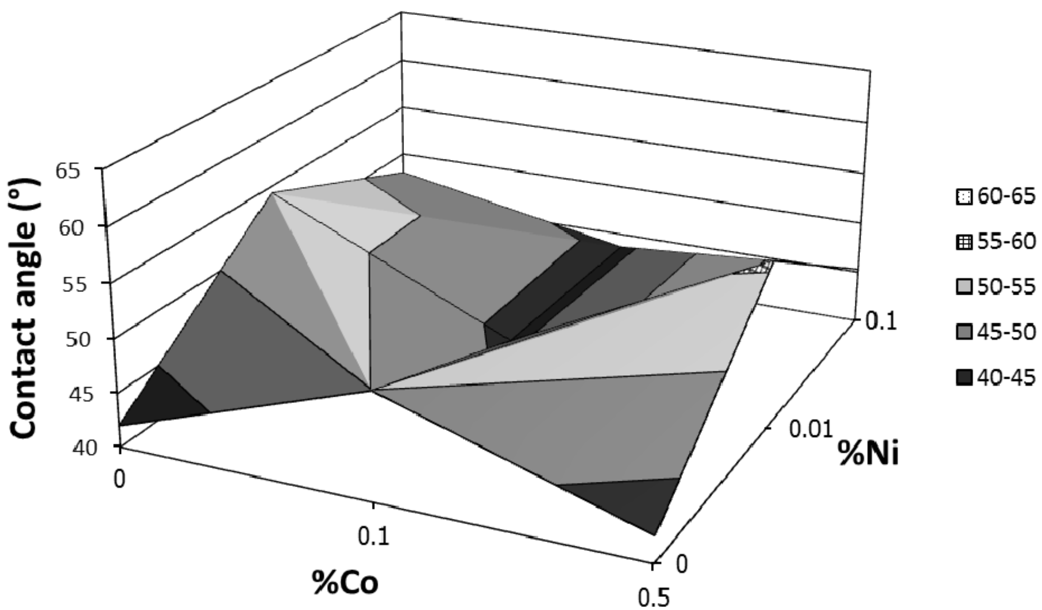

Fig 4.4 Contact-angle 3-D surface of SC-Ni-Co-In solder alloys varying amounts of Ni and Co where In is fixed at 3%

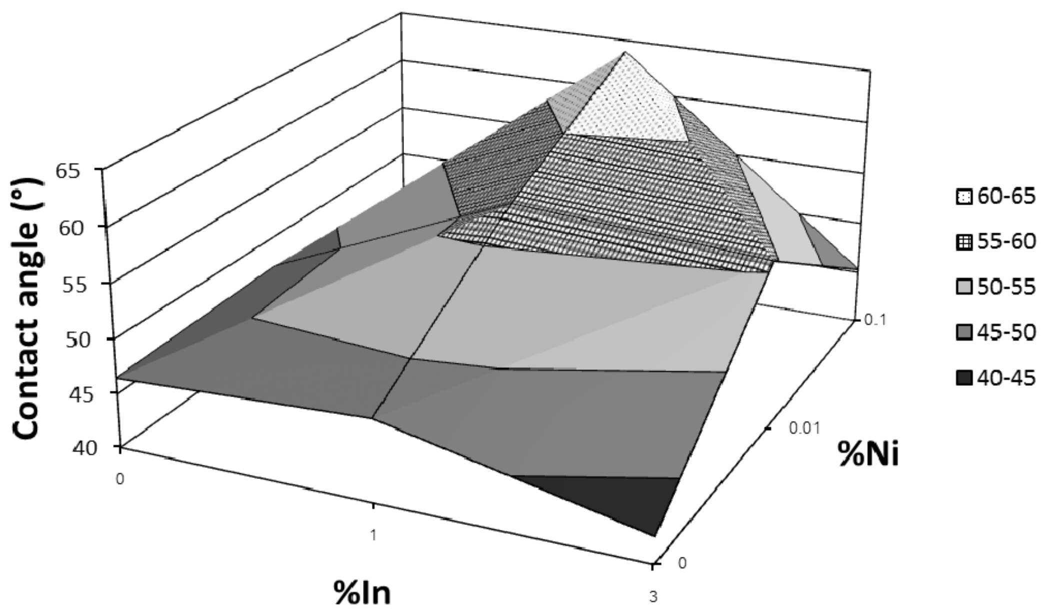

Fig 4.5 Contact-angle 3-D surface of SC-Ni-Co-In solder alloys varying amounts of Ni and In where Co is fixed at 0.5%

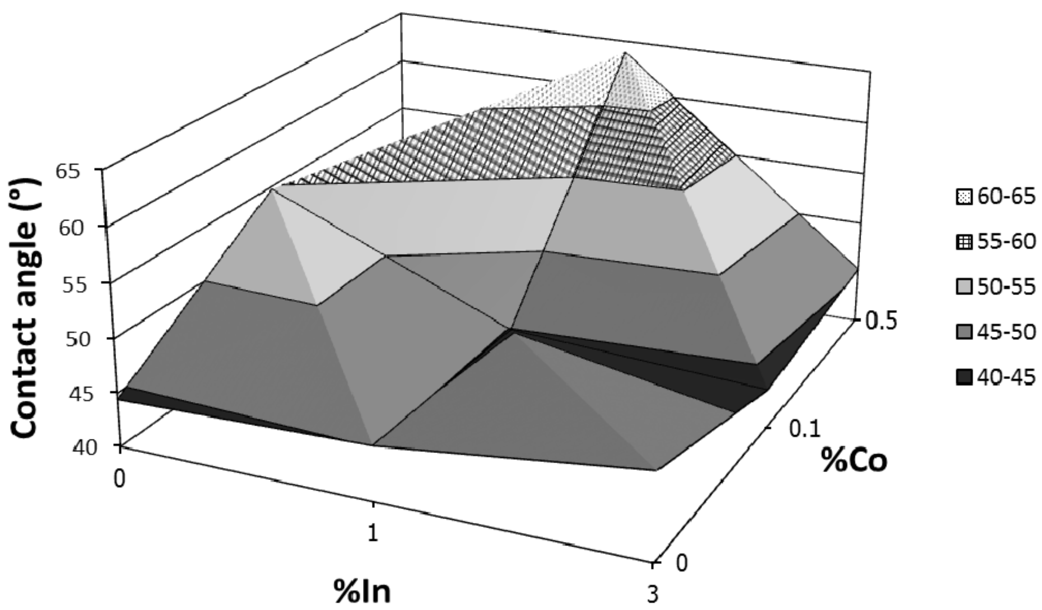

Fig 4.6 Contact-angle 3-D surface of SC-Ni-Co-In solder alloys varying amounts of In and Co where Ni is fixed at 0.1%

4.2 Melting and solidification behavior

Melting point of solder alloys is a very important aspect for soldering. In electronics, soldering essentially requires low temperature in order to prevent thermal damages to heat-sensitive components. DSC was performed to observe melting and solidification behavior of the solder alloys. In this study, the melting and solidification behavior of Sn-Cu-Ni-Co-In solder alloys were judged against the SAC305. The DSC curves are shown in Fig. 4.7. The melting and solidification behavior of the solder alloys are summarized in Table 4.1. The liquidus temperature of SC-0.01Ni-0.1Co-1In and SC-0.01Ni-0.1Co-3In were at 230ºC and 224ºC, respectively. This indicates that the addition of In can effectively decrease the liquidus temperature of Sn-Cu-Ni-Co-In solder alloys. The liquidus temperature of SC-0.01Ni-0.1Co-3In was at 224 ºC and was only 2ºC higher than that of conventional SAC305 which was at 222ºC. Apart from decreased liquidus temperature, In influence in increased solidification range because of composition shift from the eutectic. The Sn-Cu-Ni-Co-In solder alloys also show reduced undercooling

which could lead to refined microstructures. SC-0.01Ni-0.1Co-1In exhibits undercooling of 1.8ºC and no undercooling observed in SC-0.01Ni-0.1Co-3In. This thought to be due to the catalytic effects of all Ni, Co and In [1, 2, 4].

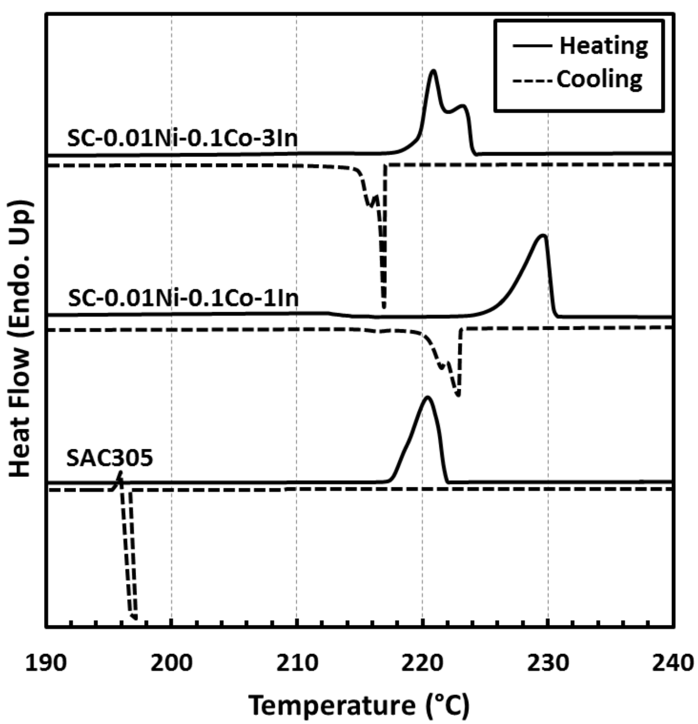

Fig.4.7 DSC curve of the selected solder alloys

Table 4.1 Melting point and solidification behavior of the selected solder alloys

Sample	Liquidus (ºC)	Solidus (ºC)	Solidification Range(ºC)	Undercooling (ºC)
SAC305	222	216	1.6	21.2
SC-0.01Ni-0.1Co-1In	230	223	8.7	1.8
SC-0.01Ni-0.1Co-3In	224	216	8	-

4.3 Electrical Resistivity

As a result of electronic packaging miniaturization and increasing power, current density in electrical interconnections is concerned. High current density promotes Joule heating and may cause electromigration [22] which results in diminished reliability of solder interconnections.

The average electrical resistivity of wire-drawn solder alloys and Sn at 298K is shown in Fig.4.8. SC-0.1Ni, SC-0.5Co and SC-3In were characterized to identify effects of single addition. The results show that addition of Ni tends to decrease the electrical resistivity of solder alloys, conversely, those of Co and In showed contrary effect. The lowest average electrical resistivity of the solder alloys was observed in the SC sample, with a magnitude of 13.4 μΩ cm. Where additions of either Ag, Co and In tends to increase the electrical resistivity of solder alloys. The resistivity of solder alloys are determined by various factor. In this case, residual strain resulted from wire drawing could not affect the electrical resistivity because these Sn-base alloys can recrystallize at temperature below ambient. Lattice-strain scattering is expected in any solder alloys containing alloying elements. According to Linde-Norbury rule, the change in electrical resistivity of metal is proportional to the square of the valence difference between solute and base metal (ΔZ^2) [11]. The value ΔZ^2 is 1 for In, 4 for Ni and Co, 9 for Ag and Cu. Therefore a small amount of Ag and Cu solute could significantly increase the electrical resistivity as can be seen from difference between solder alloys and pure Sn. A presence of IMCs in the solder matrix leads to higher electrical resistivity because IMCs naturally have higher electrical resistivity than Sn-phase. The electrical resistivity of SC-Ni-Co-In is slightly higher than that of SAC305 due to the matrix IMC in spite of the absence of Ag.

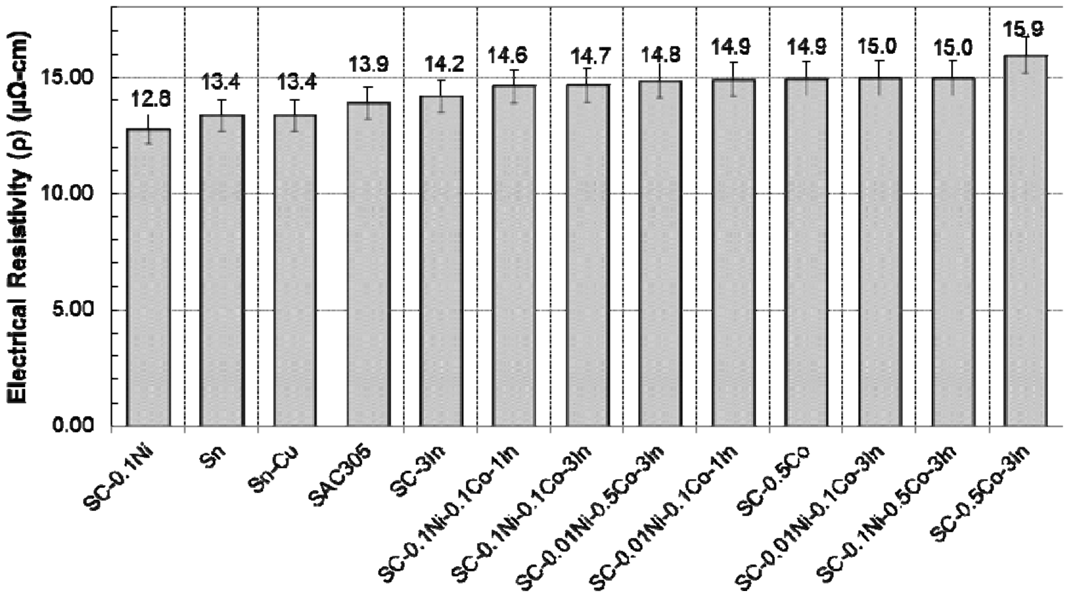

Fig.4.8 Electrical resistivity of wire-drawn solder alloys and Sn

4.4 Effects of soldering condition on microstructure and shear strength

The soldering temperature and time have significant effects on mechanical properties of solder joint. Insufficient soldering time or temperature results in low bond strength. On the other hand, excessive soldering time or temperature promotes excessive growth of IMC layer which may embrittle the solder joint. Two compositions of Sn-Cu-Ni-Co-In solder alloy were selected i.e. SC-0.01Ni-0.1Co-1In and SC-0.01-0.1Co-3In to subject to make solder joints with different soldering temperature and time listed in Table 3.1. This experiment aims to find appropriate soldering profile for Sn-Cu-Ni-Co-In solder alloys. The selected alloys are different in In content which result in different liquidus temperature. Typical cross-sectioned microstructures of solder joints made from SC-0.01Ni-0.1Co-1In and SC-0.01-0.1Co-3In with different soldering time and temperature are shown in Fig.4.9 and Fig.4.10, respectively. The soldering profile has no significant effects on solder matrix microstructures. The IMC layers at the interface were verified by EDS and found to be $(Cu,Co)_6Sn_5$. The thickness of IMC layers slightly increases with increased soldering temperature and time as shown in Fig.4.11. This is because, at the early stage of melting, the IMCs form by dissolution of Cu into

molten solder. After an IMC layer has formed, growth rate was controlled by diffusion of Cu atoms through the IMC layer [23].

The AFPB shear strength results of SC-0.01Ni-0.1Co-1In and SC-0.01-0.1Co-3In solder joints are shown in Fig.4.12. The shear strength of conventional SAC305 and SnCu soldered at their typical temperature profile is also shown as baseline. The SC-0.01Ni-0.1Co-3In is better in shear strength than SC-0.01-0.1Co-3In for all temperature profile used. The effects of temperature profile on shear strength show same trend for both SC-0.01Ni-0.1Co-1In and SC-0.01-0.1Co-3In solder joints. The solder joints soldered at 235ºC/30 sec, 240 ºC/45 sec and 245ºC/60 sec have comparable shear strength within the same solder alloy and a major drop is seen in 260ºC/120 sec solder joint. Although three temperature profiles give comparable shear strength, the temperature profile at 235ºC/30 sec was considered to be the most appropriate profile because of its lowest temperature and shortest time. Low temperature and short time of temperature profile in soldering has many merit such as energy and time saving and avoiding damage to heat-sensitive components. For these reason, temperature profile at 235ºC/30 sec was used for all other SC-Ni-Co-In solder alloys in this work. In addition, the SC-Ni-Co-In solder alloys can be soldered at lower temperature and shorter time than the conventional SAC305 and SnCu due to the effect of alloying element that promote nucleation of scallop-type Cu_6Sn_5 at the interface.

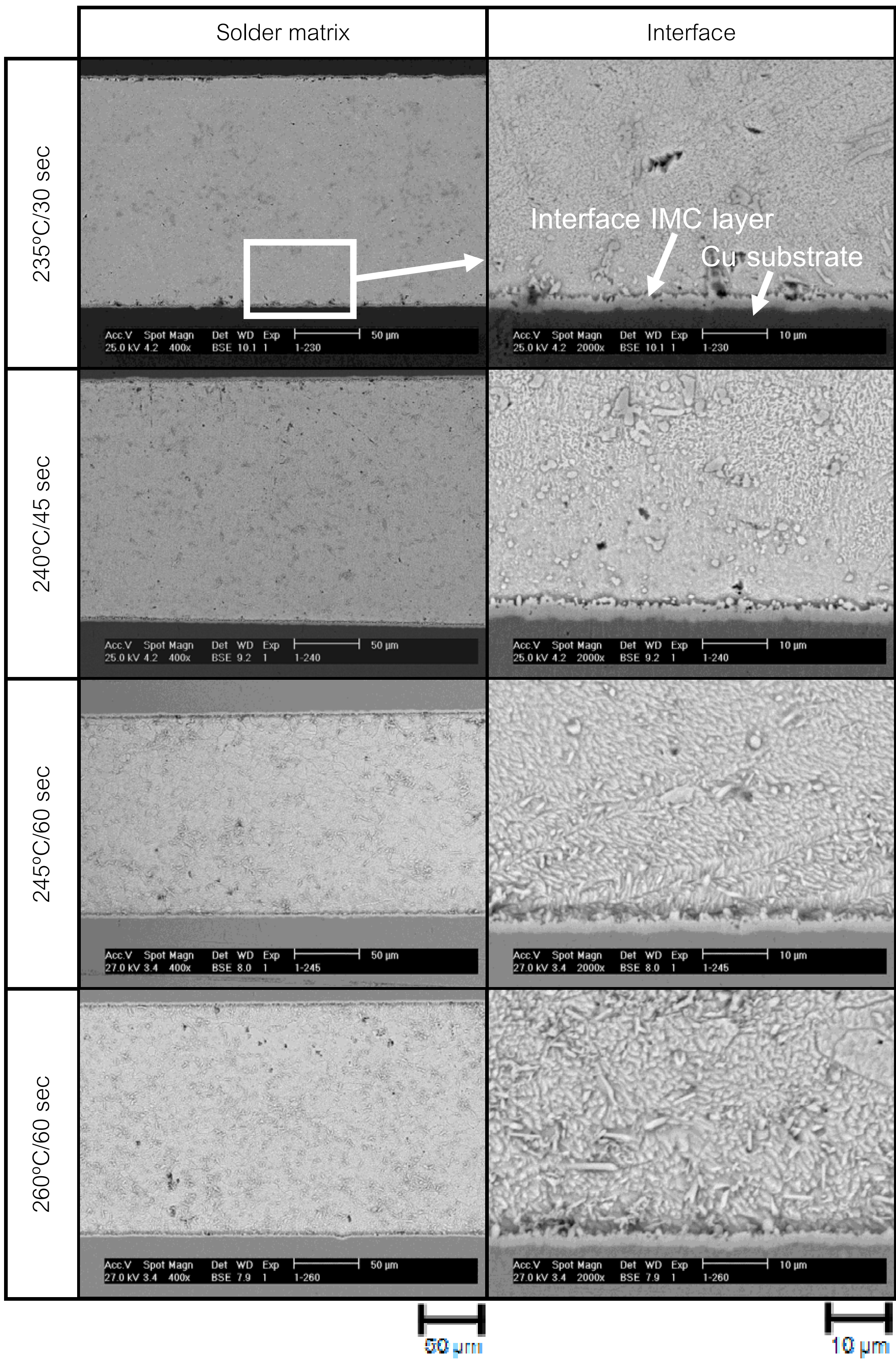

Fig.4.9 Backscattered electron micrographs of SC-0.01Ni-0.1Co-1In with various soldering time and temperature at solder matrix and solder/Cu interface

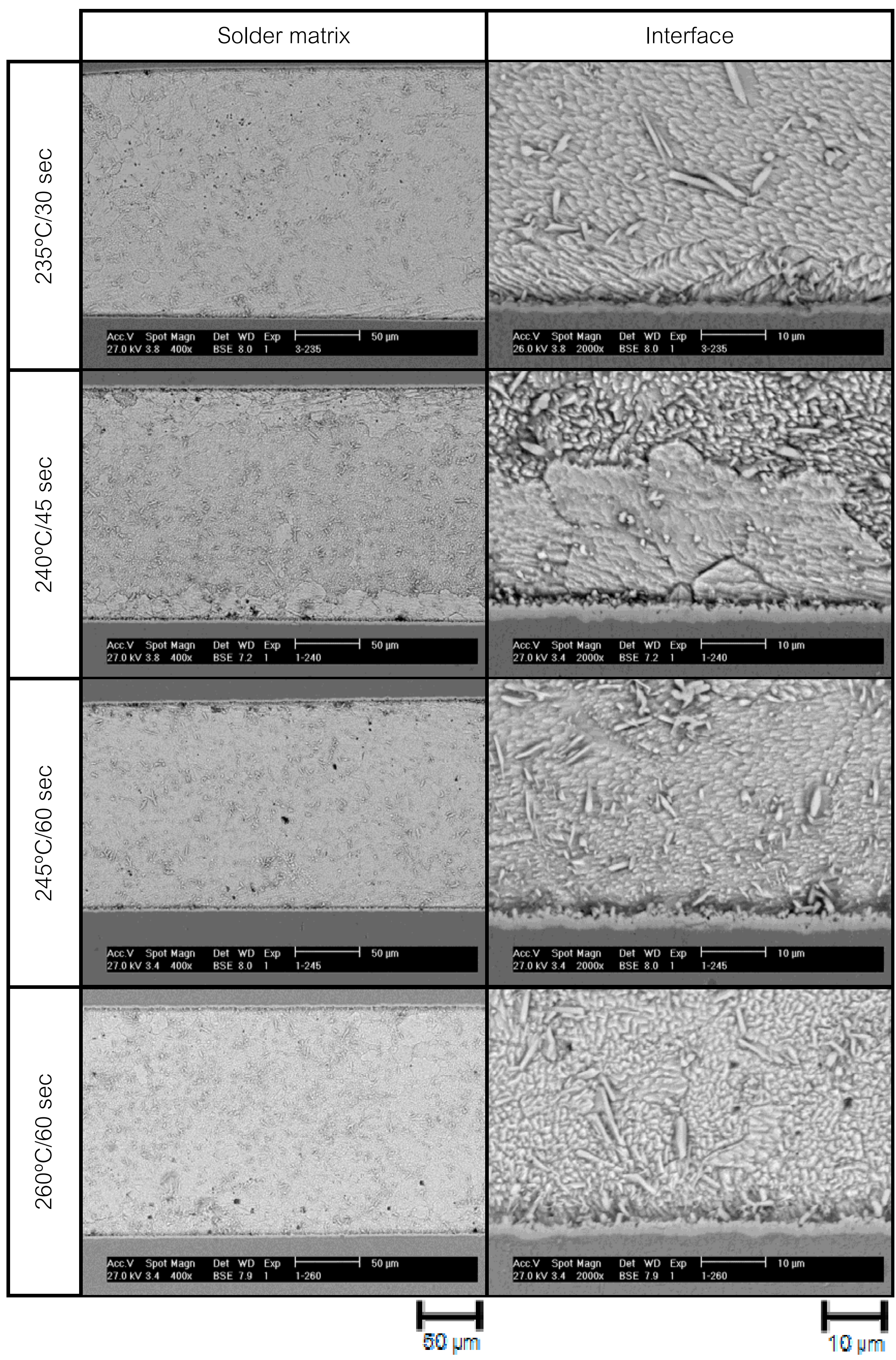

Fig.4.10 Backscattered electron micrographs of SC-0.01Ni-0.1Co-3In with various soldering time and temperature at solder matrix and solder/Cu interface

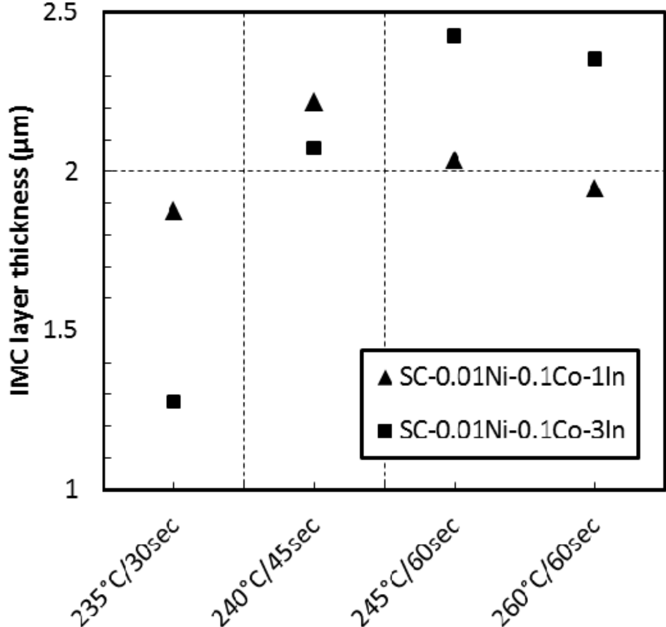

Fig.4.11 IMC layer thickness at solder/Cu interface for various soldering time and temperature

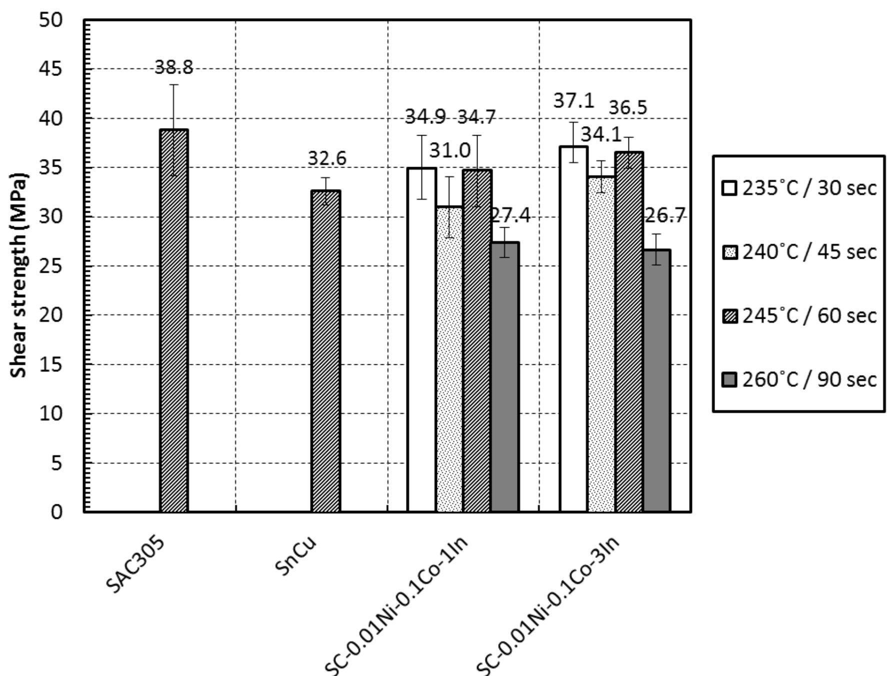

Fig.4.12 AFPB shear strength results of solder joints produced by various temperature profile comparing with SAC305 and SnCu solder joints produced by their typical temperature profile

4.5 As-soldered microstructures and shear strength

Microstructures and shear strength of SC-Ni-Co-In solder alloys were examined before isothermal aging. The selected compositions included SC-0.01Ni-0.1Co-1In, SC-0.01Ni-0.5Co-1In, SC-0.1Ni-0.1Co-1In, SC-0.1Ni-0.5Co-1In, SC-0.01Ni-0.1Co-3In, SC-0.01Ni-0.5Co-3In, SC-0.1Ni-0.1Co-3In, and SC-0.1Ni-0.5Co-3In. The soldering profile used in this experimental section is 235ºC/30 sec that showed preferred results in the previous section.

Typical cross-section BEI micrographs of the solder joint are shown in Fig.4.13-4.14. Microstructures of the conventional alloys i.e. SAC305 and SC are only consisted of Sn phase. No dispersed IMC is founded. Conversely, the microstructures of SC-Ni-Co-In alloys have small IMC dispersed in their solder matrix.

The IMC layers formed at the interface between the conventional alloys and Cu of these solder alloys have typical scallop-type morphology. The quantitative analysis by EDS indicated that these IMCs are Cu_6Sn_5. On the other hand, different morphology is formed at the interfaces of SC-Ni-Co-In alloys. In this case, the IMC layers have a needle-like morphology. The quantitative analysis by EDS indicated that the IMC formed by SC-Ni-Co-In at both interface and in the solder matrix are $(Cu,Ni,Co)_6Sn_5$ rather than Ni-Sn or Co-Sn IMC. This implied that Ni and Co could accelerate the nucleation rate of IMC and replace Cu atom in Cu_6Sn_5 without forming into IMC with Sn. The thickness of the IMC layer is greater for interfaces of SAC305 and SC than for SC-Ni-Co-In. EDS analysis taken in Sn phase showed amount of In dispersion and no Cu, Ni or Co were found.

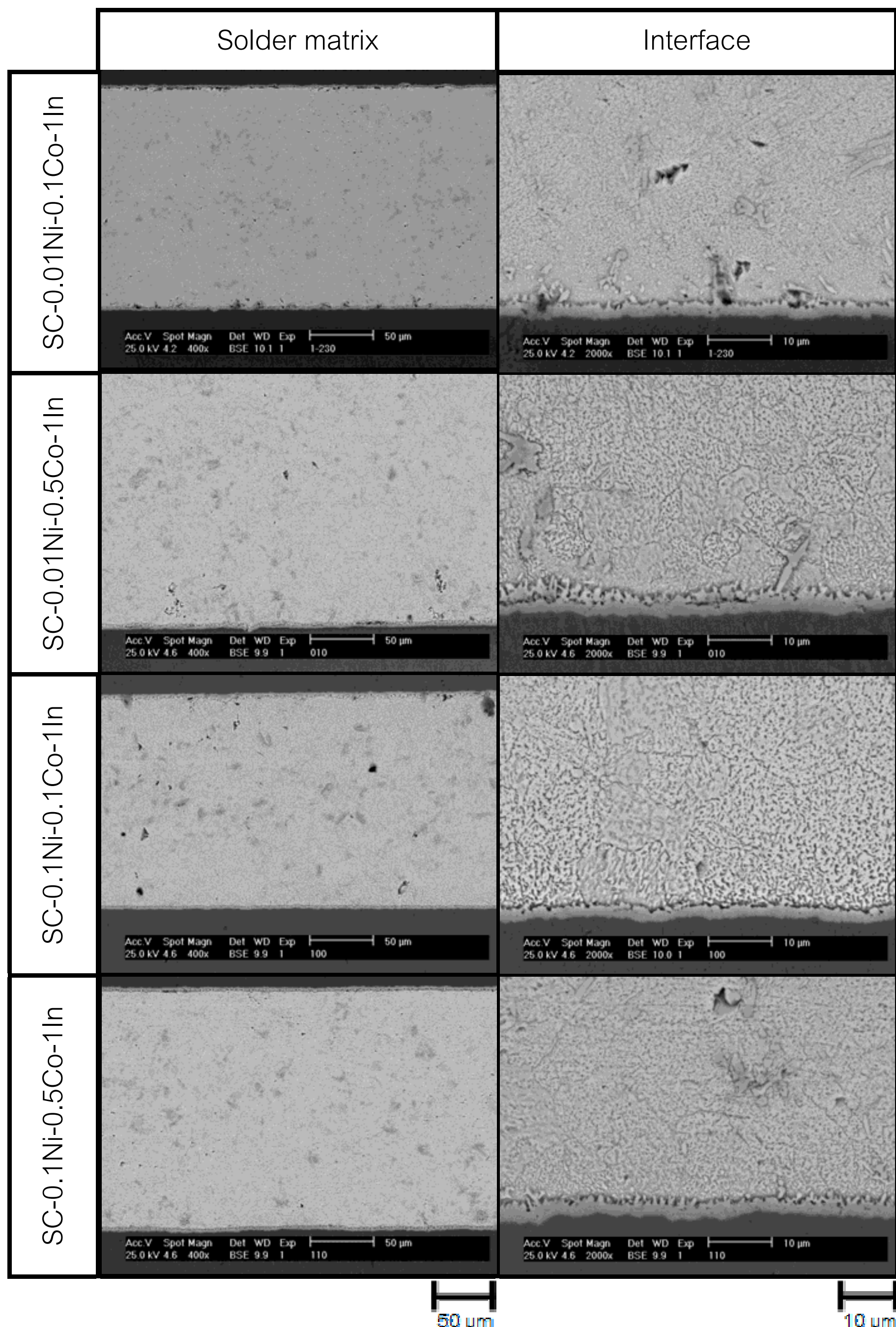

Fig.4.13 BEI micrographs of solder joints for as-soldered condition

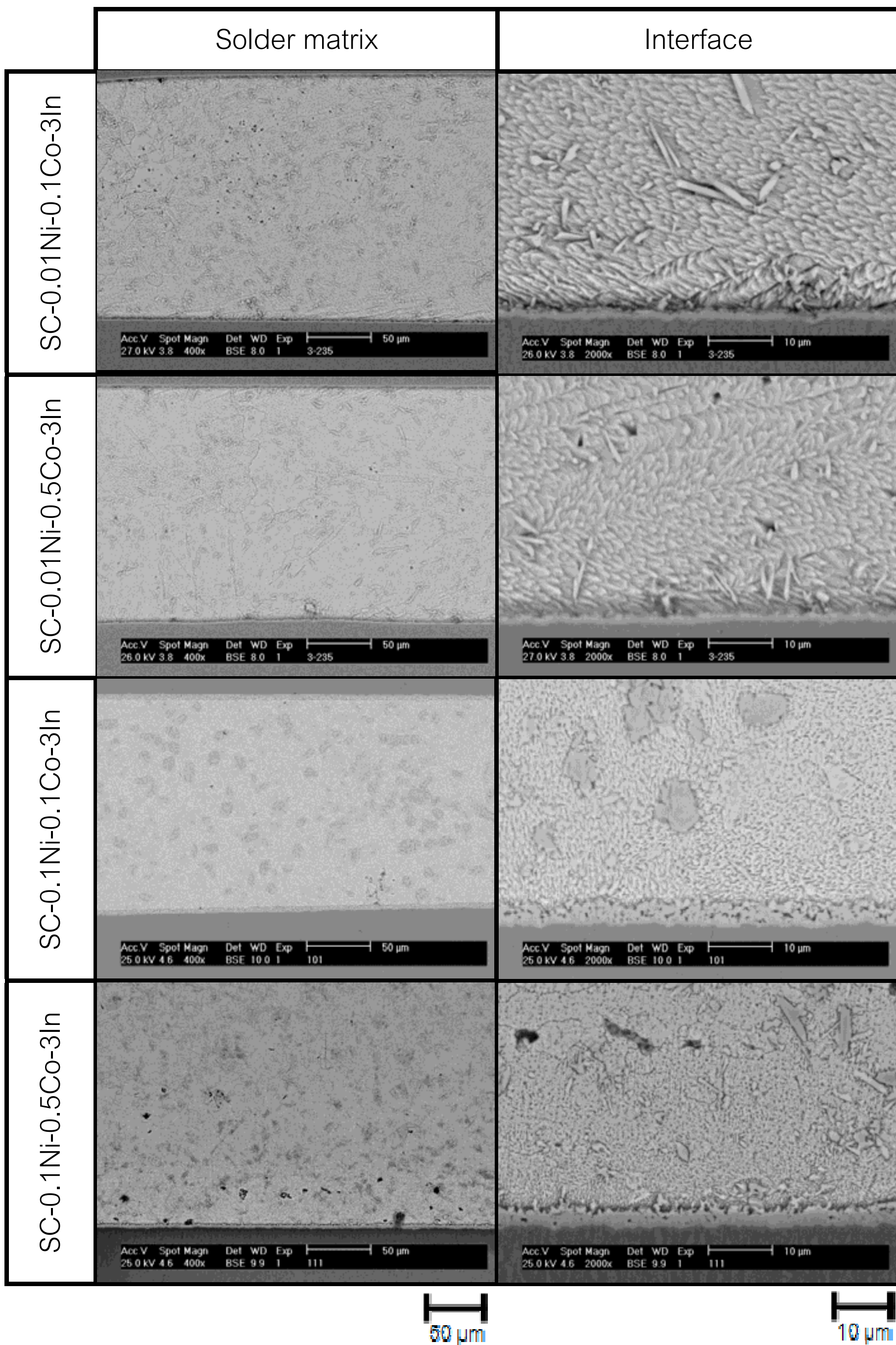

Fig.4.14 BEI micrographs of solder joints for as-soldered condition (2)

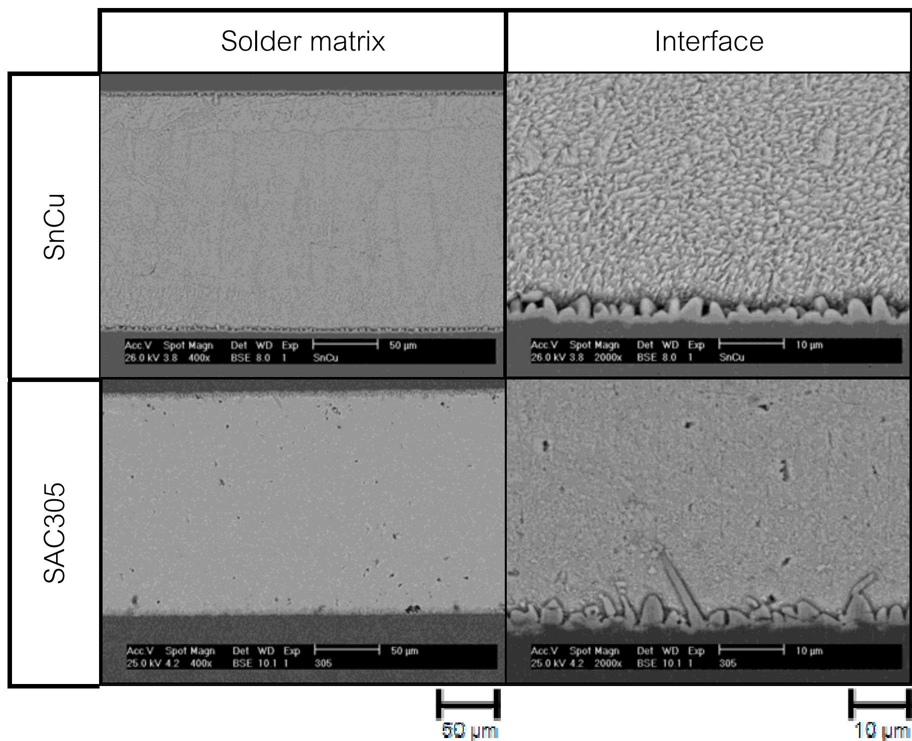

Fig.4.15 BEI micrographs of solder joints for as-soldered condition (3)

AFPB shear test results of the as-soldered solder joints are shown in Fig. 4.16. The best three of SC-Ni-Co-In are alloys with 3%In. This indicates that increasing amount of In from 1% to 3% can effectively improve shear strength of SC-Ni-Co-In alloys. The highest shear strength is shown in SC-0.01Ni-0.5Co-3In solder joint with a magnitude of 42 MPa which is higher than that of SAC305 at 39 MPa.

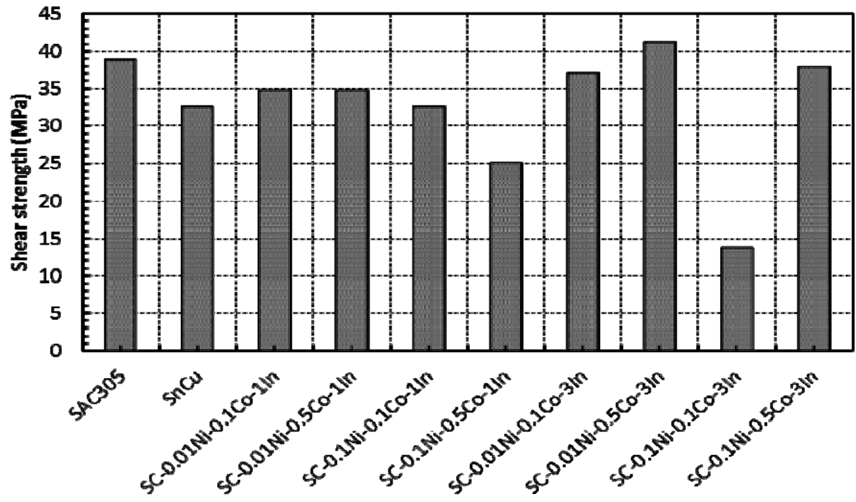

Fig. 4.16 AFPB shear strength of as-soldered solder joints

4.6 Microstructure evolution after isothermal aging

Some electronic devices operate at elevated temperature in which solders can undergo microstructural changes such as phase coarsening and excessive IMC growth. This microstructural instability can cause risk to reliability of solder joints.

Four SC-Ni-Co-In with highest shear strength from the previous section were subjected to isothermal aging at 150ºC for 1,000 hours. The selected compositions included SC-0.01Ni-0.1Co-1In, SC-0.01Ni-0.1Co-3In, SC-0.01Ni-0.5Co-3In, and SC-0.1Ni-0.5Co-3In. SAC305 was also conducted in this test for baseline. The aged solder-joint microstructures were observed every 250 hours. AFPB shear strength test were conducted on the solder joints after aging for 250 and 1,000 hours. The microstructural evolution for SAC305, SC-0.01Ni-0.1Co-1In, SC-0.01Ni-0.1Co-3In, SC-0.01Ni-0.5Co-3In, and SC-0.1Ni-0.5Co-3In solder joint is shown in Fig.4.17-4.21.

4.7 Phase identification

The IMC formation was initially characterized by EDS spot analysis on SC-0.1Ni-0.5Co-3In solder joint, the highest alloyed sample. The spot analysis was carried out on three regions i.e. solder matrix, interfacial IMC and matrix IMC as shown in Fig.4.22 for as-soldered condition and Fig.4.23 for after 1,000 hours aging. For the as-soldered condition, the interfacial and matrix IMC were found to be Cu_6Sn_5 with amount of Co segregation within this IMC thus it can be indicated as $(Cu,Co)_6Sn_5$. Indium exists as solid solution in Sn matrix hence did not combine with Cu_6Sn_5. After aging for 1,000 hours, indium is not found in the solder matrix but shows segregation in interfacial Cu_6Sn_5.

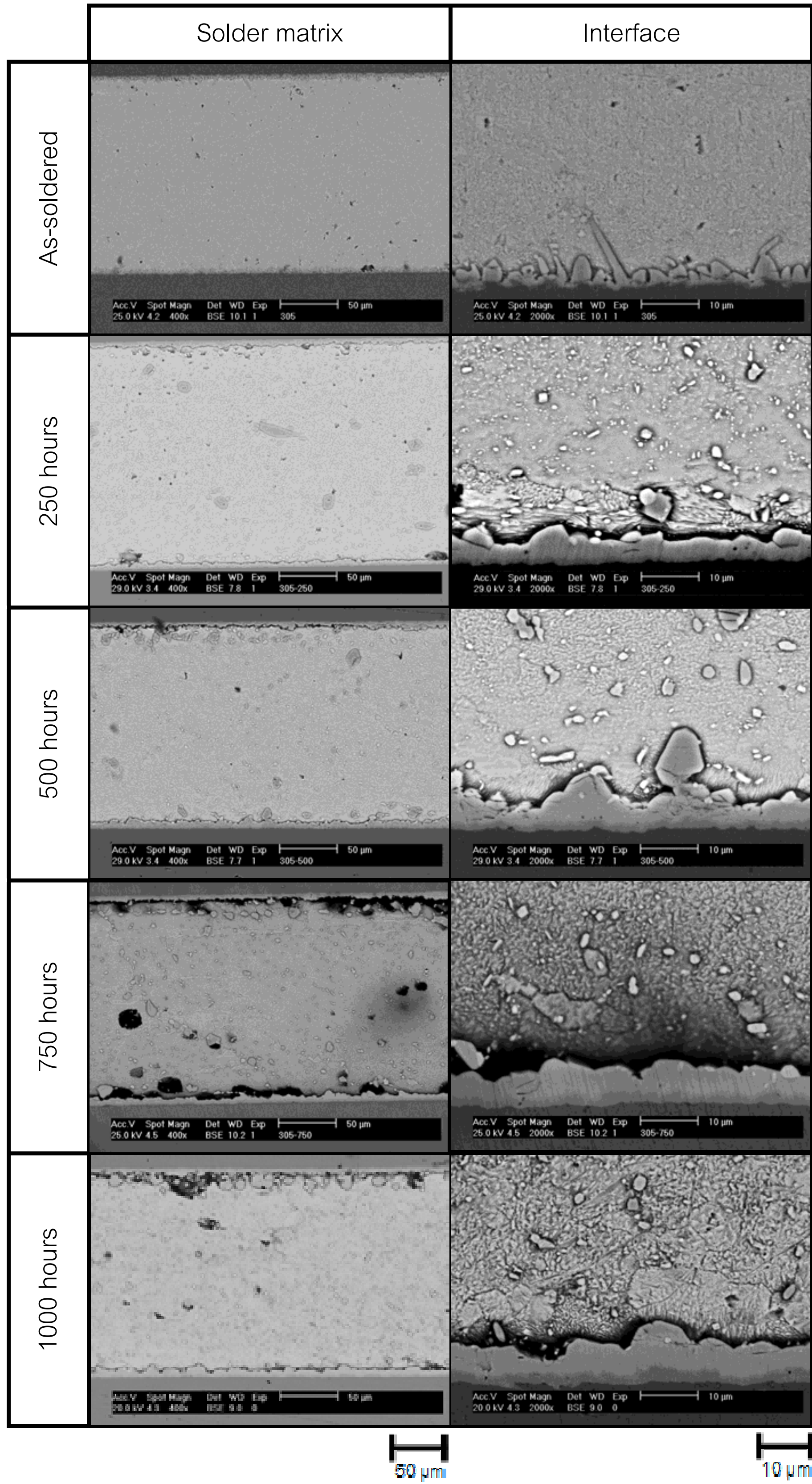

Fig.4.17 BEI micrographs showing microstructure evolution of SAC305 aged at 150°C

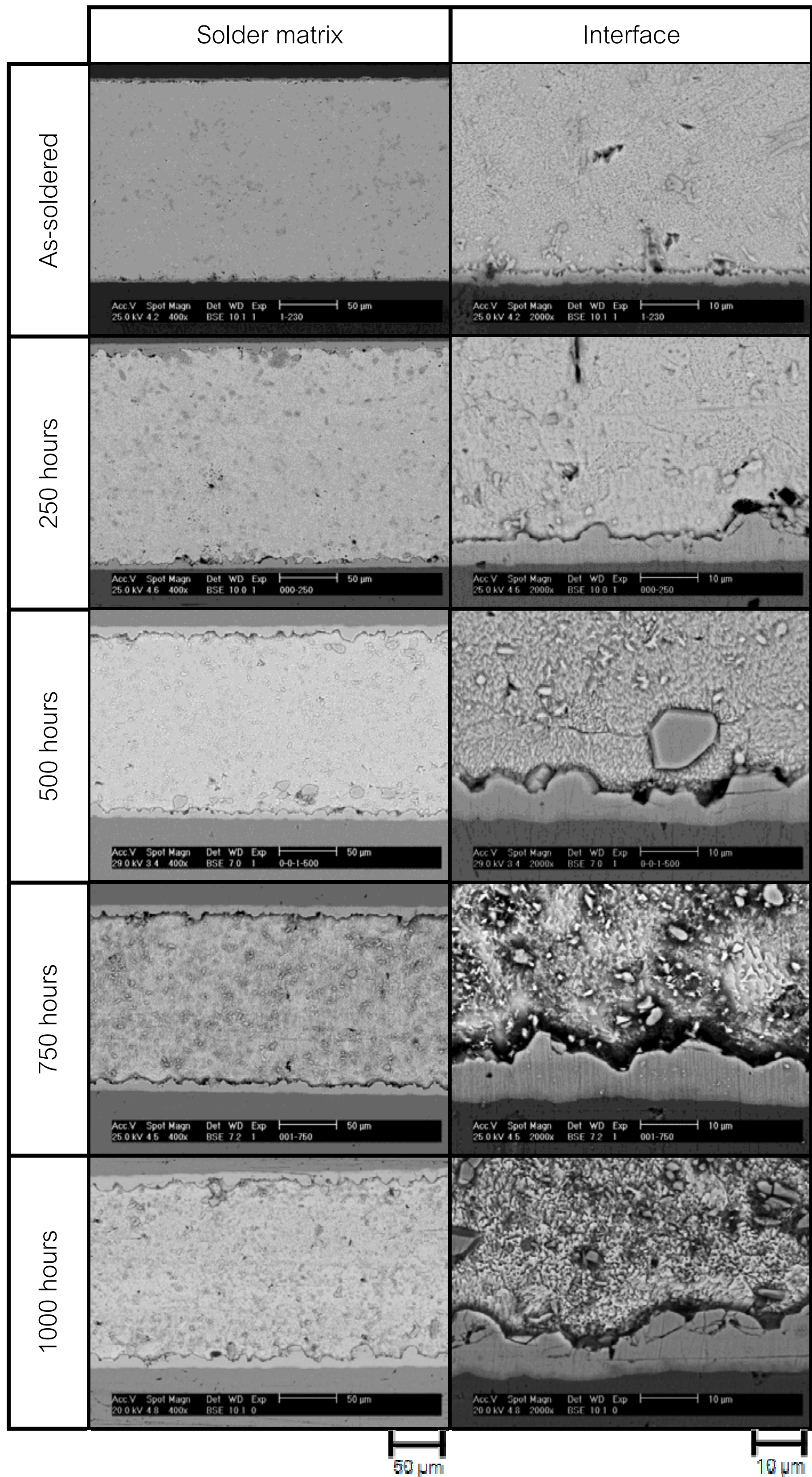

Fig.4.18 BEI micrographs showing microstructure evolution of SC-0.01Ni-0.1Co-1In aged at 150°C

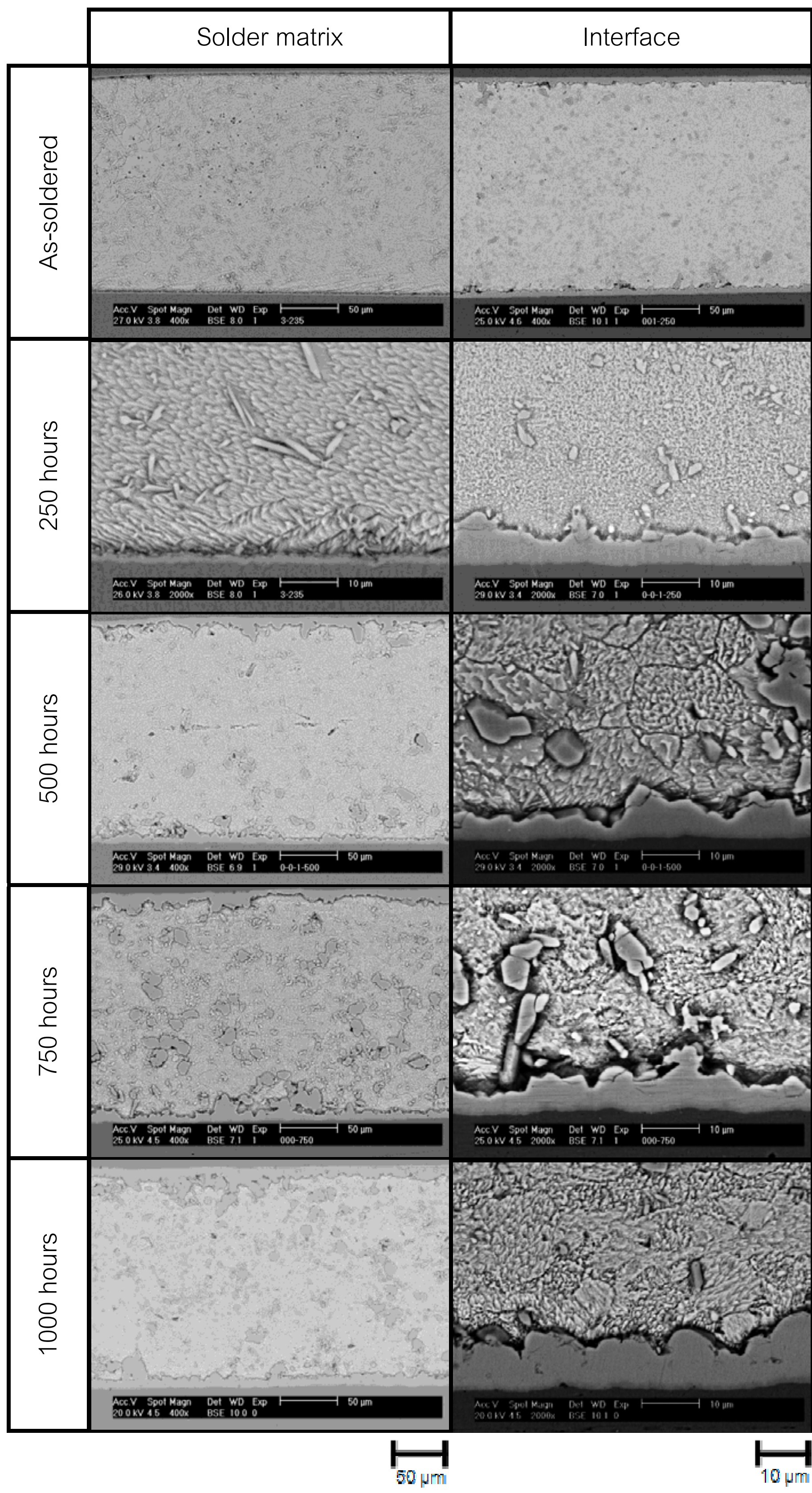

Fig.4.19 BEI micrographs showing microstructure evolution of SC-0.01Ni-0.1Co-3In aged at 150°C

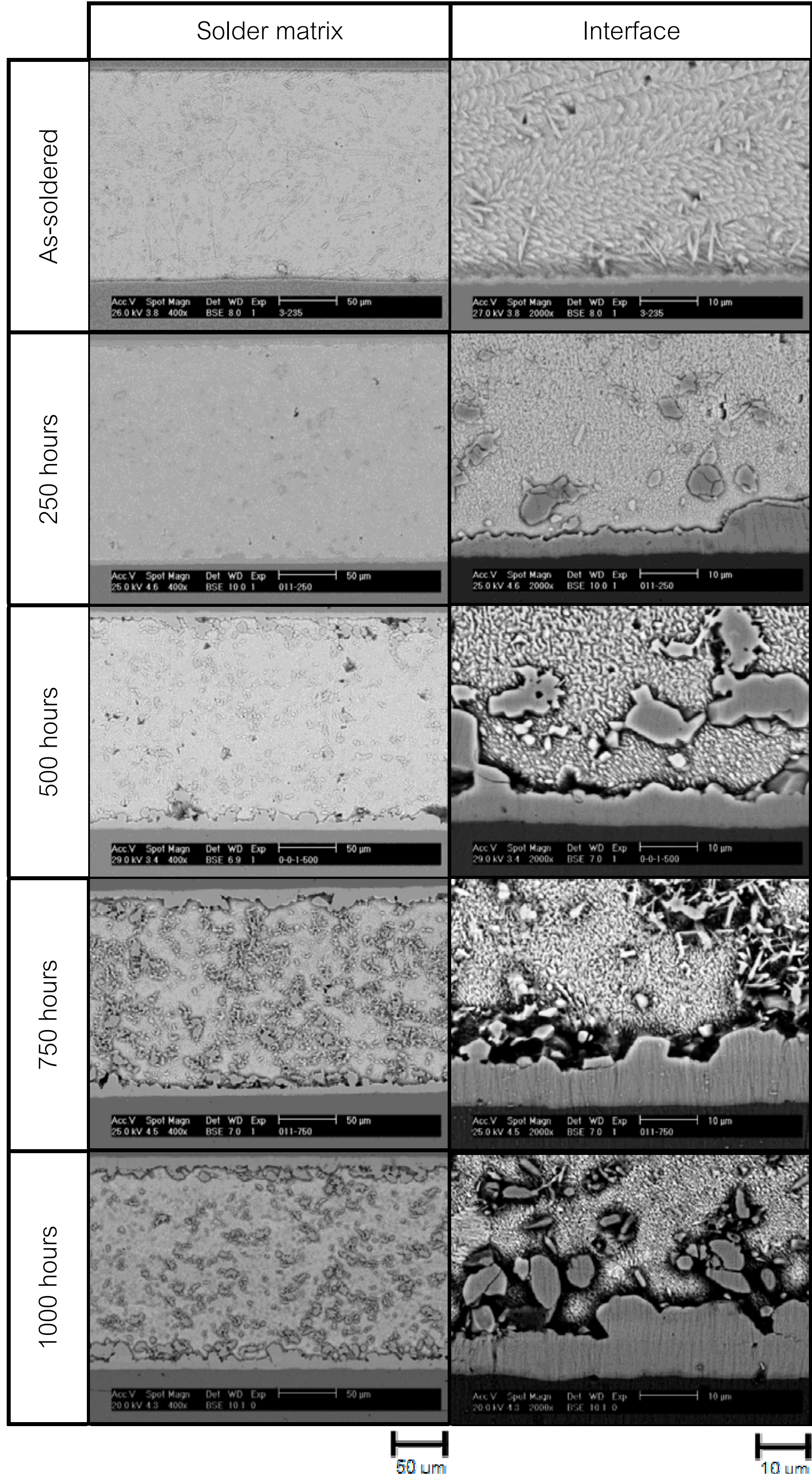

Fig.4.20 BEI micrographs showing microstructure evolution of SC-0.01Ni-0.5Co-3In aged at 150ºC

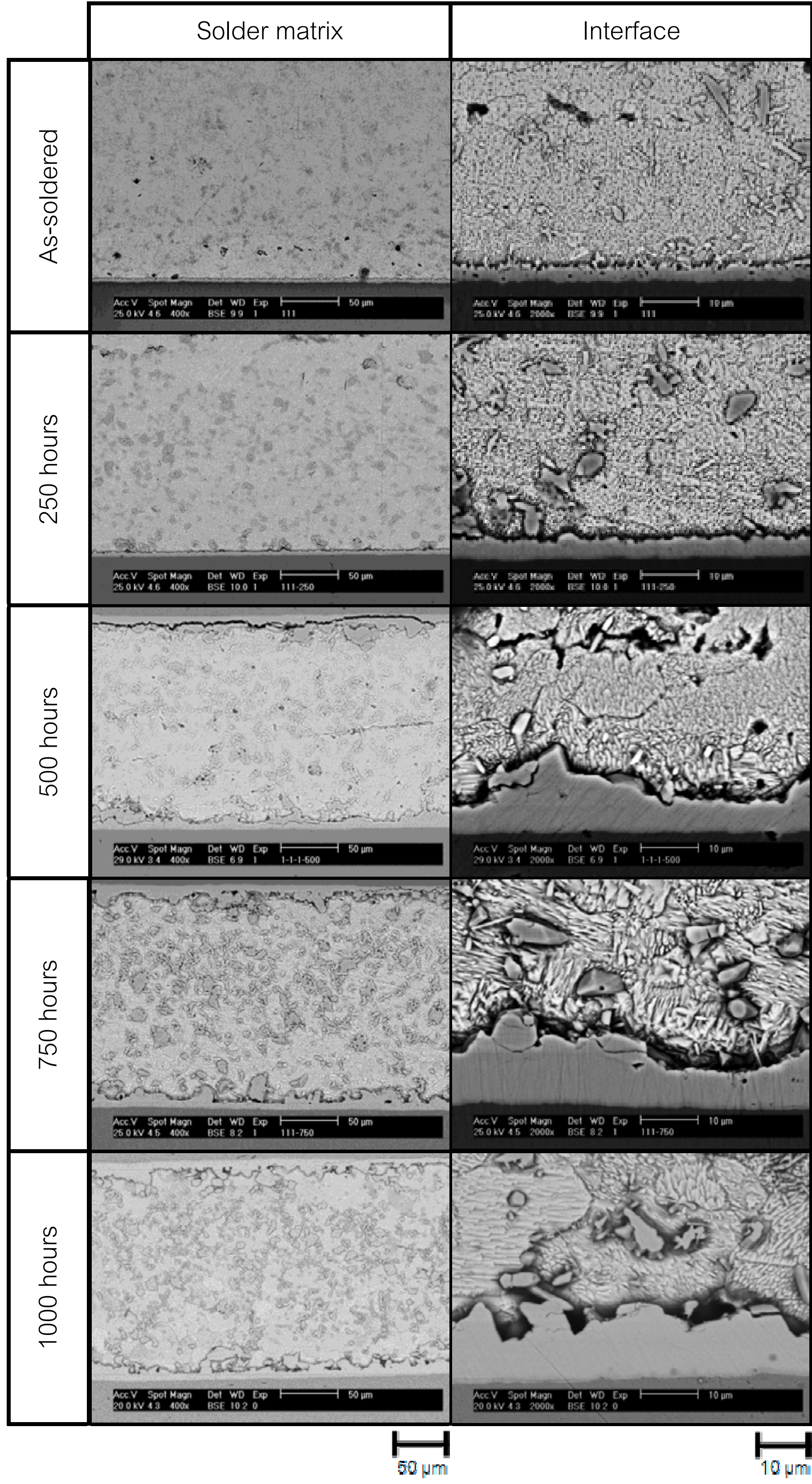

Fig.4.21 BEI micrographs showing microstructure evolution of SC-0.1Ni-0.5Co-3In aged at 150ºC

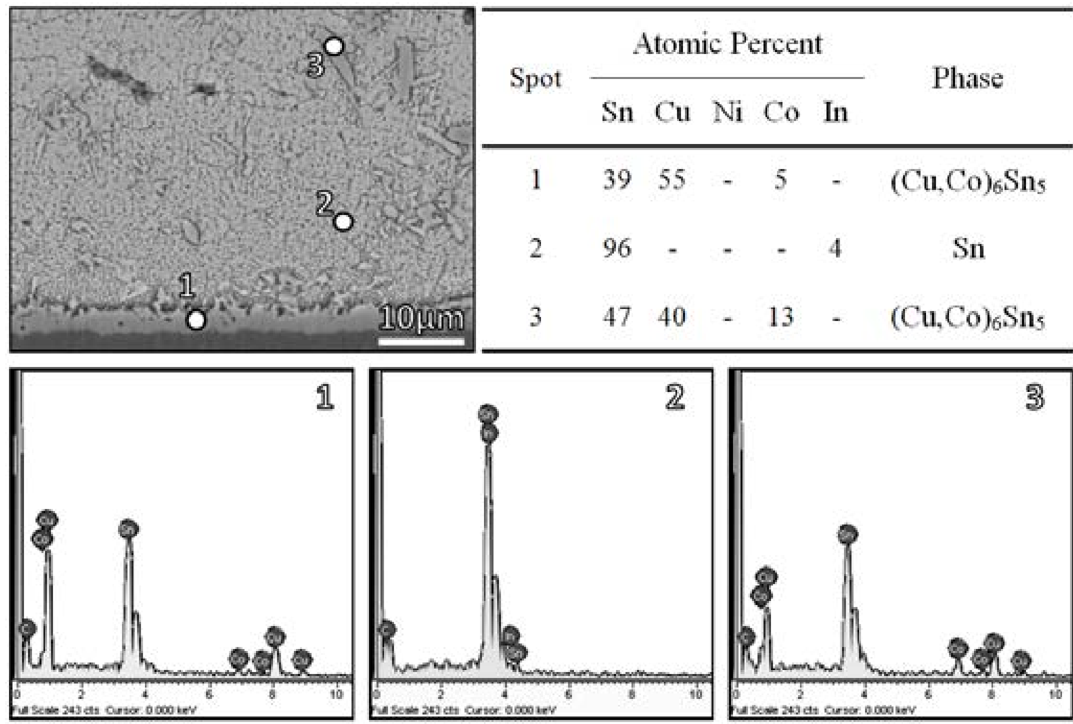

Spot	Atomic Percent					Phase
	Sn	Cu	Ni	Co	In	
1	39	55	-	5	-	$(Cu,Co)_6Sn_5$
2	96	-	-	-	4	Sn
3	47	40	-	13	-	$(Cu,Co)_6Sn_5$

Fig.4.22 Summary of EDS analysis of as-soldered SC-0.1Ni-0.5Co-3In solder joint

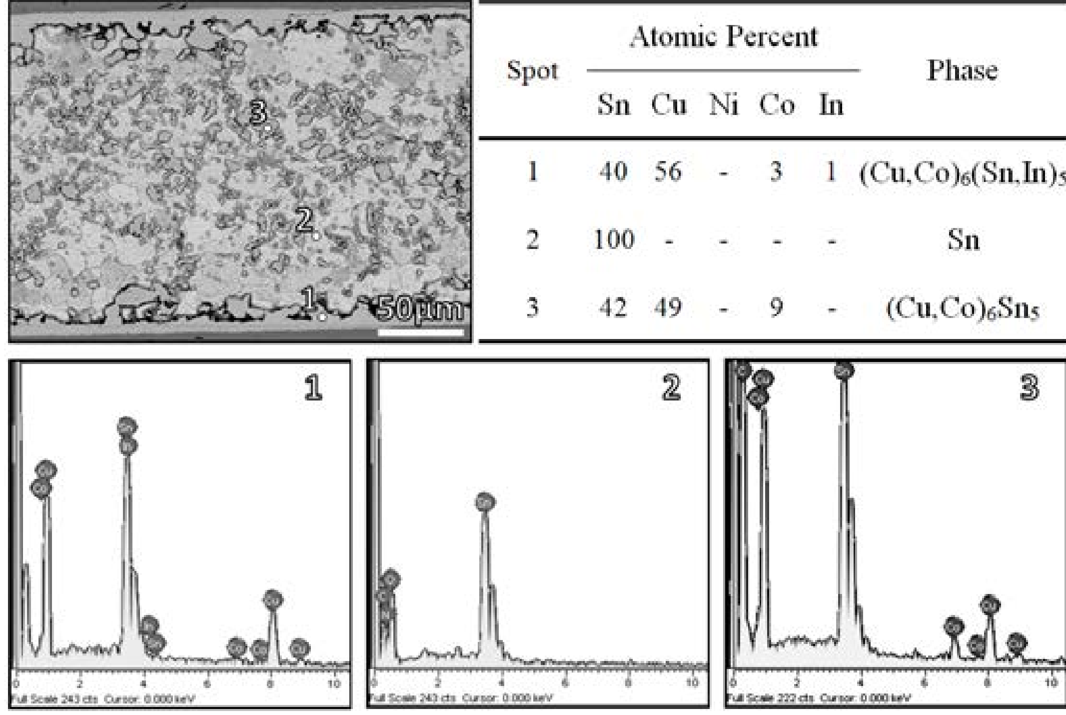

Spot	Atomic Percent					Phase
	Sn	Cu	Ni	Co	In	
1	40	56	-	3	1	$(Cu,Co)_6(Sn,In)_5$
2	100	-	-	-	-	Sn
3	42	49	-	9	-	$(Cu,Co)_6Sn_5$

Fig.4.23 Summary of EDS analysis of SC-0.1Ni-0.5Co-3In solder subjected to isothermal aging at 150ºC for 1,000 hours

4.8 Elemental distribution

EPMA analysis was carried out to observe the elemental distribution of the solder joints. Elemental mappings of SC-0.1Ni-0.5Co-3In solder joint after subjected to thermal aging at 150ºC for 0, 250 and 1,000 hours are shown in Fig.4.24-4.26, respectively. For the as-soldered condition, In dissolves in Sn matrix. Co shows segregation in both interfacial and matrix Cu_6Sn_5. The Co-rich regions present in some area. Due to minute amount, this phase is not detectable by EDS; however, it is believed to be $CoSn_2$ IMC. After isothermal aging for 250 hours, In begins to segregate in Cu_6Sn_5 near the interface next to the $(Cu,Co)_6Sn_5$ layer. Sn and In have very similar metallic radius (167 pm and 162 pm, respectively) thus In could substitute Sn atom in Cu_6Sn_5. The IMC remains as $Cu_6(Sn,In)_5$. Co remains segregated as $(Cu,Co)_6Sn_5$ at the interface and in the solder matrix. After further isothermal aging for 1,000 hours, segregation of In near the interface is clearly seen. Co still remains as a $(Cu,Co)_6Sn_5$ layer and doesn't tend to combine with $Cu_6(Sn,In)_5$ to form $(Cu,Co)_6(Sn,In)_5$. This trend is also observed for IMC in the solder matrix that In and Co tends to avoid each other. Thus, after 1,000 hours isothermal aging, comparing to typical $Cu>Cu_3Sn>Cu_6Sn_5$ IMC structure of SAC solder alloys, SC-Ni-Co-In solder alloys have a different interfacial IMC structure that is $Cu>Cu_3Sn>(Cu,Co)_6Sn_5>Cu_6(Sn,In)_5>Sn$ as illustrated schematically in Fig.4.27.

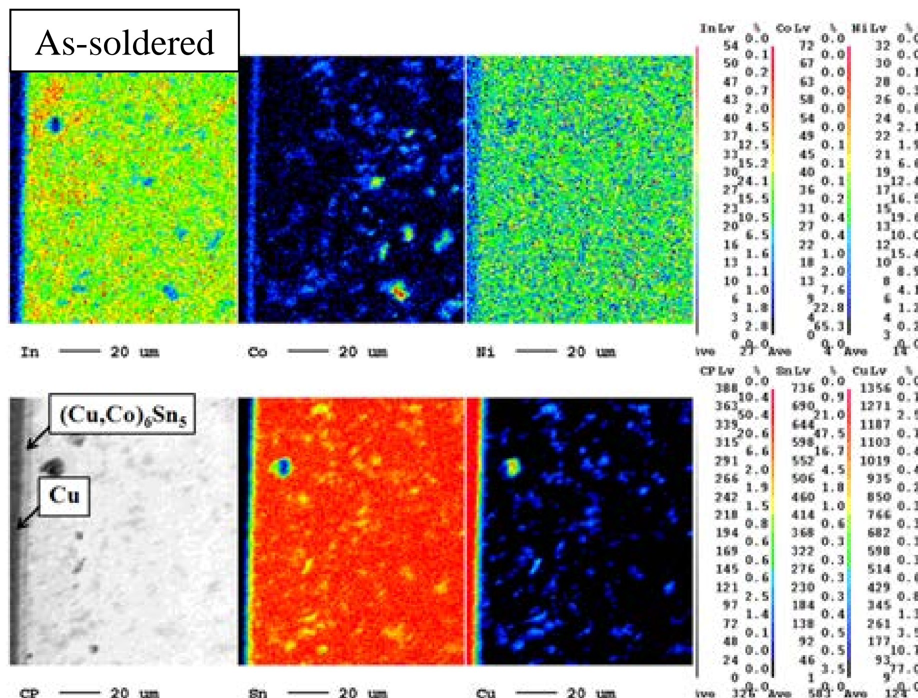

Fig.4.24 EPMA elemental mapping of SC-0.1Ni-0.5Co-3In solder joint before isothermal aging

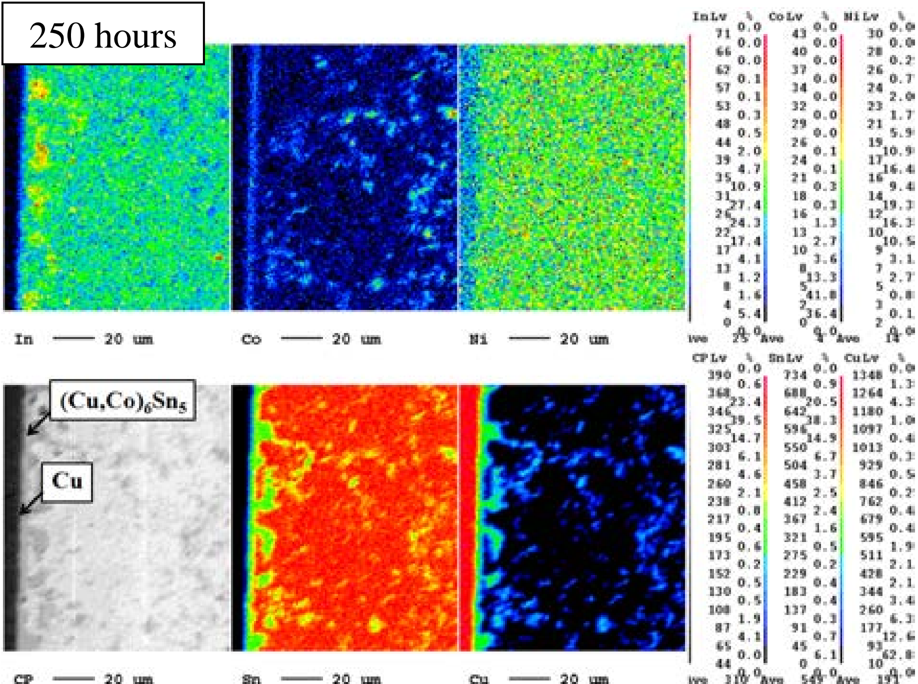

Fig.4.25 EPMA elemental mapping of SC-0.1Ni-0.5Co-3In solder joint after subjected to isothermal aging at 150°C for 250 hours

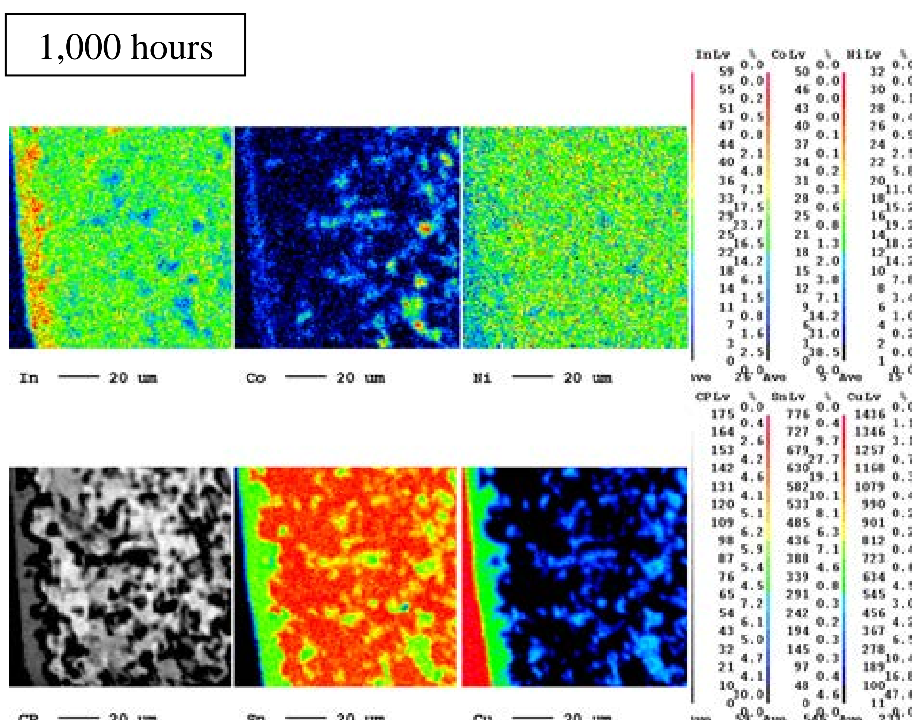

Fig.4.26 EPMA elemental mapping of SC-0.1Ni-0.5Co-3In solder joint after subjected to isothermal aging at 150°C for 1,000 hours

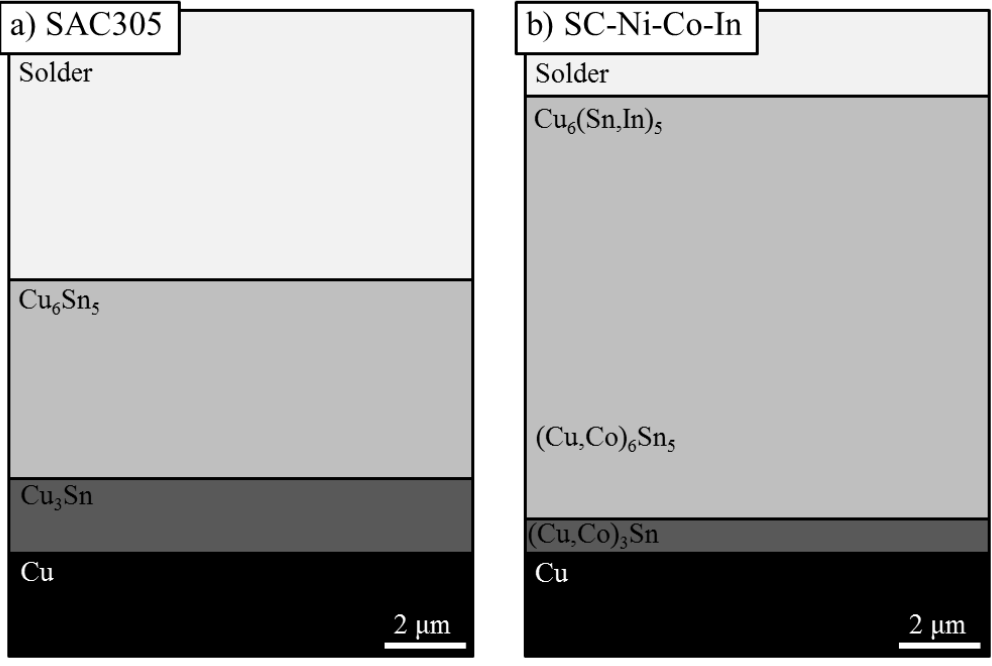

Fig.4.27 Schematic of IMC-layer structure at the interface of a) SAC and b) SC-Ni-Co-In solder joint

4.9 Growth behavior of interfacial intermetallic compounds

For all as-solidified joints, the IMC formed at the interfaces is only Cu_6Sn_5. The growth of this IMC was observed at the aged interface due to reaction between matrix Sn and Cu substrate diffused through IMC layer. After the aging time of 250 hours, the Cu_3Sn intermetallic was observed at the interfaces. This IMC appeared as a dark grey layer located at the Cu_6Sn_5/Cu interface. The formation of Cu_3Sn was accounted to two reaction; the reaction between Cu_6Sn_5 and Cu substrate and reaction between Cu atom from substrate and Sn atom diffused from solder

The growth of the Cu_6Sn_5, Cu_3Sn and total IMC thickness of each solder joint is plotted as a function of isothermal aging time in Fig. 4.28-4.30, respectively. The growth rate of Cu_3Sn is high initially and decreases as increased aging time. For SAC305, the Cu_3Sn thickness is higher as compared with that for SC-Ni-Co-In solder alloys. The thickness of Cu_6Sn_5 IMC also increases with aging time. However, Cu_6Sn_5 shows a higher thickness for SC-Ni-Co-In solder alloys. The SC-Ni-Co-In alloys with 3%In tends to have a thicker Cu_6Sn_5 layer as compared with SC-0.01Ni-0.1Co-1In. The Cu_6Sn_5 thickness appears to be similar within the 3%In group despite of the difference in the amounts of Ni and/or Co. Conversely, Cu_3Sn thickness is higher for SC-0.01Ni-0.1Co-1In.

Since at the temperature used in this research, the growth mechanism of Cu_3Sn is mainly dominated by solid state diffusion [24], the growth kinetic of Cu_3Sn layer can be expressed as:

$$x = (D_{eff}\ t)^{1/2} \qquad [4.1]$$

Where x is the thickness of Cu_3Sn, D_{eff} is the effective interdiffusion coefficient in the Cu_3Sn layer and t is the aging time.

The thickness of Cu_3Sn is plotted as a function of square root time in Fig. 4.31. The linear trend line confirms that the main growth mechanism of this IMC is solid state diffusion for all solder alloys. This indicates that Ni, Co and In additions did not change the main growth mechanism. However, the alloying element additions result in suppression of Cu_3Sn growth by the stabilization of Cu_6Sn_5, thus retard the reaction in Eq.4.2. This effect caused by Ni and Co has been reported previously [25,26]. Specifically, in this study, the EPMA mapping in Fig.4.26 shows segregation of In at the interfacial Cu_6Sn_5 of the aged sample which suggested that it could be further stabilized by In. The thickness plot in Fig.4.28 confirms the stabilization effect of In. It is clearly seen that SC-0.01Ni-0.1Co-1In has higher Cu_3Sn thickness than that of the 3%In group.

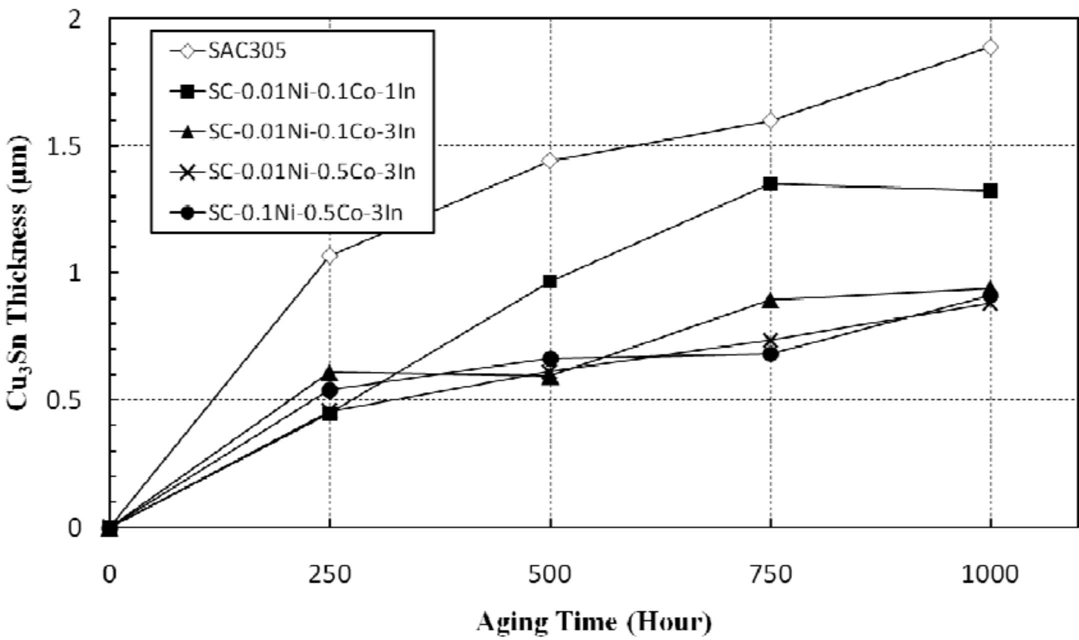

Fig.4.28 Cu_3Sn Thickness as a function of time of solder joints aged at 150°C

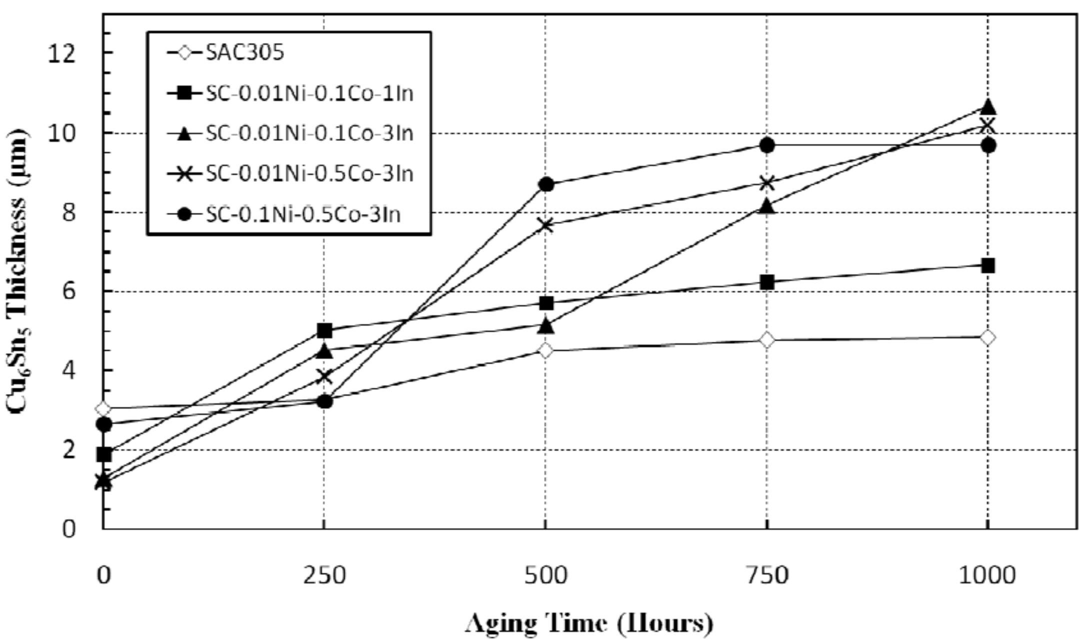

Fig.4.29 Cu_6Sn_5 Thickness as a function of time of solder joints aged at 150°C

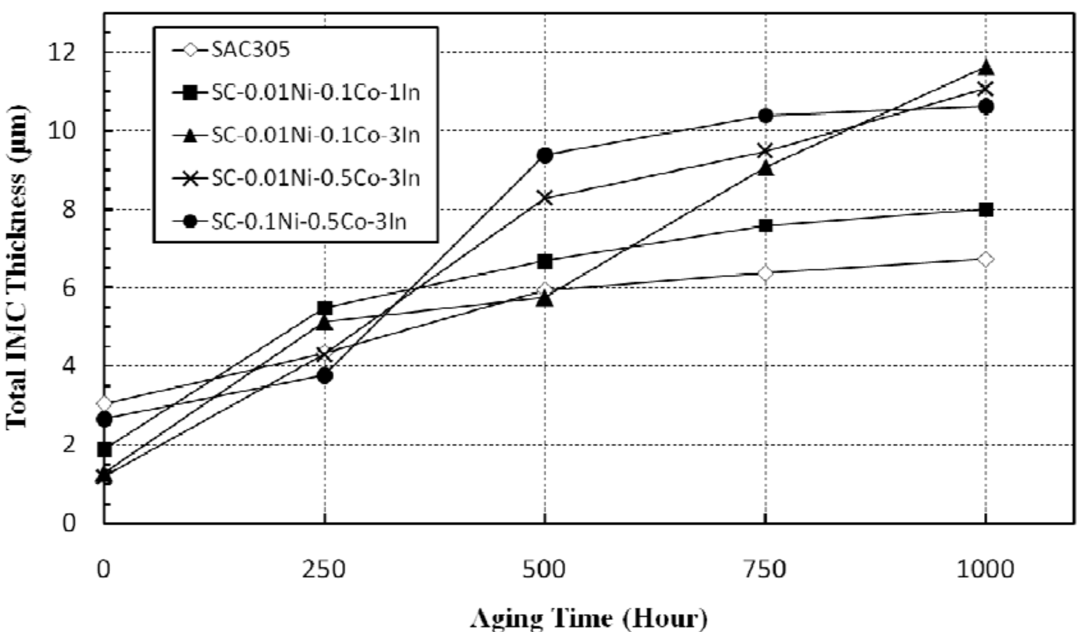

Fig.4.30 Total intermetallic compound thickness as a function of time of solder joints aged at 150°C

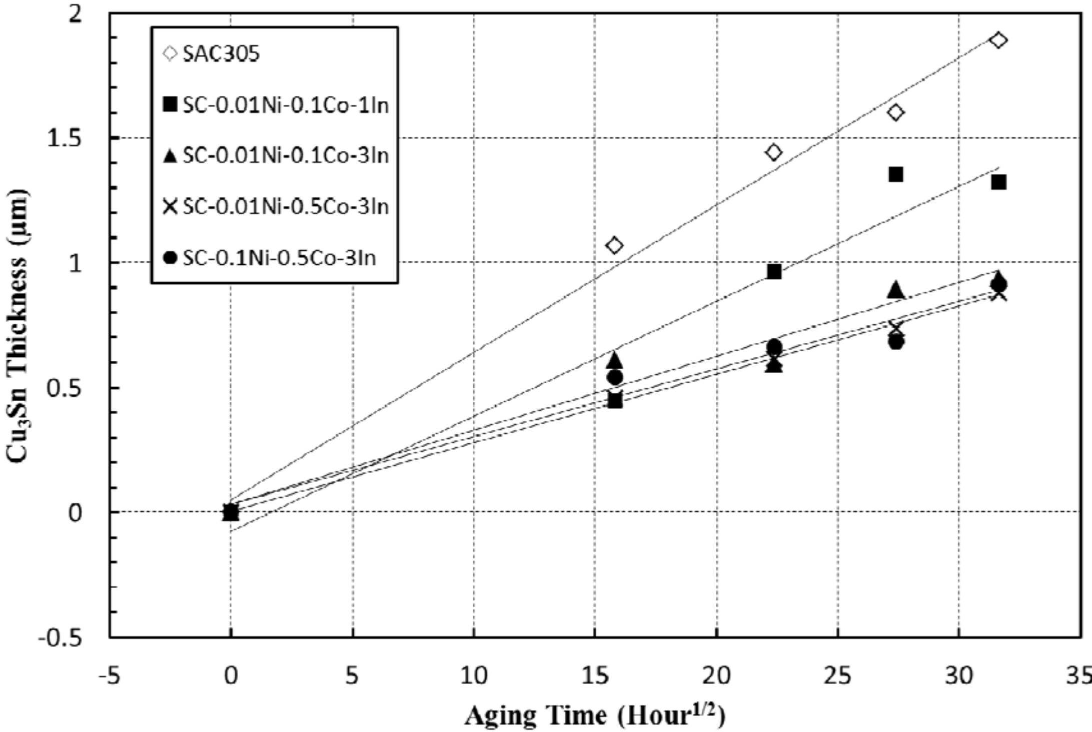

Fig.4.31 Cu_3Sn thickness as a function of square root time of the solder joints aged at 150ºC

4.10 Shear strengths after isothermal aging

AFPB shear strength test result of solder joint subjected to isothermal aging is shown in Fig.4.32. At least 4 test bars were tested for each condition. The average standard deviation of all conditions is 2.14. In as-soldered condition, the strongest joint was made from SC-0.01Ni-0.5Co-3In which is the only joint stronger than that made from SAC305. SC-0.01Ni-0.1Co-1In is the weakest joint. The shear strength of SAC305 is initially 37.5 MPa before isothermal aging. After 1,000 hours aging, its shear strength drops to 28 MPa which is 25.33% lower than the as-reflow value. SAC305 solder joint is the weakest joint after 1,000 hours aging. The AFPB shear strength drop of SAC305 solder joint of the same aging temperature was previously reported by Anderson et al.[14]. The value is 14.9% after 100 hours and 30.3% after 1,000 hours. The average value of four SAC alloys was 33.425% as shown in Fig.4.33 [14]. The SC-

Ni-Co-In alloys maintain their shear strength well after isothermal aging. The strongest joint was again made from SC-0.01Ni-0.5Co-3In which shows only 2.18% shear strength drop. The weakest joint of SC-Ni-Co-In alloys is again SC-0.01Ni-0.1Co-1In which shows 8.31% shear strength drop. Average as-aged shear strength drop of four SC-0.01Ni-0.5Co-3In is 3.82%.

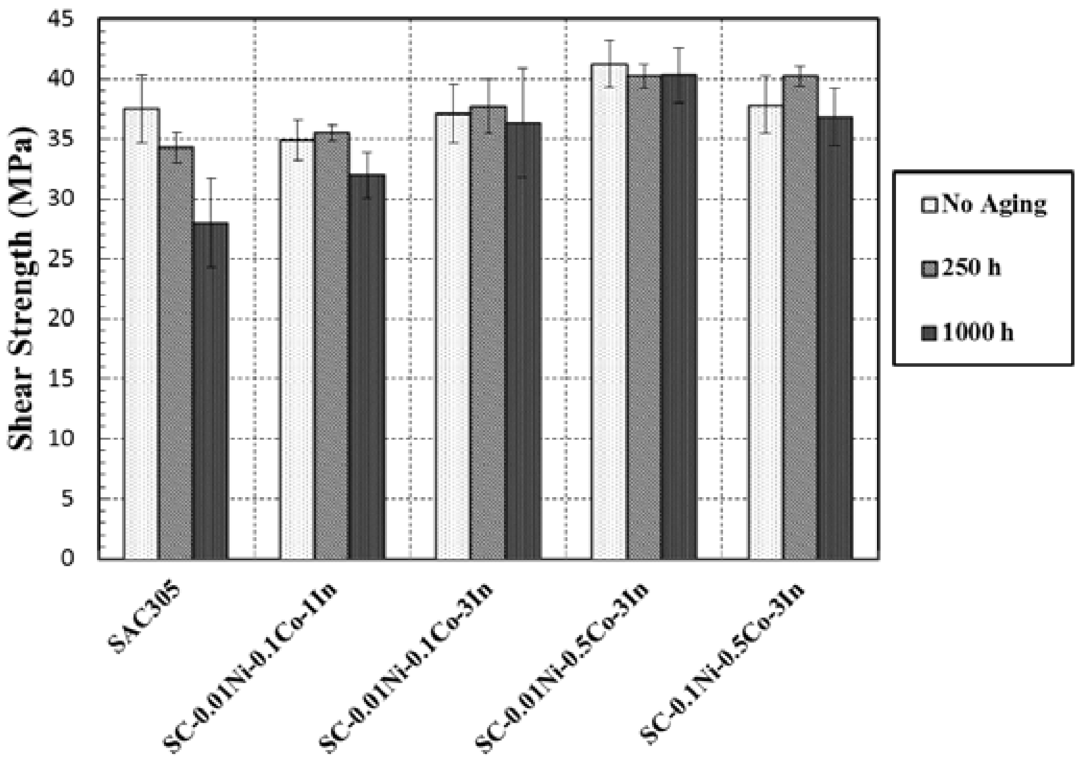

Fig.4.32 AFPB shear test results of SC-Ni-Co-In solder joints showing maximum shear strength as a function of aging time, SAC305 also shown as baseline

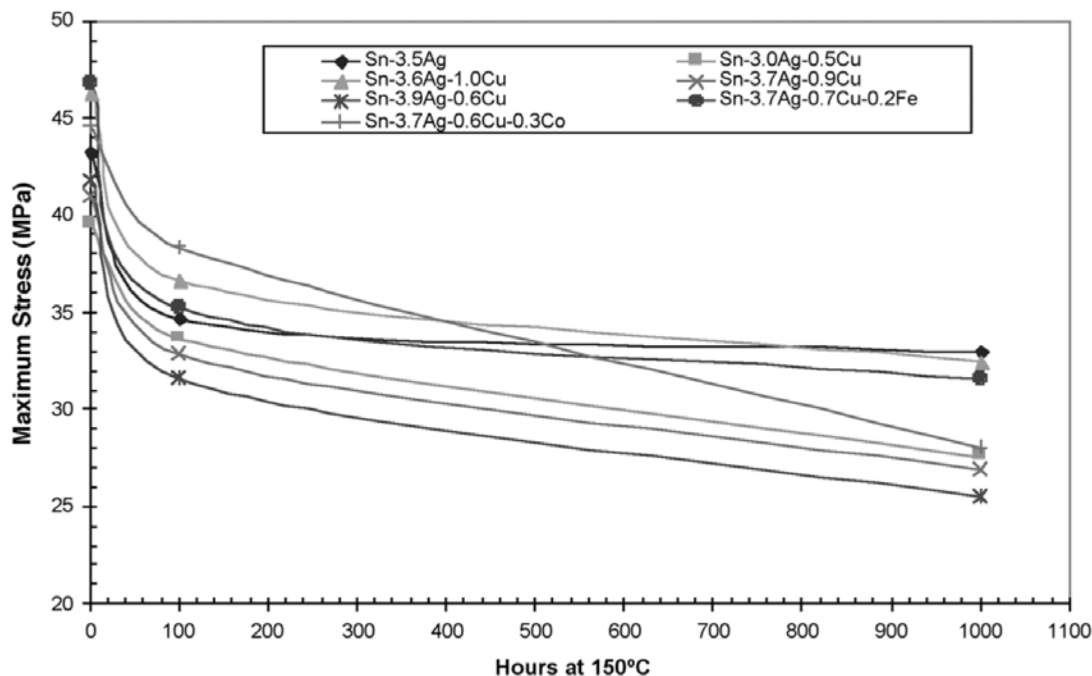

Fig.4.33 AFPB shear test results of SAC solder joints showing maximum shear strength as a function of aging time [14]

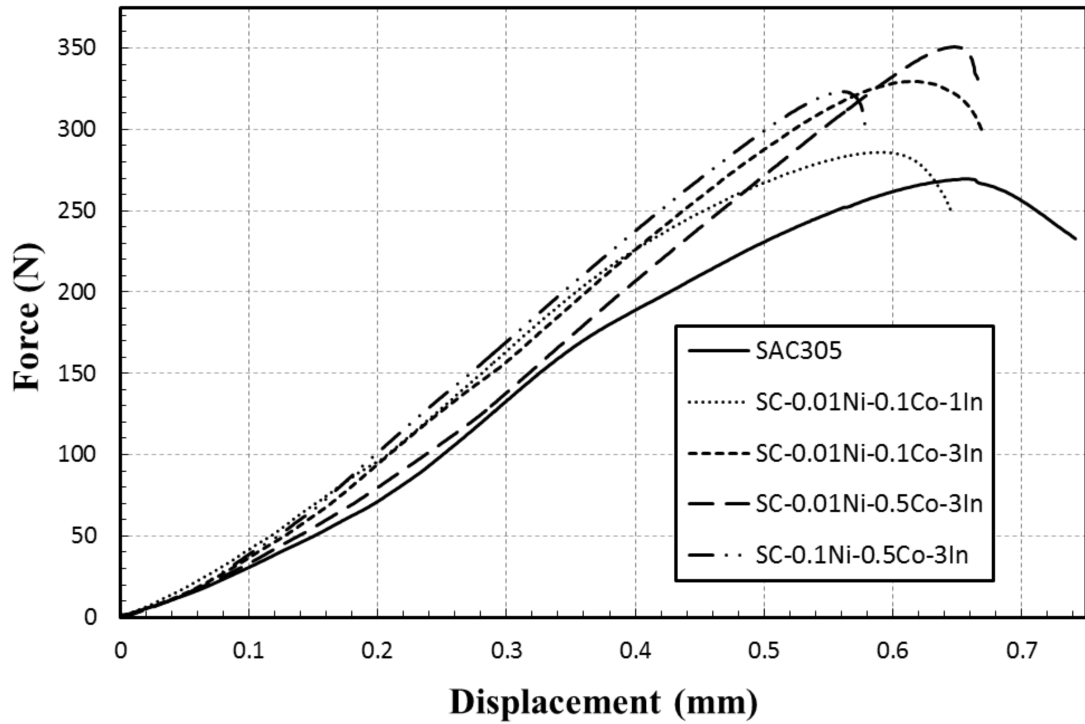

Fig.4.34 Load-displacement curves of solder joints aged at 150ºC for 1,000 hours

The load-displacement curve of the solder joints aged for 1,000 hours is shown in Fig.4.34. For SAC305 solder joint, its slope changes when the displacement reaches 0.32 mm. This behavior can also be seen in SC-0.01Ni-0.1Co-1In, where SC-Ni-Co-In alloys with 3%In display constant slopes. The strongest SC-0.01Ni-0.5Co-3In solder joint has about the same displacement at maximum load as that of SAC305. This increase in shear modulus of SC-Ni-Co-In with 3%In may be attributed to the IMC in the solder matrix which serves as the dislocation obstacles.

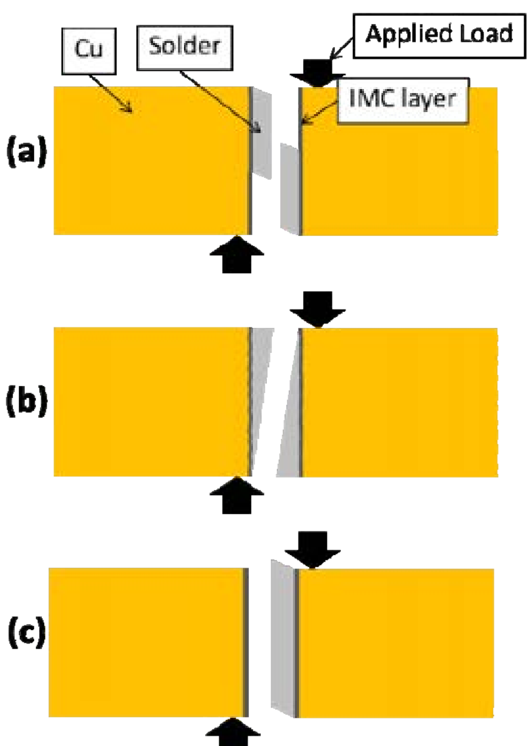

Fig.4.35 Illustrations of shear failure mode observed in AFPB shear test: (a) cracks open at both side of the solder/IMC interface and grow along the interface, (b) cracks open at both side of the solder/IMC interface and grow along solder, (c) cracks open at a side of the solder/IMC interface and grow along the interface

Cross-section images of failed solder joint were categorized into three failure modes as illustrated in Fig.4.35. The first failure mode in Fig.4.35a shows that localized shear occurred at both side of solder joint. The cracks are observed to initiate and growth along the solder matrix next to the interfacial IMC layer at both ends of

solder joint. The cracks come cross the solder matrix to join each other at the middle of solder joint. For the second mode in Fig.4.35b, cracks also initiate at both sides of solder joint but growth within the solder matrix. The third mode in Fig.4.35c shows that localized shear occurred at one side of solder joint. The crack is observed along interfacial IMC layer.

The shear failure mode of solder joints is summarized in Tab.4.2 for as-soldered and 1,000 hours aged conditions. The strong solder joints i.e. as-soldered SAC305, as-soldered SC-0.01Ni-0.5Co-3In, as-soldered SC-0.1Ni-0.5Co-3In, 1,000 hours aged SC-0.01Ni-0.5Co-3In and 1,000 hours aged SC-0.1Ni-0.5Co-3In usually fail by mode (a). The weak solder joints i.e. 1,000 hours aged SAC305, 1,000 hours aged SC-0.01Ni-0.1Co-1In usually fail by mode (b). This behavior is due to the stress distribution in solder joints. A uniform stress distribution in the solder joint leads to failure mode (a). On the other hand, if sites for local stress concentration are present in the solder joint such as poor distribution of IMCs and initial cracks, it will fail by mode (b).

Table 4.2 Summary of shear failure mode of solder joints

Solder alloys	Failure mode	
	As soldered	1,000-hour aged
SAC305	a	c
SC-0.01Ni-0.1Co-1In	b	c
SC-0.01Ni-0.1Co-3In	c	c
SC-0.01Ni-0.5Co-3In	a, c	a
SC-0.1Ni-0.5Co-3In	a, b	a

SAC305 exhibits change in failure mode from (a) to (b) after 1,000 hours aging. This may be due to local stress concentration by large locally IMC formation after aging. For SC-Ni-Co-In solder joint, instead of stress developing at a few locations, the IMCs in the solder matrix are uniformly distributed thus serve as multiple sites of local stress concentration so that stress dissipation through the solder joint is more homogeneous. Such uniform stress distribution leads to higher overall shear stress.

CHAPTER V
CONCLUSIONS

New solder alloys of Sn-Cu-Ni-Co-In system were synthesized and characterized to understand the effects of Ni, Co and In additions on Sn-Cu based solder alloys. Key soldering properties for electronics applications were characterized i.e. wettability, solidification behavior, electrical resistivity, microstructure evolution after isothermal aging and shear strength in order to verify the optimum amount of Ni, Co and In, and appropriate reflow soldering condition for this solder alloys. The properties of Sn-Cu-Ni-Co-In were compared to baseline obtained from those of conventional Pb-free solder alloys i.e. Sn-0.7Cu and SAC305.

Comparing to the eutectic Sn-0.7Cu, Sn-Cu-Ni-Co-In alloys with optimum amount of Ni, Co and In show enhanced shear strength and reduced melting temperature without posting immoderately negative effects on other key soldering properties. Amongst all SC-Ni-Co-In solder alloys tested, SC-0.01Ni-0.5Co-3In and SC-0.1Ni-0.5Co-3In are considered to be the candidates to be alternative alloys aside from the conventional Sn-Ag-Cu and Sn-Cu alloys. With lower cost, they show comparable properties with SAC305. Specifically, these alloys can effectively maintain their shear strength after subjected to high temperature operating environment. Sn-Cu-Ni-Co-In solder joints capably maintain their shear strengths after isothermal aging at 150ºC due to uniform dispersion of intermetallic compound in the solder matrix which serves as dislocation obstacles and multiple sites for local stress concentration.

The experimental results and discussions have leaded to the following conclusions:

5.1 Effects of Ni, Co and In additions on wettability

5.1.1 Co and In additions to Sn-Cu based solder alloy tend to decreased its spread area and increase its wetting angle.

5.1.2 SC-Ni-Co-In alloys with 0.1% Ni have better wettability than that of SC-Ni-Co-In with 0.01%Ni.

5.2 Solidification behavior of SC-Ni-Co-In solder alloys

5.2.1 SC-Ni-Co-In solder alloys with 3%In have 2ºC higher melting point than the conventional SAC305.

5.2.2 Ni, Co and In additions result in increased solidification range of Sn-Cu solder alloy to about 8ºC due to the off-eutectic compositions.

5.2.3 Ni, Co and In additions effectively suppress undercooling to near zero by catalytic effect.

5.3 Effects of Ni, Co and In additions on electrical resistivity

5.3.1 Co and In tends to increase the electrical resistivity of Sn-Cu solder alloys due to IMC formation in the solder matrix

5.3.2 The average electrical resistivity of SC-Ni-Co-In solder alloys is higher than that of SAC305 by magnitude of 0.9 μΩ-cm.

5.4 Effects of reflow soldering conditions on shear strength of SC-Ni-Co-In solder joints

5.4.1 The best shear strength was observed in solder joint subjected to reflow soldering conditions of 235ºC/30 sec and 245ºC/60 sec for both 1% and 3% In.

5.4.2 The reflow soldering condition of 235ºC/30 sec is considered the most appropriate because of lower energy and time consumptions than that of 245ºC/60 sec condition.

5.5 Effects of Ni, Co and In additions on shear strength of Sn-Cu based solder alloy before isothermal aging

5.5.1 The optimum amount of Ni, Co and In additions can effectively improve shear strength of Sn-Cu based solder alloy

5.5.2 The 3% In group show significant improvement in shear strength when compared to the 1% In group

5.5.3 SC-Ni-Co-In with 3% In show comparable shear strength to that of SAC305

5.6 Shear strength of SC-Ni-Co-In solder joints after isothermal aging

5.6.1 SAC305 show as-aged shear strength of 28 MPa which is 25.33% lower than that of as-soldered condition.

5.6.2 Average as-aged shear strength drop of four SC-Ni-Co-In solder alloys is 3.82%.

5.6.3 SC-0.01Ni-0.5Co-3In is the strongest solder joint for both as-soldered and as-aged conditions with shear strengths of 41.2 MPa and 40.3 MPa, respectively.

REFERENCES

[1] Cheng, F., Nishikawa, H., Takemoto, T.. Microstructural and mechanical properties of Sn–Ag–Cu lead-free solders with minor addition of Ni and/or Co. Journal of Materials Science 43 (May 2008): 3643-3648.

[2] Anderson, I.E., et al.. Alloying effects in near-eutectic Sn-Ag-Cu solder alloys for improved microstructural stability. Journal of Electronic Materials 30 (September 2001): 1053-1058.

[3] Gao, F., Takemoto, T., Nishikawa, H., Komatsu, A.. Microstructure and mechanical properties evolution of intermetallics between Cu and Sn-3.5Ag solder doped by Ni-Co additives. Journal of Electronic Materials 35 (May 2006): 905-911.

[4] Kanlayasiri, K., Mongkolwongrojn, M., Ariga, T.. Influence of indium addition on characteristics of Sn-0.3Ag-0.7Cu solder alloy. Journal of Alloys and Compounds 485 (October 2009): 225-230.

[5] Šebo, P., Švec, P., Janikovic, D., Štefánik, P.. Influence of thermal cycling on shear strength of Cu-Sn3.5AgIn-Cu joints with various content of indium. Journal of Alloys and Compounds 463 (September 2008): 168-172.

[6] Sharif, A., Chan, Y.C.. Effect of indium addition in Sn-rich solder on the dissolution of Cu metallization. Journal of Alloys and Compounds 390 (March 2005): 67-73.

[7] Šebo, P. et al.. Effect of indium on the microstructure of the interface between Sn3.13Ag0.74CuIn solder and Cu substrate. Journal of Alloys and Compounds 480 (July 2009): 409-415.

[8] National Center for Manufacturing Sciences. NCMS lead-free solder project final report. 3025 Boardwalk, Ann Arbor, MI: National Center for Manufacturing Sciences, 1999.

[9] Courtesy of Research International. Solder Reflow Technology Handbook [Online]. 2009. Available from: http://www.research-intl.com/reflowtechbook.htm [2009, September 4]

[10] Ho, C.E., Yang, S.C., Kao, C.R., Interfacial reaction issues for lead-free electronic solders. Journal of Materials Science: Materials in Electronics 18 (June 2007):1\55–174.

[11] Xu, L.H., Pang, J. H. L.. Effect of intermetallic and kirkendall voids growth on board level drop reliability for SnAgCu lead-free BGA solder joint. In Patrick Thompson et al. (eds.), 56th Electronic Components and Technology Conference, 8-15. 538 Johnson Avenue, Floor 2, Brooklyn, NY: Inc. The Printing House, 2006.

[12] Chiu, T.C., Zeng, K., Stierman, R., Edwards, D., Ano, D.. Effect of thermal aging on board level drop reliability for Pb-free BGA packages. In David McCann et al. (eds.), 54th Electronic Components and Technology Conference, 1256-1262. 538 Johnson Avenue, Floor 2, Brooklyn, NY: The Printing House, 2004.

[13] Tsai, J.Y., Hu, Y.C., Tsai, C.M., Kao, C.R.. A study on the reaction between Cu and Sn3.5Ag solder doped with small amounts of Ni. Journal of Electronic Materials 32 (November 2003): 1203-1208.

[14] Anderson, I.E., Harringa, J.L.. Elevated temperature aging of solder joints based on Sn-Ag-Cu: Effects on joint microstructure and shear strength. Journal Of Electronic Materials 33 (December 2004):1485-1496.

[15] Anderson, I.E., Harringa, J.L.. Suppression of void coalescence in thermal aging of tin-silver-copper-X solder joints, Journal of Electronic Materials 35 (January 2006): 1-13.

[16] Wang, Y.W., Lin, Y.W., Tu, C.T., Kao, C.R., Effects of minor Fe, Co, and Ni additions on the reaction between SnAgCu solder and Cu, Journal of Alloys and Compounds 478 (June 2009): 121-127.

[17] Anderson, I.E., Harringa, J.L.. Beneficial alloy effects in tin-silver-copper-X solder joints for high temperature applications. In John Stephens et al. (eds.), 3rd International Brazing and Soldering Conference, 18–25. Materials Park, 9639 Kinsman Road, OH: ASM International, 2006.

[18] Cook, B.A. et al.. Shear deformation in Sn-3.5Ag and Sn-3.6Ag-1.0Cu solder joints subjected to asymmetric four-point bend tests. Journal of Electronic Materials 30 (September 2001): 1214-1221

[19] Ünal, Ö., Barnard, D.J., Anderson, I.E.. A shear test method to measure shear strength of metallic materials and solder joints using small specimens. Scripta Materialia 40 (January 1999): 271-276.

[20] Chen, W. et al.. Effects of Ag on microstructures, wettabilities of Sn–9Zn–xAg solders as well as mechanical properties of soldered joints. Journal of Materials Science: Materials in Electronics 21 (May 2010): 461-467.

[21] Butler, J. A. V..The thermodynamics of the surfaces of solutions. In Eric Keightly Rideal et al. (eds), The Royal Society of London, 348-375. 1932.

[22] Tang, Z., Shi, F.G., Effects of preexisting voids on electromigration failure of flip chip solder bumps. Microelectronics Journal 32 (July 2001): 605-613.

[23] Laurila, T., Vuorinen, V., Kivilahti, J.K.. Interfacial reactions between lead-free solders and common base materials. Materials Science and Engineering: R 49 (March 2005): 1–60.

[24] Shanga, P.J., Liua, Z.Q., Panga, X.Y., Lia, D.X., Shanga, J.K., Growth mechanisms of Cu_3Sn on polycrystalline and single crystalline Cu substrates. Acta Materialia 57 (September 2009) 4697-4706.

[25] Liu, P., Yao, P., Liu, J., Evolutions of the interface and shear strength between SnAgCu–*x*Ni solder and Cu substrate during isothermal aging at 150°C. Journal of Alloys and Compounds. 486 (November 2009): 474-479.

[26] Haseeb, A.S.M.A., Leng, T.S.. Effects of Co nanoparticle addition to Sn-3.8Ag-0.7Cu solder on interfacial structure after reflow and ageing. Intermetallics 19 (May 2011): 707-712.

[27] Vuorinen, V., Laurila, T., Mattila, T., Heikinheimo, E., Kivilahti, J.K.. Solid-state reactions between Cu(Ni) alloys and Sn. Journal of Electronic Materials 36 (October 2007): 1355-1362.

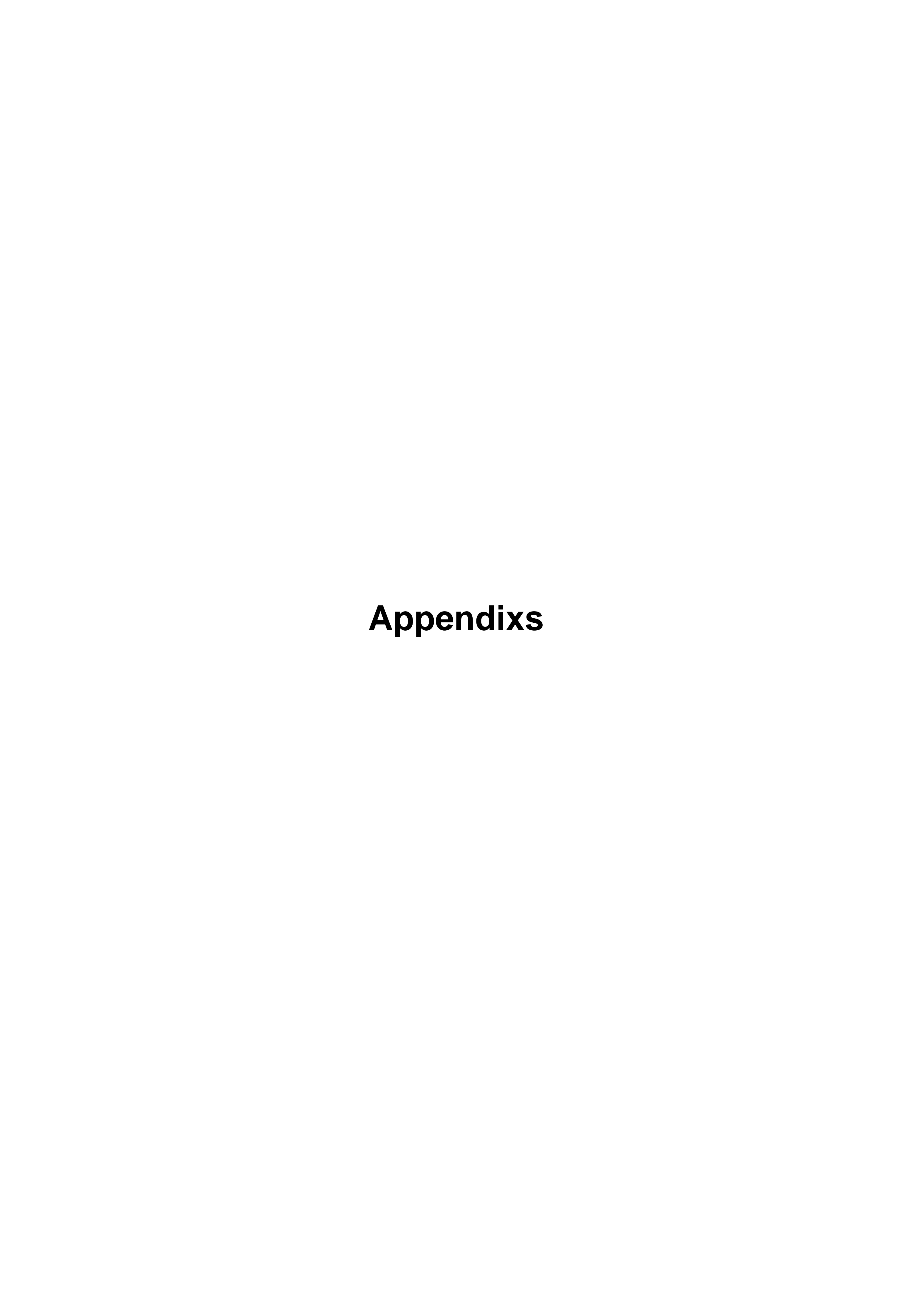

Appendixs

APPENDIX A

ICP-AES Analysis

ICP-AES Analysis

The solder alloy compositions were verified using inductively coupled plasma atomic emission spectroscopy (ICP-AES). The results of the selected alloys, SAC305, SC-0.1Ni-0.5Co-1In, SC-0.01Ni-0.5Co-3In, SC-0.1Ni-0.5Co-3In and SC-0.1Ni-0.5Co-3In (retest) are shown in Fig. A.1-A.5, respectively. The results are summarized in Table A.1.

Table A.1 ICP-AES results

Solder Alloys	Composition (wt.%)					
	Sn	Ag	Cu	Ni	Co	In
SAC305 (Sn-3.0Ag-0.5Cu)		2.89	0.48			
SC-0.1Ni-0.5Co-1In			0.58	0.084		0.89
SC-0.01Ni-0.5Co-3In			0.63	0.006		2.39
SC-0.1Ni-0.5Co-3In			0.67	0.068		2.49

สถาบันวิจัยและพัฒนาอัญมณีและเครื่องประดับแห่งชาติ (องค์การมหาชน) (สวอ)
The Gem and Jewelry Institute of Thailand (Public Organization) (GIT)

รายงานผลการวิเคราะห์ / Assay Report

เลขที่ / No ASI1008-082 Issue No. 0007126

วันที่รับของ 18/08/10 วันที่วิเคราะห์ 30/08/10

ลักษณะของวัตถุ / Specimen characteristic Alloy

น้ำหนักก่อนวิเคราะห์ / Weight before assaying 0.36 g

น้ำหนักหลังวิเคราะห์ / Weight after assaying 0.15 g

รายละเอียด / Description SAC305

วิธีการวิเคราะห์ / Method of Assaying ICP (Inductively Couple Plasma)

ผลการวิเคราะห์ / Result

ธาตุ / element	ร้อยละ / percent	หมายเหตุ / remark
Ag (Silver)	2.89	
Cu (Copper)	0.48	

(จักรพันธ์ สุวรรณวิจิตร)
ผู้รับรอง/Approved

(มนัสพงษ์ แววศรี)
ผู้ตรวจสอบ/Assayer

Fig. A.1 ICP result of SAC305

สถาบันวิจัยและพัฒนาอัญมณีและเครื่องประดับแห่งชาติ (องค์การมหาชน) (สวอ)
The Gem and Jewelry Institute of Thailand (Public Organization) (GIT)

รายงานผลการวิเคราะห์ / Assay Report

เลขที่ / No ASI1008-083 Issue No. 0007126
วันที่รับของ 18/08/10 วันที่วิเคราะห์ 30/08/10
ลักษณะของวัตถุ / Specimen characteristic Alloy
น้ำหนักก่อนวิเคราะห์ / Weight before assaying 0.33 g
น้ำหนักหลังวิเคราะห์ / Weight after assaying 0.31 g
รายละเอียด / Description 1 In

วิธีการวิเคราะห์ / Method of Assaying ICP (Inductively Couple Plasma)

ผลการวิเคราะห์ / Result

ธาตุ / element	ร้อยละ / percent	หมายเหตุ / remark
Ni (Nickel)	0.084	
Cu (Copper)	0.58	
In (Indium)	0.89	

(จักรพันธ์ สุวรรณวิจิตร)
ผู้รับรอง/Approved

(มนัสพงษ์ แวววศรี)
ผู้ตรวจสอบ/Assayer

Fig. A.2 ICP result of SC-0.1Ni-0.5Co-1In

สถาบันวิจัยและพัฒนาอัญมณีและเครื่องประดับแห่งชาติ (องค์การมหาชน) (สวอ)
The Gem and Jewelry Institute of Thailand (Public Organization) (GIT)

รายงานผลการวิเคราะห์ / Assay Report

เลขที่ / No ASI1007-026 Issue No. 0007049

วันที่รับของ 21/07/10 วันที่วิเคราะห์ 23/07/10

ลักษณะของวัตถุ / Specimen characteristic Alloy

น้ำหนักก่อนวิเคราะห์ / Weight before assaying 0.51 g

น้ำหนักหลังวิเคราะห์ / Weight after assaying 0.42 g

รายละเอียด / Description No. A

วิธีการวิเคราะห์ / Method of Assaying ICP (Inductively Couple Plasma)

ผลการวิเคราะห์ / Result

ธาตุ / element	ร้อยละ / percent	หมายเหตุ / remark
Cu (Copper)	0.63	
Ni (Nickel)	0.006	
In (Indium)	2.39	

(จักรพันธ์ สุวรรณวิจิตร) (ธิดารัตน์ เมืองไทย)

Fig. A.3 ICP result of SC-0.01Ni-0.5Co-3In

สถาบันวิจัยและพัฒนาอัญมณีและเครื่องประดับแห่งชาติ (องค์การมหาชน) (สวอ)
The Gem and Jewelry Institute of Thailand (Public Organization) (GIT)

รายงานผลการวิเคราะห์ / Assay Report

เลขที่ / No ASI1007-027 Issue No. 0007049

วันที่รับของ 21/07/10 วันที่วิเคราะห์ 23/07/10

ลักษณะของวัตถุ / Specimen characteristic Alloy

น้ำหนักก่อนวิเคราะห์ / Weight before assaying 0.54 g

น้ำหนักหลังวิเคราะห์ / Weight after assaying 0.43 g

รายละเอียด / Description No. B

วิธีการวิเคราะห์ / Method of Assaying ICP (Inductively Couple Plasma)

ผลการวิเคราะห์ / Result

ธาตุ / element	ร้อยละ / percent	หมายเหตุ / remark
Cu (Copper)	0.67	
Ni (Nickel)	0.006	
In (Indium)	2.49	

ธิดารัตน์ เมืองไทย

(จักรพันธ์ สุวรรณวิจิตร) (ธิดารัตน์ เมืองไทย)

ผู้รับรอง/Approved ผู้ตรวจสอบ/Assayer

Fig. A.4 ICP result of SC-0.1Ni-0.5Co-3In

สถาบันวิจัยและพัฒนาอัญมณีและเครื่องประดับแห่งชาติ (องค์การมหาชน) (สวอ)
The Gem and Jewelry Institute of Thailand (Public Organization) (GIT)

GIT

รายงานผลการวิเคราะห์ / Assay Report

เลขที่ / No ASI1008-084 Issue No. 0007126

วันที่รับของ 18/08/10 วันที่วิเคราะห์ 30/08/10

ลักษณะของวัตถุ / Specimen characteristic Alloy

น้ำหนักก่อนวิเคราะห์ / Weight before assaying 0.33 g

น้ำหนักหลังวิเคราะห์ / Weight after assaying 0.31 g

รายละเอียด / Description 3 In

วิธีการวิเคราะห์ / Method of Assaying ICP (Inductively Couple Plasma)

ผลการวิเคราะห์ / Result

ธาตุ / element	ร้อยละ / percent	หมายเหตุ / remark
Ni (Nickel)	0.068	

(จักรพันธ์ สุวรรณวิจิตร) (มนัสพงษ์ แววศรี)

Fig. A.3 ICP result of SC-0.1Ni-0.5Co-3In (retest)

APPENDIX B

Thermodynamic Approach for Interface Thickening

Thermodynamic Approach for Interface Thickening

In order to explain the growth behavior of interfacial Cu_6Sn_5 and Cu_3Sn, thermodynamic approach is taken into consideration. In the work by Vuorinen el al., effects of Ni addition on growth behavior of interfacial Cu_6Sn_5 and Cu_3Sn in Sn/Cu diffusion couple was studied [27]. The system is considered to be local equilibrium system which equilibrium exists only at the interface between different phases. The Gibbs energy diagram of the binary Sn-Cu system was calculated at 125°C, including the effects of dissolved Ni as shown in Fig. B.1 [27]. Sn atoms diffuse from interface I to II (through Cu_6Sn_5) by the driving force for diffusion of about 3,100 J/mol (ΔG_{Sn}) and that of Cu atoms from interface III to II (through Cu_3Sn) is about 10,000 J/mol (ΔG_{Cu}) in the diffusion couple. When 1at.% Ni is added in to $(Cu,Ni)_6Sn_5$, its gibbs energy decreases to $g^{\eta*}$ and the driving forces for the diffusion changes to ΔG^{*}_{Sn} and ΔG^{*}_{Cu}. When 5at.% Ni is added in to $(Cu,Ni)_6Sn_5$, its gibbs energy decreases to $g^{\eta**}$ and the driving forces for the diffusion changes to ΔG^{**}_{Sn} and ΔG^{**}_{Cu}. This thesis found that In tends to segregate into the Cu_6Sn_5 at the interface and Cu_6Sn_5 layer of all three solder alloys with 3%In is significantly thicker than that of the solder alloy with 1%In. These indicate that In also effects in stabilization of Cu_6Sn_5 as well as Ni. The effect of Co in stabilization of Cu_6Sn_5 has been previously revealed [2].

The diffusion flux of component i (J_i) is proportional to the driving force according to Nernst–Einstein relation:

$$J_i = C_i M_i \frac{\partial \mu_i}{\partial x} \qquad [B.1]$$

where C is concentration [mol/m^3], M is mobility, R = universal gas constant, and T = absolute temperature.

Thus, the changes in diffusion fluxes in the intermetallic compound layers resulted from the additions of Ni, Co and In can result in the observed changes in the thickness of the intermetallic compound layers. Fig. B.2 again shows intermetallic compound structure (Fig. 4.27) with approximated intrinsic fluxes through the layers.

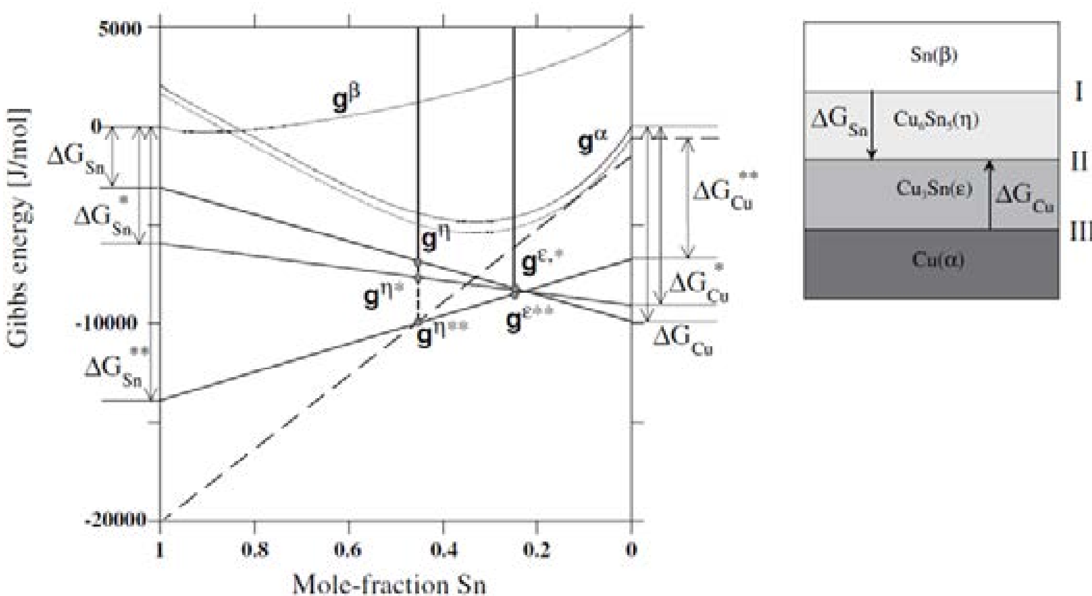

Fig. B.1 Gibbs energy diagram of binary Sn-Cu system at 150°C showing the driving forces for the diffusion of Sn and Cu atoms across the interfaces [27].

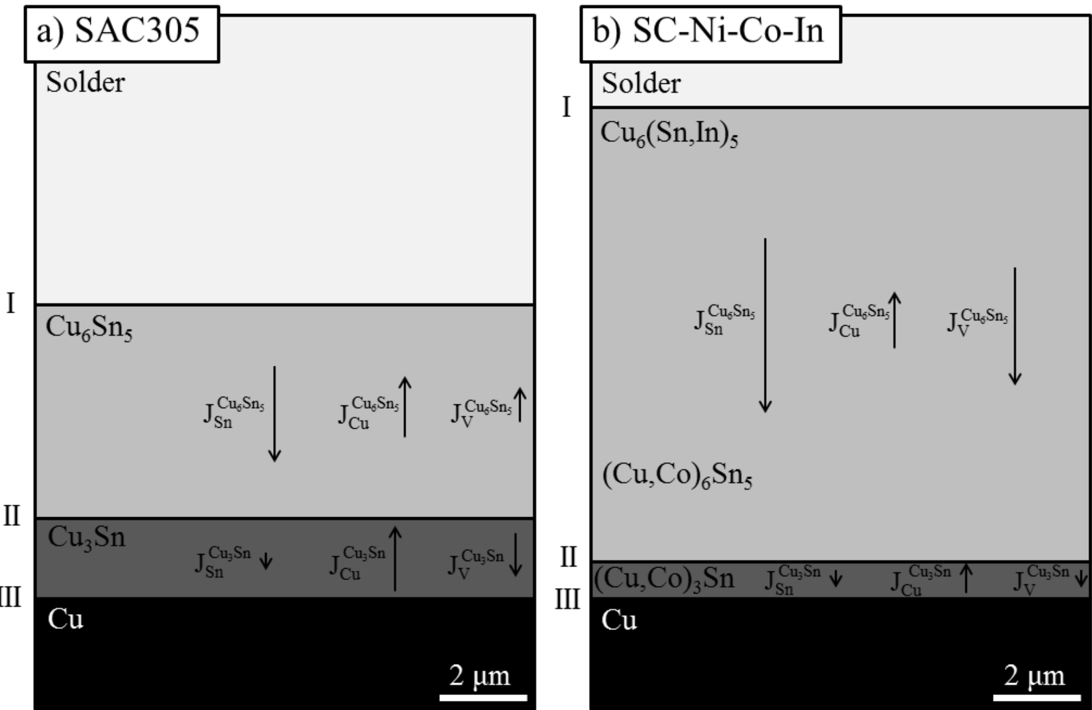

Fig. B.2 Intermetallic compound structure of as-aged solder joints. Note that the flux vectors are not to scale.

APPENDIX C

Measurement of IMC Thickness

Measurement of IMC Thickness

IMC Thickness at the solder joint interface was measured by SemAfore software. The thickness was reported as an average value of at least 10 measurements for smooth layer i.e. Cu_3Sn and as-soldered Cu_6Sn_5, and 20 measurements for rough layer i.e. aged Cu_6Sn_5. In order to avoid cognitive bias, position of thickness measurement is equidistant. Example for measurement of thicknesses of as-soldered Cu_6Sn_5, 1000-hour aged Cu_6Sn_5 and Cu_3Sn, are shown in Fig.C.1, C.2, and C.3, respectively.

Effects of inclination resulted from machining and metallographic preparation on measured thickness can be expressed by Eq. C.1

$$x_m = x_p \cos\theta \quad [C.1]$$

where x_m is the measured thickness, x_p is the thickness perpendicular to the substrate surface, and θ is the inclination angle as illustrated in Fig. C.4. However, the inclination angle should never exceed 5°. By taking $\theta = 5^{\circ}$, the Eq. C.1 is again written as:

$$x_m = 0.9962 x_p \quad [C.2]$$

which makes the error negligible.

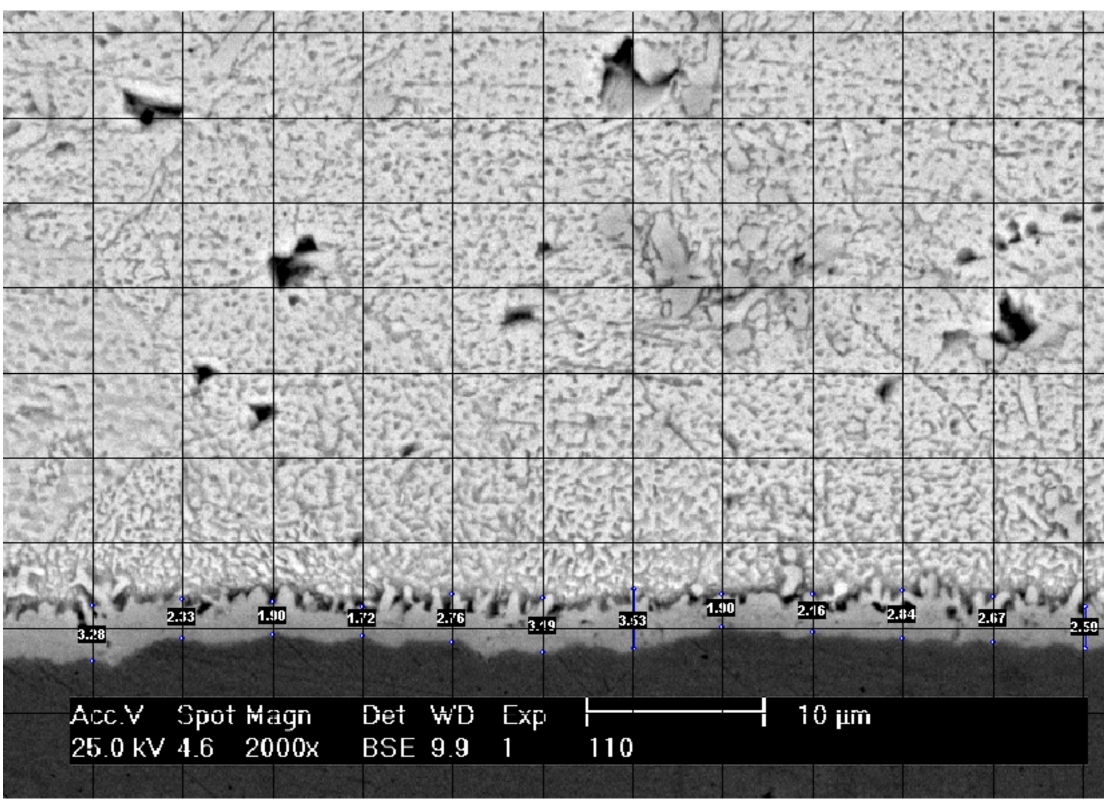

Fig. C.1 Example of thickness measurement of as-soldered Cu_6Sn_5

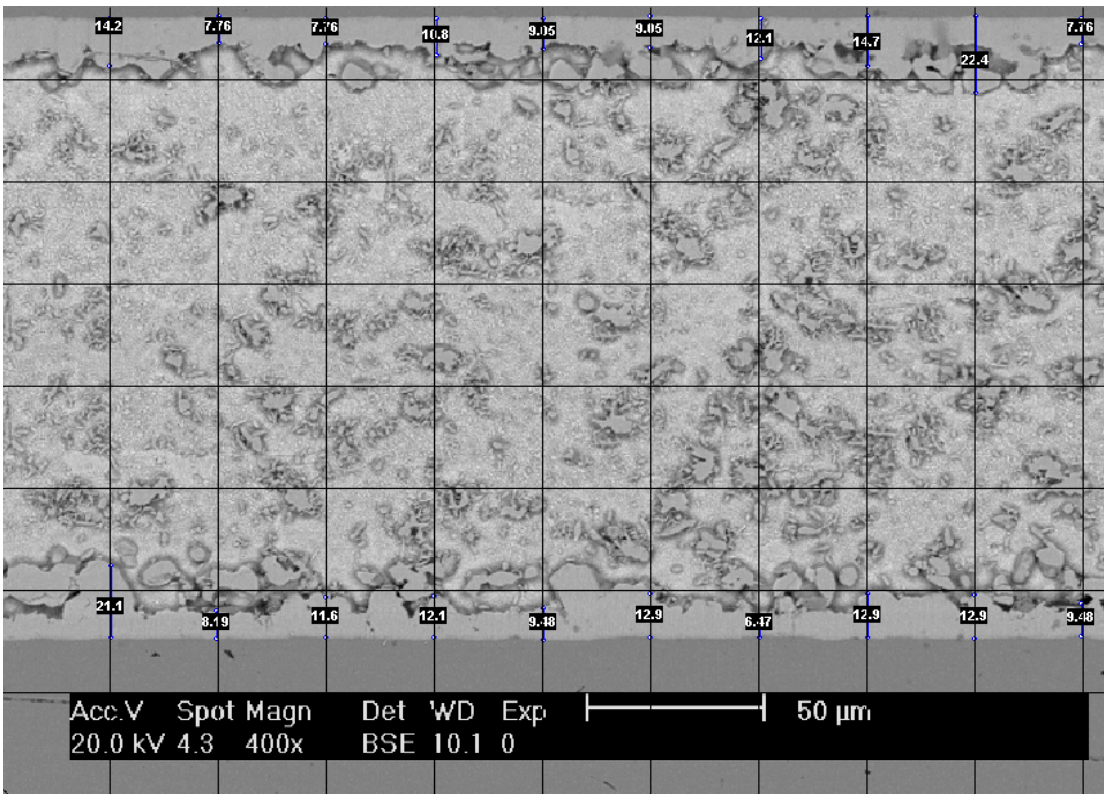

Fig. C.1 Example of thickness measurement of 1000-hour aged Cu_6Sn_5

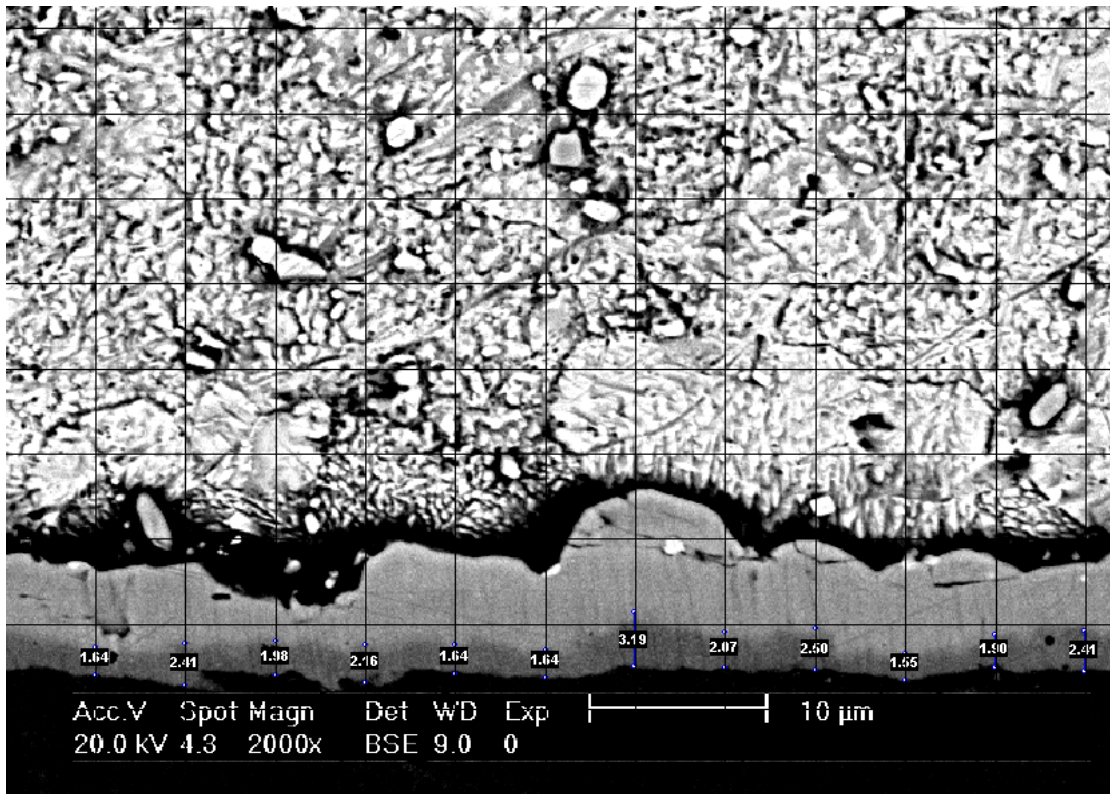

Fig. C.1 Example of thickness measurement of Cu_3Sn

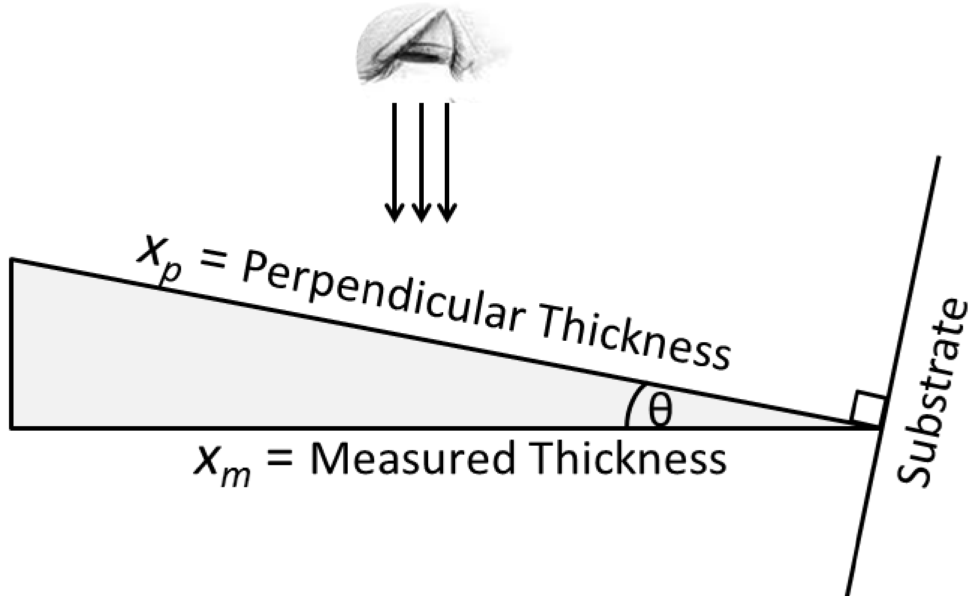

Fig. C.4 Effects of inclination resulted from machining and metallographic preparation on measured thickness

Biography

Pitinan Piyavatin was born on December 6, 1985 in Saraburi. He graduated from Chulalongkorn University with Bachelor Degree of Engineering in Metallurgical Engineering in 2008. He has been a Master student at Department of Metallurgical Engineering, Chulalongkorn University since 2008.